2018

Adaptive backstepping control of quadrotors with neural-network

Wang, Zhengqi

Lakehead University

Adaptive backstepping control of quadrotors with neural-network

by

Zhengqi Wang

Under the Supervision of Dr. Xiaoping Liu

For Fulfilling the Partial Requirements of the Master of Science in the Electrical and Computer Engineering

Lakehead University, Thunder Bay, Ontario, Canada

April. 2018

Acknowledgements

Firstly I would like to show my fully appreciation to my supervisor Dr. Xiaoping Liu. He is well knowledged in the control theory field. He can always be helpful with my thesis project. Also he helped me with my daily lives during the very first several days in Lakehead University. Then I would like to appreciate my to reviewers, Dr. Uddin and Dr. Yushi Zhou. They gave me a lot of useful advices on my thesis project as well as my thesis paper.

Also I would like to express my thanks to my colleagues, Mr. Tianqi Xi, Miss Ning Che. They accompany with me for the whole period of my master thesis study. And fully thanks to the former Masters thesis student Mr. Xiao Cui and Miss Kaiyu Zhao. During the start period of my thesis project, they helped me a lot to understand the complex system. Also, Mr. Xiao Cui helped me a lot with my life during the first several months in Thunder Bay. He can always be helpful with me in both academy and daily life. There's no doubt that we have become life-long friends.

Besides, I would like to express my heartfelt thanks to Lakehead University International Centre, Faculty of Graduate Studies and Lakehead University Robotics Lab. They gave me the fundamental support to complete my thesis.

Finally, I appreciate my family, my father and mother. Without their mental and financial support, I couldn't have the opportunity to study abroad in such an exceptional university.

Sincerely
Zhengqi Wang

Abstract

A quadrotor is a type of unmanned aerial vehicles. It has been widely used in aerial photography. The quadrotor has the capability of vertical takeoff and landing, which is very useful in small or narrow areas. The mechanical structure of a quadrotor is also simple, which makes it easy to produce and maintain. It is a strong candidate for a future means of transportation. In practical applications, it is commonly controlled by a proportional integral derivative controller.

In this thesis, two nonlinear controllers are designed to control the attitude and the position of a quadrotor by using the backstepping technique. The attitude is estimated by a nonlinear attitude estimator, which is based on a nonlinear explicit complementary filter. It uses data from a six axis inertial measurement unit and a three axis magnetometer to calculate the estimated attitude. To avoid the singularity problem like "gimbal lock" in Euler angle attitude representation, the unit quaternion attitude representation is applied in the controller derivation. However, the Euler angle representation is easier for people to imagine the actual attitude of a quadrotor. To make it more readable, the results of the experiments are converted to the Euler angle representation. During the derivation of a backstepping controller, a neural-network is applied to estimate the nonlinear terms in the system. The universal approximation theorem is the principle for the estimation of nonlinear terms. Besides, a two step controller is derived by modifying the backstepping controller with four steps. The two step controller is developed by an adaptive method for both the nonlinear terms and the moment of inertia. Analysis shows the boundedness of the closed-loop system with both controllers.

Finally, the proposed controllers are tested on a true quadrotor system. Experimental results show the effectiveness of the two proposed controllers. Also, comparison between two controllers are carried out. In addition, some future works are discussed.

Contents

List of Figures

List of Tables

List of Abbreviations

ICAO – International Civil Aviation Organization.
UAV – Unmanned Aerial Vehicle.
VTOL – Vertical Take Off and Landing.
BLDC – BrushLess Direct Current.
AHRS – Attitude and Heading Reference System.
RLG – Ring Laser Gyroscope.
IMU – Inertial Measurement Unit.
MEMS – Micro Electronic Mechanical Systems.
UAS – Unmanned Aircraft System.
KF – Kalman Filter.
EKF – Extended Kalman Filter.
UKF – Unscented Kalman Filter.
GPS/INS – Global Positioning System/Inertial Navigation System.
PID – Proportional Integral Derivative.
LQR – Linear Quadratic Regulator.
SMC – Sliding Mode Control.
CMAC – Cerebellar Model Arithmetic Computer.
RBF – Radial-Basis-Function.
FIR – Finite Impulse Response.
FFT – Fast Fourier Transform.
RC – Resistor Capacitor.
NED – North East Down.
PFD – Primary Flight Display.
DCM – Direction Cosine Matrix.
RC – Radio Control.
DC – Direct Current.
AC – Alternating Current.
ESC – Electronic Speed Controller.

LiPo – Lithium Polymer.
APM – Ardupilot Mega.
GCC – GNU Compiler Collection.
CPU – Central Processing Unit.
RTOS – Real Time Operating System.
PPM – Pulse Position Modulation.
RSSI – Received Signal Strength Indicator.
PWM – Pulse Width Modulation.
FPU – Floating Point Unit.
DMIPS – Dhrystone Million Instructions Per Second.
PC – Personal Computer.

Chapter 1

Introduction

1.1 Definition of a UAV

According to the official document from International Civil Aviation Organisation (ICAO), an Unmanned Aerial Vehicle (UAV) is a pilotless aircraft, which is flown without a pilot-in-command on-board and is either remotely and fully controlled from another place (ground, another aircraft, space) or programmed and fully autonomous [1].

1.2 Classifications

A UAV can be a fixed-wing airplane in Fig. 1.1 and Fig. 1.2, a rotorcraft in Fig. 1.3, Fig. 1.4 and Fig. 1.5 and other aerial vehicles such as a blimp or balloon in Fig. 1.6 and even a flapping wing vehicle in Fig. 1.7. It can used for either military purpose in Fig. 1.1, Fig. 1.2 and Fig. 1.3 or civil purpose in Fig. 1.4 and Fig. 1.5.

Figure 1.1: RQ-4 Global Hawk UAV

Fig. 1.1 shows an unmanned surveillance aircraft called RQ-4 Global Hawk developed by Northrop Grumman. It is powered by a Rolls-Royce AE 3007 turbofan engine. The engine features 8500 lbs of thrust and over 23 million hours of demonstrated reliability. The wingspan of Global Hawk is 131 ft. This feature helps it to fly long distance without

refueling for over 32 hours. Its operational range is 12300 nautical miles. Also its maximum altitude is 60000 ft due to the powerful turbofan engine [2].

Figure 1.2: MQ-9 Reaper UAV

The MQ-9 Reaper, as shown in Fig. 1.2, is an armed, multi-mission, medium-altitude, long-endurance remotely piloted aircraft that is employed primarily against dynamic execution targets and secondarily as an intelligence collection asset [3]. Compared with RQ-4 Global Hawk, it is more light weighted, which also means more agile and more suitable to the front line of wars or conflicts. The rear mounted turboprop engine is its feature which is uncommon in the manned airplane due to the difficulty for balancing the center of gravity. For MQ-9 Reapter, a lot of video equipment is arranged on the nose of the airplane to gain a better view. As a result, the power plant is moved to the rear of the airplane. Also, a turboprop engine is more fuel efficient which improves its range and reduces cost. However, a turboprop engine powered MQ-9 can not be compared with a turbofan engine powered RQ-4 in terms of maximum altitude, speed and range. More details can be refereed to Table 1.1.

Table 1.1: MQ-9 UAV Specification

Primary function	find, fix, and finish targets
Maximum thrust	900 shaft hp
Wingspan	66 ft (20.1 m)
Length	36 ft (11 m)
Height	12.5 ft (3.8 m)
Empty weight	4,900 lbs (2,223 kg)
Maximum takeoff weight	10,500 lbs (4,760 kg)
Fuel capacity	4,000 lbs (602 gal)
Payload	3,750 lbs (1,701 kg)
Speed	cruise speed around 230 mph (200 kt)
Range	1,150 mi (1,000 nautical mi)
Ceiling	Up to 50,000 ft (15,240 m)

As shown in Fig. 1.3, MQ-8B Fire Scout is a helicopter UAV developed by Northrop Grumman. It is designed to provide unprecedented situational awareness and precision targeting support for the U.S. Navy. Unlike RQ-4 and MQ-9, MQ-8B doesn't need a runway to take off or land. Like a manned helicopter, it only needs a helipad. In addition, it is able to take off and land autonomously from any suitably-equipped air-capable warship and

Figure 1.3: MQ8B Helicopter UAV

at unprepared landing zones [4]. Also the entire flight can be fully automatically operated. That is much different from the RQ-4 and MQ-9, because both of them need one or two crew members to remotely pilot the aircraft. More details about MQ-8B can be refereed to Table 1.2.

Table 1.2: MQ-8B Fire Scout UAV Specification

Rotor diameter	27.50 ft (8.4 m)
Width	6.20 ft (1.9 m)
Length	23.95 ft (7.3 m)
Height	9.71 ft (2.9 m)
Weight	3,150 lbs (1428.8 kg)
Payload	3,750 lbs (1,701 kg)
Speed	85 kt
Range	596 nautical mi/7.75 hrs with baseline payload
Ceiling	12,500 ft (3.8 km)
Payload	300 lbs
Typical payload	150 lbs

Figure 1.4: Phantom 4 Advanced Quadrotor UAV

Fig. 1.6 shows a tethered balloon UAV used by a climate research facility of the US government [5]. Using such a balloon to do some research about atmosphere is easy and

Figure 1.5: Inspire 2 Quadrotor UAV

Figure 1.6: A Tethered Balloon UAV

reliable. Also it is much safer than using a UAV airplane or rotorcraft. The tether cable can hold electrical wires as well as optical fibers which means its data link can be extremely faster and more reliable. However, deploying such a big object is a huge task for workers and also costs a lot of time. Moreover, it doesn't have the ability to move itself, so all the movement must be achieved by tethered cables.

Figure 1.7: Festo's "SmartBird" Flapping Wing UAV

Inspired by the herring gull, Festo developed a flapping wing UAV called SmartBird as shown in Fig. 1.7. It features outstanding aerodynamics and maximum agility and is able to take off, cruise and land autonomously [6]. Due to the flapping wing mechanism, the system can be extremely efficient. According to the research in [7], the average proplusive efficiency is 54% for the designed flapping wing vehicle. And it is a strong candidate for future means of transportation. However, besides its known advantages, the current technology for it is still limited. A lot of difficulties and drawbacks are not overcome [8].

1.3 Definition and Features of a Quadrotor

Quadrotor as shown in Fig. 1.4 and Fig. 1.5 is a rotor aircraft which is powered by four rotors. It has Vertical Take Off and Landing (VTOL) capability [9]. It has a simple structure with four motors and each of the motors has a propeller attached. To increase the reliability, layouts with more than four motors are introduced which are usually called multirotors or multicopters. But quadrotors are still popular because they are simple and cheap. Moreover, motor failure is not usually happened due to the advanced BrushLess Direct Current (BLDC) motor and motor controller technologies. The additional motors indeed don't increase too much reliability but decrease efficiency. This is caused by the additional weight and drags introduced by the motors and propellers. As a result, the flight range and time of the multicopters with more than four rotors are shorter than that of the quadrotors under the same conditions.

Unlike traditional helicopters, a simple and common quadrotor usually uses pitch fixed propellers [10]. The final output of controller is only four angular velocities of motors. The pitch or roll angle of the quadrotor can be changed by simply increasing one side motors' speed and decreasing the other side motors' speed. The yaw angle can be adjusted by increasing a diagonal pair of motors' speed and decreasing the other pair's speed.

Phantom 4 Advanced as shown in Fig. 1.4 is a medium sized quadrotor UAV which can be placed in a regular sized school bag. It is the latest version of DJI Phantom series quadrotor UAVs (announced in April, 2017). The details of Phantom 4 Advanced can be refereed to Table 1.3 [11].

Table 1.3: Phantom 4 Advanced Quadrotor UAV Specification

Weight (battery and propellers included)	1368 g
Diagonal size (propellers excluded)	350 mm
Max ascent speed	s-mode: 6 m/s
Max descent speed	s-mode: 4 m/s
Max speed	s-mode: 45 mph (72 kph)
Max tilt angle	s-mode: 42°
Max angular speed	s-mode: 250°/s
Max service ceiling above sea level	19685 ft (6000 m)
Max wind speed resistance	10 m/s
Max flight time	approx. 30 min
Operating temperature range	32°F to 104°F (0°C to 40°C)

Inspire 2 is a large sized professional aerial flimmaking quadrotor UAV as shown in Fig. 1.5. The arm of Inspire 2 can moves upwards in order to obtain a good view for the camera mounted beneath. The gimbal of Inspire 2 can freely rotate for 330°on each direction. Details can be refereed to Table 1.4 [12].

Table 1.4: Inspire 2 Quadrotor UAV Specification

Max take off weight	8.82 lbs (4000 g)
Diagonal distance (propeller excluded)	23.8 in (605 mm, landing mode)
Max ascent speed	s-mode: 6 m/s
Max descent speed	vertical: 4 m/s
Max speed	s-mode: 58 mph (94 kph)
Max tilt angle	s-mode: 40°
Max angular velocity	pitch/roll: 300°/s yaw: 150°/s
Max take off sea level	2500 m
Max wind speed resistance	10 m/s
Max flight time	dual battery 27 min
Operating temperature range	32°F to 104°F (0°C to 40°C)

1.4 Attitude Estimator

Although the attitude estimator is not the focus of this thesis, it indeed plays a vital role in the whole quadrotor UAV system. Also, it is true for almost any kind of aircraft, even for submarines. Sometimes, the attitude estimator is also called a Attitude and Heading Reference System (AHRS).

Unlike manned aircraft, it is not practical for a small quadrotor UAV to carry on a heavy and expensive Ring Laser Gyroscope (RLG). So far, the only Inertial Measurement Unit (IMU) solution is a gyroscope based on Micro Electronic Mechanical Systems (MEMS). However, the performance and the accuracy of a MEMS gyroscope is much worse than a RLG, even worse than a mechanical gyroscope. Aside from gyroscope, accelerometer and magnetometer are in the same situation.

For attitude estimation, it is easy to carry out the integration method. Time integration of the rotation rate from gyroscope readings is Euler angles. The integration method is practical for a RLG but not for a MEMS gyroscope because the gyro drift for a MEMS gyroscope is much greater than a RLG. Such a drift makes the readings unacceptable for the Unmanned Aircraft System (UAS). To solve this problem, some sensor fusion algorithm is required.

Kalman Filter (KF) [13] and Extended Kalman Filter (EKF) are two traditionally used methods for attitude estimation. The filter name Kalman is the primary developer of the algorithm. Generally, KF is an algorithm that combines multiple measurements with noise and inaccuracy, then produces a more accurate estimates of the unknown variables than estimates based on a single measurement. KF is widely applid in several fields such as aerospace navigation, battery charging system, motor controller and weather forecasting. It is an ideal solution for attitude estimation according to the facts of sensors in the last two paragraph. KF theory has been developed and applied by many reserachers [14]. Meanwhile, there are a lot of books and articles, which focus on the explanation of KF and EKF [15–17]. The KF and EKF were applied to the navigation system during the famous Apollo moon project by NASA, USA [18]. The detail of the application can be refereed to [19]. With unit

quaternion attitude representation, the EKF was implementated on a quadrotor UAV system in [20, 21]. Furthermore, Unscented Kalman Filter (UKF) can be also used as an attitude estimator [22]. In [23], a comparison of UKF and EKF was carried out. An application of adaptive high-gain EKF to a quadrotor navigation system was introduced by [24]. However, the attitude part of [24] was represented by Euler angle representations. In addition to attitude estimation, KF and EKF can be used on position estimation as a Global Positioning System/Inertial Navigation System (GPS/INS) fusion algorithm. Together with AHRS, KF and EKF can be used to build up a complete navigation system.

Recently, several new attitude estimators are developed. There are mainly 2 types of approach: complementary filter and gradient descent algorithm.

Typical research about complementary filter based attitude estimator is given by Tarek Hamel and Robert Mahony [25, 26]. Some further research is carried out for this kind of filters by [27].

Research about gradient descent algorithm based attitude estimator is mainly conducted by Madgwick [28,29]. However, the test performance is not extremely better than complementary filter in [27].

Some practical tests of these attitude estimators have been conducted. Due to the limited computational speed for the real time system, KF and EKF consume too much time in one loop and affect the general performance of the quadrotor system. And it can not draw a conclusion that which is better between CF and gradient descent algorithm. Considered the consistency of experiments and convience for comparison with archived thesis, the attitude estimator in [27] was finally used.

1.5 Controller Algorithm

Unlike the attitude estimator, there are various methods for the controller design of a quadrotor. Basically, there are two kinds for controllers: linear controllers and nonlinear controllers.

1.5.1 Linear Controllers

Generally, Proportional Integral Derivative (PID) controller is a basic and commonly used controller algorithm. It is also true for most industrial fields. It can be directly used in a quadrotor system even without a linearization. There is no doubt that PID controller is a very practical, easy and reliable method and there is indeed some research about PID controllers on quadrotor systems [30]. However, the PID controller is a linear controller and the quadrotor UAV is a nonlinear system. So, one of linear controller design method is to linearize the nonlinear model for a quadrotor UAV system first and the PID control is developed based on the linearized model. Besides PID, a Linear Quadratic Regulator (LQR) controller is also a linear controller for quadrotor UAV systems. Bouabdallah, Noth

and Siegwart did a research work about the comparison of PID and LQR controllers on quadrotor UAV systems in [31]. In [32], the nearly same research was conducted and then the PID tuned by the LQR controller was tested.

1.5.2 Nonlinear Controllers

For a quadrotor UAV system, a straightforward control strategy is to use nonlinear controllers. So far, most of nonlinear controllers have been designed by using the Lyapunov based methods. The backstepping method is a proved approach. It is applied in [33–39]. However, most of these backstepping controllers are developed for attitude control based on the nonlinear models in Euler angle representation. In [40], a backstepping method was used to design a trajectory tracking controller and an H_∞ controller was used to stabilize the attitude of a quadrotor. Sliding Mode Control (SMC) is another possible approach for the control of a quadrotor. In [41], an adaptive SMC for quadrotor attitude stabilization and altitude tracking was proposed. A comparison between backstepping and SMC for a quadrotor application can be found in [33]. Besides, there are also other methods for the control of a quadrotor, such as state feedback [42], feedback linearization [43], etc.

1.5.3 Adaptive Control

To estimate unknown parameters or unknown nonlinearities, nonlinear adaptive control has been used in quadrotor systems. Most of the nonlinear adaptive controllers are developed by using Lyapunov stability theory. In [38, 42], the adaptive method was used to compensate disturbances. A research about model reference adaptive control was proposed in [44]. It includes the comparison of direct and indirect model reference adaptive control for a quadrotor. A nonlinear function approximator called Cerebellar Model Arithmetic Computer (CMAC) was employed for the direct approximate-adaptive control of a quadrotor in [45]. A robust adaptive-fuzzy control method was carried out in [46]. This paper introduces an approach to prevent the drift of fuzzy membership centers.

1.5.4 Neural Network Applications to Controller Design

The controller design is based on the dynamic model. However, the dynamic model is derived by using the current physical theory instead of matching mathematical model from experiment. So, the dynamic model itself is not accurate. The dynamic model is limited in a very ideal environment which is hardly to find in the real world. A lot of disturbances are hard to be included accurately in the dynamic model. Since the designed controller is based on the inaccurate dynamic model of a quadrotor UAV system, the control performance of the closed-loop system may deteriorate, especially in a windy weather. To overcome this issue, the robust control theory can be applied. In [47], a typical robust control for a quadrotor system was designed by H_∞ control method. Also a model predictive controller was introduced in this research. Another approach to solve the model uncertainty issue is to apply neural network. Early in 1989, it was proved that a multilayer feedforward network

can be used as a universal approximator to estimate a continuous function [48]. Later in 1991, Park and Sandberg shows that Radial-Basis-Function (RBF) networks can be used to approximate an nonlinear function [49]. According to the research in [50], the perceptron type networks with two hidden layers have universal approximation capabilities. A later research in [51] shows that a feed-forward network with a single hidden layer and sigmoidal functions is able to approximate continuous functions.

On the quadrotor system, an application of neural network with PID controller was proposed in [52]. However, in this research, instead of being directly used as an approximator, the neural-network is used to provide the coefficients of a Finite Impulse Response (FIR) approximator. In [53], the researchers mainly used an output feedback controller and introduced a neural network to learn the complete dynamics of the quadrotor online. Obviously, estimating the quadrotor dynamics online has a lot of advantages over the robust control. The disturbances can be varied from place to place. Also for the fuel powered quadrotors, their mass is decreasing during the flight process, which leads to a change of dynamic model. The proper implementation of neural network to learn the dynamics online would perfectly solve these issues.

1.6 Research Motivation

As showed in Subsection 1.5.2, the research with proper application of backstepping to a quadrotor platform is still insufficient. In [33], there are no experimental result for the position control. In [34, 35, 38], only simulation results are provided. In addition, most literatures use Euler angle attitude representation [33–35, 38, 54]. These researches can not overcome the singularity problem caused by Euler angle attitude representation. Above all, these are the main reasons to conduct this thesis.

Inspired by [54, 55], and by referring to the previous thesis work in [36, 37, 56], this thesis actually does the "future works" in their thesis. According to these research, it can be clarified that the Euler angle representation is improper to be used in a controller design for a quadrotor UAV. So, the Euler angle representation is no longer used in the controller design of this research.

According to the research in [48–51], it can be concluded that the neural-network is an ideal approximator for the uncertain terms. Also, its capability with the attitude control of a quadrotor is proved in [36]. Since there has been little related research about its application on the position tracking of a quadrotor UAV so far, it is conducted in this thesis.

Above all, Adaptive backstepping control of quadrotors with neural-network is developed in this thesis.

1.7 Thesis Contribution

The contributions of this thesis are shown as below.

- A method to measure the moment of inertia is implemented in Chapter 2, which was proposed in [57] and improved in [56]. To collect the oscillation data, a nonlinear attitude estimator proposed in [27] is used. To get the natural frequencies for each axis of the quadrotor, the Fast Fourier Transform (FFT) has been applied.
- Two adaptive backstepping position tracking controllers are proposed based on the unit quaternion representation in Chaper 4. In order to smooth the position data collected from the GPS, a Resistor Capacitor (RC) low pass filter is implemented. A complementaty filter proposed in [27] is used to estimate the attitude of the quadrotor.
- The uncertain nonlinear terms are estimated by an adaptive neural-network algorithm in Section 4.2. In addition, an adaptive method is also implemented for the estimation of moment of inertia. Both simulation results and outdoor flight testing results on the quadrotor are presented.

1.8 Thesis Outline

Six chapters are included in this thesis. Chapter 1 gives an introduction to quadrotor UAVs. Attitude estimators and controller algorithms for quadrotor UAVs are also reviewed in this chapter.

Chapter 2 presents the measurement of the moment of inertia and some basic mathematical concepts and properties which are used in the rest of this thesis. Chapter 3 consists of the details about the quadrotor hardware layout. Chapter 4.1 gives a dynamic model for a quadrotor UAV. Two unit quaternion based position tracking controller are developed in Chapter 4. An adaptive neural-network algorithm is used to estimate the nonlinear terms and an adaptive algorithm is employed to estimate the moment of inertia.

Finally, Chapter 5 summarizes the thesis work and suggests the visions of future research work.

Chapter 2

Preliminaries

This chapter is composed of two sections. The first section provides a mathematical model and experimental results for calculation of the moment of inertia. The second section focuses on the attitude representations. Three types of attitude representations are introduced and their properties are provided. In addition, the conversion among the three representations are discussed as well.

2.1 Moment of Inertia

Moment of inertia is a crucial part of a quadrotor UAV model. Also it is a component of the controller derived in Chapter 4.

Moment of inertia is a property of an object. The moment of inertia can be calculated by formulas related to the object's geometry shape. Also it can be measured by experiment. For the calculation method, the shape of the quadrotor is complex. Also some of the measurements are difficult to carry out. And for the experimental method, it's prone to interference from environmental changes such as winds and vibration. To reduce the error and simplify this process, the experimental method was used. And over 3 times of experiments were carried out. The average of 3 experiment results was calculated. However, whatever method used, it is very difficult to obtain the accurate values for the moment of inertia. So an adaptive method is applied in Chapter 4.

Due to the limitation of the lab equipment, a simple method implemented by a Bifilar pendulum [36, 56, 57] was used in Fig. 2.1.

Figure 2.1: Measuring the Moment of Inertia

2.1.1 Derivations

The kinetic energy for the suspended quadrotor consists of rotational kinetic energy as well as a small amount of kinetic energy caused by movement of vertical axis, that is,

$$E_k = \frac{1}{2} I\omega^2 + \frac{1}{2} m\dot{z}^2 \tag{2.1}$$

where I denotes the moment of inertia, ω represents the angular velocity, m is the mass of the quadrotor, $\dot{z}$ denotes the velocity of vertical movement.

Neglecting the very small amount of elastic potential energy caused by suspension wire, choosing the lowest point as zero reference for potential energy results in

$$E_p = mg(l - l\cos\theta) \tag{2.2}$$

where g denotes the gravitational acceleration, l is the distance from the centre of the quadrotor to the junction of suspension wire, θ represents the angle from current position to the neutral position with respect to the testing axis, which can be obtained from the attitude estimator by converting the unit quaternion to Euler angle.

Define

$$L = E_k - E_p \tag{2.3}$$

The Euler-Lagrange equation for L is given by

$$\frac{\partial L}{\partial \theta} - \frac{d}{dt}\left(\frac{\partial L}{\partial \dot{\theta}}\right) = 0 \tag{2.4}$$

Substituting (2.3) into (2.4) results in

$$\left(I + ml^2\right)\ddot{\theta} + mgl\sin\theta = 0 \tag{2.5}$$

Since θ is relatively small, $\sin\theta \approx \theta$, which, together with (2.5), implies that

$$\left(I + ml^2\right)\ddot{\theta} + mgl\theta = 0 \tag{2.6}$$

Performing a Laplace transform of (2.6) gives

$$\left(I + ml^2\right)s^2 + mgl = 0 \tag{2.7}$$

which means that

$$s^2 + \frac{mgl}{I + ml^2} = 0 \tag{2.8}$$

Comparing (2.8) with the standard second order system $s^2 + 2\zeta\omega_n + \omega_n^2$ yields the following natural frequency

$$\omega_n = \sqrt{\frac{mgl}{I + ml^2}} \tag{2.9}$$

Finally, an expression for I can be determined from

$$I = \frac{mgl}{\omega_n^2} - ml^2 \tag{2.10}$$

with ω_n being calculated from the test.

2.1.2 Experimental Results

To get the natural frequency ω_n, FFT method was used. The experiment was carried out by rotating the quadrotor to a big angle and releasing it to let it oscillate freely. To satisfy the condition mentioned in (2.6), only the oscillation data whose amplitude is between $\pm 10°$ was used.

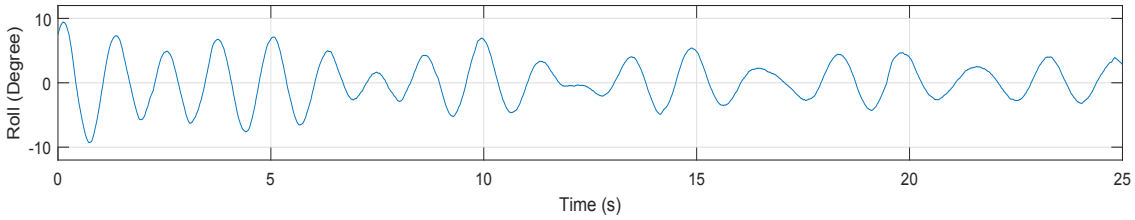

Figure 2.2: Oscillation of Roll Angle

The natural frequency ω_n are read from FFT figure in Fig. 2.3, Fig. 2.5 and Fig. 2.7 by capturing the first visible peak of the figures, which is labelled in these figures. From these figures, it can be observed that the largest peak occurs at a very low frequency. And there

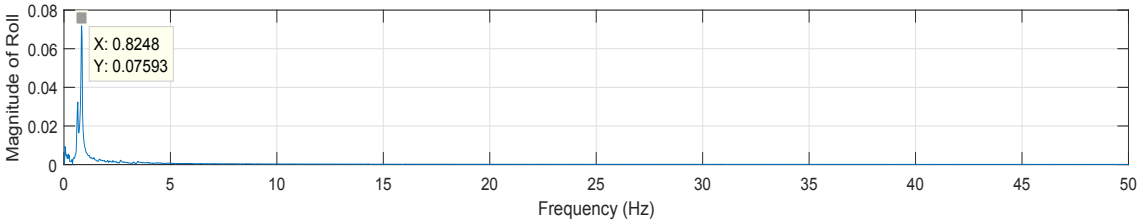

Figure 2.3: FFT of Roll Angle

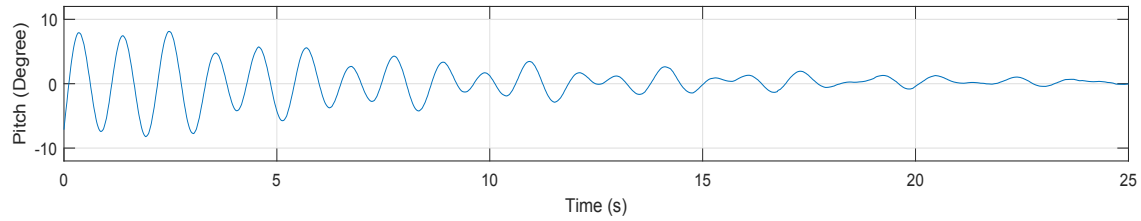

Figure 2.4: Oscillation of Pitch Angle

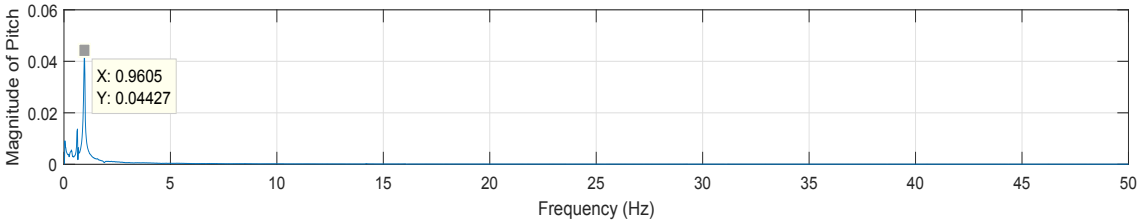

Figure 2.5: FFT of Pitch Angle

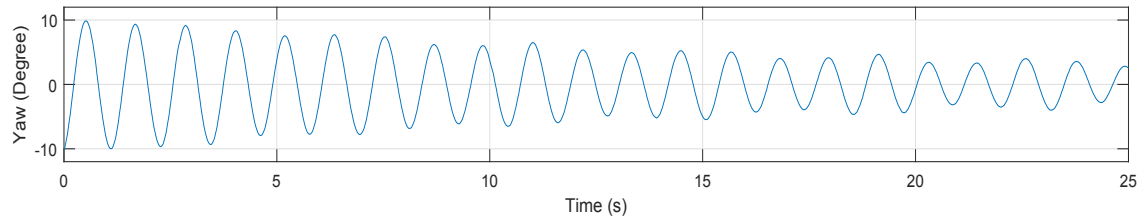

Figure 2.6: Oscillation of Yaw Angle

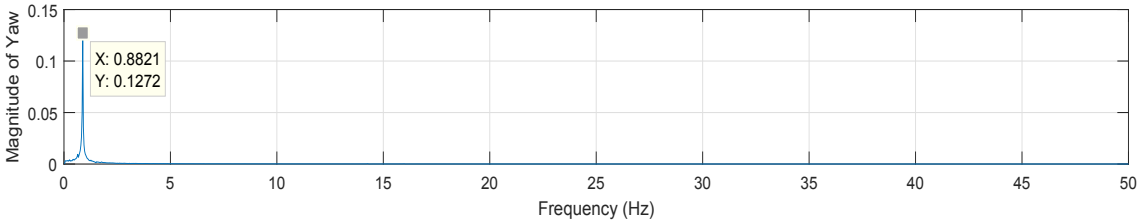

Figure 2.7: FFT of Yaw Angle

is also a peak around 98 Hz. They are not the frequency of interest. A parameter table is shown in Table 2.1.

Table 2.1: Model Parameters

Parameter	Description	Roll (x Axis)	Pitch (y Axis)	Yaw (z Axis)
ω_n	natural frequency	0.9605 Hz	0.8248 Hz	0.8821 Hz
I	moment of inertia	0.0113 $kg \cdot m^2$	0.0085 $kg \cdot m^2$	0.0122 $kg \cdot m^2$
m	total mass of the quadrotor	0.526 kg		
g	gravitational acceleration	9.81 m/s^2		
l	distance from the center to the suspension point	0.0905 m	0.0905 m	0.1125 m

2.2 Attitude Representations

There are mainly 3 different types of attitude representations used in the thesis: Euler angle representation, unit quaternion representation and rotation matrix representation [58]. Each of them has its own characteristic. To avoid singularity problem and simplify calculation as much as possible, unit quaternion attitude representation is mainly used in controller design. To make results more readable, Euler angle representation is used in simulation and experimental analyses and it is mostly offline converted from unit quaternion. Rotation matrix is mainly used to transform expressions back and forth from the inertial frame to body frame.

2.2.1 Frames

There are basically two frames used in this thesis: inertial frame and body (fixed) frame. The coordinate direction of the body frame is shown in Fig. 2.8. The inertial frame is set as the same to the local navigation frame. The direction of the inertial frame is defined as North East Down (NED).

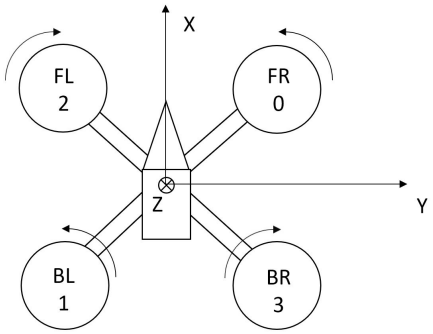

Figure 2.8: Body Frame

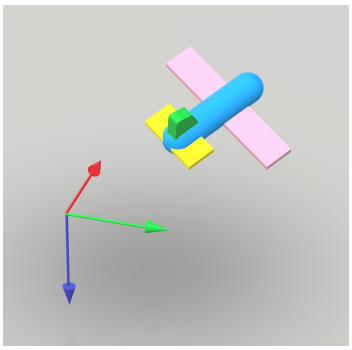

Figure 2.9: Body Frame and Inertial Frame

2.2.2 Euler Angle

Figure 2.10: A Boeing Style PFD

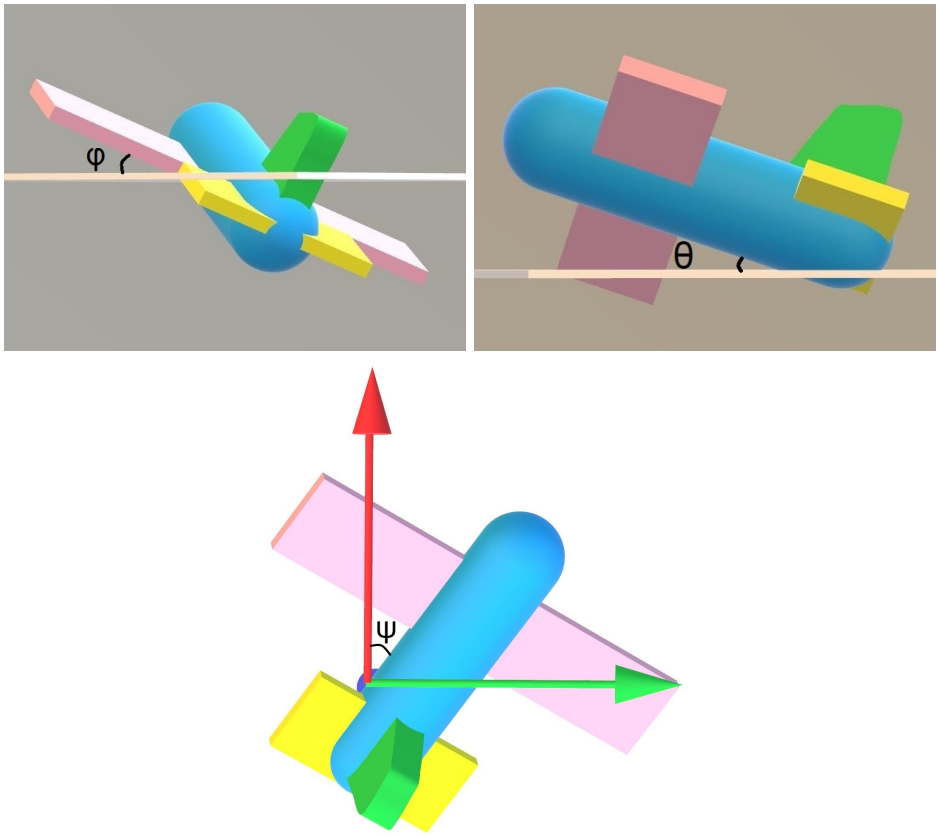

Figure 2.11: Euler Angle

Euler angle attitude representation is commonly used in flight instruments as shown in Fig. 2.10 because it is easy to visualize an attitude by pilots. However, it has a singularity problem when a specific axis goes to 90 degrees. This phenomenon is usually called “gimbal lock” [59].

Commonly the attitude representation in 3D space requires three components of Euler angle: roll(ϕ), pitch(θ) and yaw(ψ). For roll and pitch angles, the reference is the horizontal line. For yaw angle, the reference is usually chosen to be in the geographical north direction or the magnetic north direction as indicated in Fig. 2.11.

2.2.3 Rotation Matrix

As mentioned earlier, a rotation matrix is produced by rotation. The rotation matrix is widely used in robotic field. Furthermore, it has no singularity problem. However, it involves too much computation which limits its application in real time embedded system [37].

The rotation matrix is also called Direct Cosine Matrix (DCM) [60]. The rotation matrix in 3D space is advanced from the rotation matrix in 2D space. Obviously, a 3D rotation can be separated into the following 3 single axis rotations:

$$R_x = \begin{bmatrix} 1 & 0 & 0 \\ 0 & \cos\phi & -\sin\phi \\ 0 & \sin\phi & \cos\phi \end{bmatrix}, R_y = \begin{bmatrix} \cos\theta & 0 & \sin\theta \\ 0 & 1 & 0 \\ -\sin\theta & 0 & \cos\theta \end{bmatrix}, R_z = \begin{bmatrix} \cos\psi & -\sin\psi & 0 \\ \sin\psi & \cos\psi & 0 \\ 0 & 0 & 1 \end{bmatrix} \tag{2.11}$$

which implies that the 3D rotation matrix can be calculated by

$$\begin{aligned} R &= R_z R_y R_x \\ &= \begin{bmatrix} \cos\theta\cos\psi & \cos\psi\sin\theta\sin\phi - \cos\phi\sin\psi & \sin\phi\sin\psi + \cos\phi\sin\theta\cos\psi \\ \cos\theta\sin\psi & \cos\phi\cos\psi + \sin\phi\sin\theta\sin\psi & \cos\phi\sin\theta\sin\psi - \sin\phi\cos\psi \\ -\sin\theta & \sin\phi\cos\theta & \cos\phi\cos\theta \end{bmatrix} \end{aligned} \tag{2.12}$$

The rotation matrix has the following useful properties

$$R^T = R^{-1} \tag{2.13}$$

Due to the basic matrix properties

$$RR^{-1} = R^{-1}R = I_3 \tag{2.14}$$

the rotation matrix satisfies the identities

$$RR^T = R^T R = I_3 \tag{2.15}$$

Let ${}^b_aR$ and ${}^c_bR$ denote a rotation matrix from frame a to frame b and a rotation matrix from frame b to frame c. Then, the rotation matrix from frame a to frame c is given by

$${}^c_aR = {}^c_bR\,{}^b_aR \tag{2.16}$$

The following property can be easily proved.

$$det(R) = \pm 1 \tag{2.17}$$

In this thesis, it is restricted to $det(R) = 1$, which is called proper, so that it meets the requirement of the research. Otherwise, the rotation matrix is improper, which means that the rotation does not represent a rigid body transformation [37].

2.2.4 Unit Quaternion

A unit quaternion is an ideal attitude representation because it avoids the singularity problem meanwhile it doesn't involve too much computation because it has only four components [61]. However, the unit quaternion representation is the most difficult representation to understand and it is basically impossible for human to visualize an attitude from a unit quaternion. So the experimental results based on the unit quaternion representation will be converted to the representation with Euler angles.

The unit quaternion representation is based on the fact that any rigid body rotation can be expressed by a single rotation around a fixed axis [9, 62]. Generally, a quaternion is a hyper complex number with three imaginary parts. Mathematically, a quaternion can be written as [63]

$$Q = q_0 + q_1 i_1 + q_2 i_2 + q_3 i_3 \tag{2.18}$$

Like traditional complex numbers, it obeys

$$i_k^2 = -1 \quad k = 1, 2, 3 \tag{2.19}$$

In this thesis, the basic representation for a quaternion is a vector array with 4 components, as shown below.

$$Q = \begin{bmatrix} q_0 \\ \mathbf{q} \end{bmatrix} = \begin{bmatrix} q_0 \\ q_1 \\ q_2 \\ q_3 \end{bmatrix} = \begin{bmatrix} \cos\frac{\mu}{2} \\ \mathbf{k}\sin\frac{\mu}{2} \end{bmatrix} \tag{2.20}$$

where μ is the rotation angle about the axis defined by unit vector $\mathbf{k}$, q_0 is called the scalar part of Q and $\mathbf{q}$ is called the vector part of Q [61, 64, 65].

The inverse of a quaternion is defined as

$$Q^{-1} = \begin{bmatrix} q_0 \\ -\mathbf{q} \end{bmatrix} \tag{2.21}$$

The norm of a quaternion is given by

$$\|Q\| = \sqrt{q_0^2 + q_1^2 + q_2^2 + q_3^2} \tag{2.22}$$

The basic property for a unit quaternion is the norm of itself equal to 1 [66], that is,

$$q_0^2 + q_1^2 + q_2^2 + q_3^2 = 1 \tag{2.23}$$

Let P and Q represent two quaternions defined by

$$P = \begin{bmatrix} p_0 \\ \mathbf{p} \end{bmatrix} \quad Q = \begin{bmatrix} q_0 \\ \mathbf{q} \end{bmatrix} \tag{2.24}$$

Then, the product of the quaternions P and Q is defined as

$$P \odot Q = \begin{bmatrix} p_0 q_0 - \mathbf{p}^T \mathbf{q} \\ q_0 \mathbf{p} + p_0 \mathbf{q} + \mathbf{p} \times \mathbf{q} \end{bmatrix} \tag{2.25}$$

On the other hand, the error between the quaternions P and Q can be determined by $Q^{-1} \odot P$, that is,

$$\begin{aligned} Q_e &= Q^{-1} \odot P \\ &= \begin{bmatrix} p_0 q_0 + \mathbf{p}^T \mathbf{q} \\ q_0 \mathbf{p} - p_0 \mathbf{q} - \mathbf{q} \times \mathbf{p} \end{bmatrix} \\ &= \begin{bmatrix} p_0 q_0 + p_1 q_1 + p_2 q_2 + p_3 q_3 \\ p_1 q_0 - p_0 q_1 - p_3 q_2 + p_2 q_3 \\ p_2 q_0 + p_3 q_1 - p_0 q_2 - p_1 q_3 \\ p_3 q_0 - p_2 q_1 + p_1 q_2 - p_0 q_3 \end{bmatrix} \end{aligned} \tag{2.26}$$

The identity quaternion is defined as $Q_I = \begin{bmatrix} 1 & 0 & 0 & 0 \end{bmatrix}^T$. Normally, an attitude represented by Q_I means that the vehicle is levelled and the nose of the vehicle points to the north. Also, if a quaternion error is Q_I, then there's no error.

It is easy to prove that

$$Q^{-1} \odot Q = Q \odot Q^{-1} = Q_I \tag{2.27}$$

(2.27) means that there's no error between Q and Q (Q^{-1} and Q^{-1}).

2.2.5 Conversions among Three Representations

In the thesis, all of three attitude representations are used. So the conversions among these three types of representations are important and frequently used.

Euler angle to unit quaternion representation

$$Q = \begin{bmatrix} q_0 \\ q_1 \\ q_2 \\ q_3 \end{bmatrix} = \begin{bmatrix} \cos\frac{\phi}{2}\cos\frac{\theta}{2}\cos\frac{\psi}{2} + \sin\frac{\phi}{2}\sin\frac{\theta}{2}\sin\frac{\psi}{2} \\ -\cos\frac{\phi}{2}\sin\frac{\theta}{2}\sin\frac{\psi}{2} + \sin\frac{\phi}{2}\cos\frac{\theta}{2}\cos\frac{\psi}{2} \\ \cos\frac{\phi}{2}\sin\frac{\theta}{2}\cos\frac{\psi}{2} + \sin\frac{\phi}{2}\cos\frac{\theta}{2}\sin\frac{\psi}{2} \\ \cos\frac{\phi}{2}\cos\frac{\theta}{2}\sin\frac{\psi}{2} - \sin\frac{\phi}{2}\sin\frac{\theta}{2}\cos\frac{\psi}{2} \end{bmatrix} \tag{2.28}$$

Unit quaternion to Euler angle representation

$$\begin{bmatrix} \phi \\ \theta \\ \psi \end{bmatrix} = \begin{bmatrix} atan2\left(2\left(q_0q_1+q_2q_3\right), 1-2\left(q_1^2+q_2^2\right)\right) \\ asin\left(2\left(q_0q_2-q_3q_1\right)\right) \\ atan2\left(2\left(q_0q_3+q_1q_2\right), 1-2\left(q_2^2+q_3^2\right)\right) \end{bmatrix} \tag{2.29}$$

where $atan2$ denotes the four quadrant inverse tangent, which is developed from $arctan$ function, and $asin$ (also expressed as $arcsin$) represents the inverse sine function.

Euler angle to rotation matrix representation

The expression for conversion from Euler angle to rotation matrix is the same as equation (2.12).

Quaternion to rotation matrix representation

The rotation matrix from the inertial frame to the body frame is

$$\begin{aligned} {}^b_I\mathbf{R} &= I + 2S\left(q\right)^2 - 2q_0S\left(q\right) \\ &= \begin{bmatrix} 1 & 0 & 0 \\ 0 & 1 & 0 \\ 0 & 0 & 1 \end{bmatrix} + 2\begin{bmatrix} 0 & -q_3 & q_2 \\ q_3 & 0 & -q_1 \\ -q_2 & q_1 & 0 \end{bmatrix}\begin{bmatrix} 0 & -q_3 & q_2 \\ q_3 & 0 & -q_1 \\ -q_2 & q_1 & 0 \end{bmatrix} - 2q_0\begin{bmatrix} 0 & -q_3 & q_2 \\ q_3 & 0 & -q_1 \\ -q_2 & q_1 & 0 \end{bmatrix} \\ &= \begin{bmatrix} -2q_2^2-2q_3^2+1 & 2q_0q_3+2q_1q_2 & 2q_1q_3-2q_0q_2 \\ 2q_1q_2-2q_0q_3 & -2q_1^2-2q_3^2+1 & 2q_0q_1+2q_2q_3 \\ 2q_0q_2+2q_1q_3 & 2q_2q_3-2q_0q_1 & -2q_1^2-2q_2^2+1 \end{bmatrix} \end{aligned} \tag{2.30}$$

The rotation matrix from the body frame to the inertial frame is [65]

$$\begin{aligned} {}^I_b\mathbf{R} &= I + 2S\left(q\right)^2 + 2q_0S\left(q\right) \\ &= \begin{bmatrix} 1 & 0 & 0 \\ 0 & 1 & 0 \\ 0 & 0 & 1 \end{bmatrix} + 2\begin{bmatrix} 0 & -q_3 & q_2 \\ q_3 & 0 & -q_1 \\ -q_2 & q_1 & 0 \end{bmatrix}\begin{bmatrix} 0 & -q_3 & q_2 \\ q_3 & 0 & -q_1 \\ -q_2 & q_1 & 0 \end{bmatrix} + 2q_0\begin{bmatrix} 0 & -q_3 & q_2 \\ q_3 & 0 & -q_1 \\ -q_2 & q_1 & 0 \end{bmatrix} \\ &= \begin{bmatrix} -2q_2^2-2q_3^2+1 & 2q_1q_2-2q_0q_3 & 2q_0q_2+2q_1q_3 \\ 2q_0q_3+2q_1q_2 & -2q_1^2-2q_3^2+1 & 2q_2q_3-2q_0q_1 \\ 2q_1q_3-2q_0q_2 & 2q_0q_1+2q_2q_3 & -2q_1^2-2q_2^2+1 \end{bmatrix} \end{aligned} \tag{2.31}$$

Unless specially indicated, in this thesis, $\mathbf{R}$ stands for ${}^b_I\mathbf{R}$. In other words, all the rotation matrix representations of attitude are from the inertial frame to the body fixed frame.

Chapter 3

Experimental Platform

The experimental platform for this thesis is based on a popular racing quadrotor QAV250, as indicated in Fig. 3.1.

Figure 3.1: Experimental Platform

3.1 Mechanical Frame

The main frame of the quadrotor is in "x" shape. Unlike the quadrotor in "+" shape, its stability performace is better. Also, an "x" shape quadrotor can be converted from a "+" shape without any mechanical change.

3.2 Radio Control System

Figure 3.2: Spektrum DX8 G2 Radio Control System

The Spektrum Radio Control (RC) system, as shown in Fig. 3.2, is used to remote control the quadrotor. It is widely used in the aeromodelling field as well as micro UAV field. It is featured with DSMX protocol which is of excellent reliability and performance.

3.3 Motors

Figure 3.3: Tarot MT2204 BLDC Motor

Four BLDC motor, as displayed in Fig. 3.3, are used for actuating the quadrotor, which have a lot of advantages over traditional Direct Current (DC) brushed motors. Without contacts for brush, the BLDC motor becomes more efficient because the friction caused by electrical brush is avoided. This feature also increases the system reliability by reducing electrical contact components. The drawbacks of the BLDC motors are mainly related to cost. Since it has nonlinear characteristics and it is driven by 3 phase Alternating Current

(AC) power, a brushless Electronic Speed Control (ESC) must be used to regulate the motor speed. Table 3.1 shows some important specifications of the motors used in the thesis. For detailed information, refer to [67].

Table 3.1: Tarot MT2204 2300KV Motor Specification

Propeller	KV(RPM/V)	Max Current	Cell Count	Connector
6045	2300KV	13A	2-3S LiPo	5mm Bullet

3.4 ESC

Figure 3.4: EMAX BLheli 12A ESC

ESC is basically a BLDC motor driver as shown in Fig. 3.4. Its main function is to control the output of a BLDC motor. According to different applications, the output can be speed, power, torque, etc. The ESC used by quadrotor is actually a torque controller. Meanwhile, it can be a speed controller in other researches [9, 56]. It depends on the settings for ESC. Generally, the task of ESC is to convert the signal from the flight controller and DC battery power to a three phase driving current for the BLDC motor. Moreover, it is able to convert the high voltage from the battery to 5V as a power for the flight controller and other low voltage equipment. The relationship between ESC input signal and output thrust of the power assembly is nearly linear. Some experiments were also carried out to prove this feature (for test results, see Appendix G).

3.5 Battery

Battery is the power source for the quadrotor. As shown in Fig. 3.5, Lithium Polymer (LiPo) battery is an ideal battery for quadrotors and other small UAVs. Compared to the Nickelmetal hydride battery or Nickelcadmium battery, it is much lighter with the same

Figure 3.5: LiPo Battery

capacity. Another crucial advantage of LiPo battery is the high discharge rate. This feature enables the battery to supply enough power to the motors which can lift up the quadrotor. However, LiPo battery also has some disadvantages. The most notable disadvantage of LiPo battery is that it is flammable. To ensure safety, LiPo battery should always be stored in a cool place within a fireproof bag.

3.6 Flight Controller

In order to do a real flight test, two types of flight controller boards are used.

3.6.1 APM 2.8 Autopilot System

Arduino Pilot Mega (APM) is a mature open sourced autopilot system, which is displayed in Fig. 3.6. It is based on an Atmel AVR 8 bit microprocessor. The main microprocessor is Atmega 2560. Also thanks to Arduino open sourced system, the programming of the microprocessor becomes relatively easy. However, due to the limited functionalities of Arduino, APM development team gave up using Arduino and switched to GNU Compiler Collection (GCC) open sourced compiler. Also, due to the limited performance of the microprocessor, since ArduCopter version 3.3, APM development team finally gave up using AVR based board and switched to faster hardware like Pixhawk, etc.

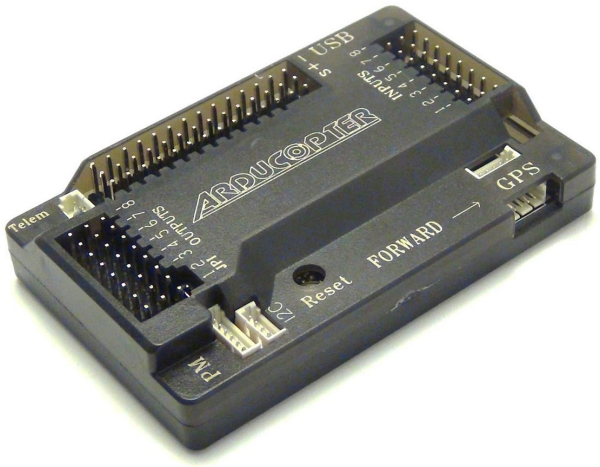

Figure 3.6: APM 2.8 Autopilot System

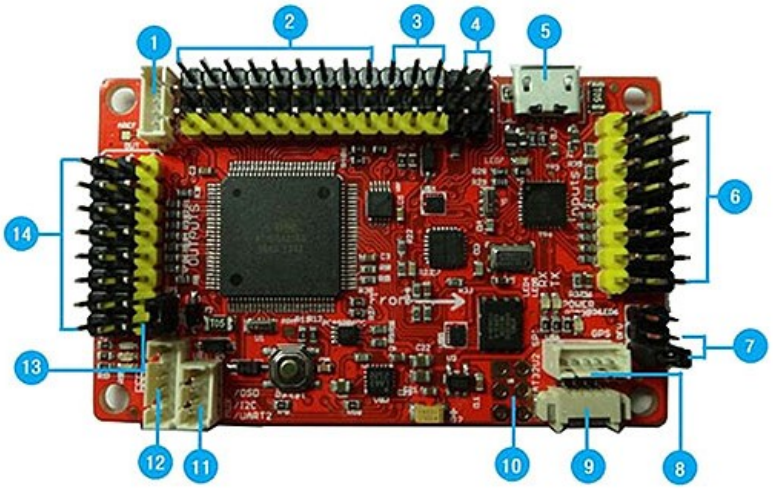

1. Data Transmission Port
2. Analog Sensor Port
3. Autostability Gimbal Output
4. Atmega2560 SPI Online Programming Port
(Be Useful For Optical Flow Sensor)
5. USB Port
6. Remote Control Input
7. Function Selection Jumper
8. GPS Port
9. 12c External Compass Port
10. Atmega32U2 SPI Online Programming Port
11. Multifunction Configurable Mux Port
(OSD is The Defaulted Output)
12. Current Voltage Port
13. ESC Power Supply Selection Jumper
14. ESC Output Port

Figure 3.7: APM 2.8 Circuit Board with Instructions

Fig. 3.7 is a picture of the circuit board of APM with instructions [68]. APM 2.8 is not an original version of APM. Most of its design is the same as APM 2.6. The main difference is that the APM 2.8 adds the onboard magnetometer and has more choices of power supply. These features are more suitable to the experimental environments. So, the APM 2.8 is

chosen instead of the APM 2.6.

3.6.2 Pixhawk 2.4.8 Autopilot System

Figure 3.8: Pixhawk Autopilot System

To overcome the hardware limit of APM autopilot system, Pixhawk autopilot system in Fig. 3.8 is used. Equiped with a 32 bit ARM Cortex M4 based STM32F4 series microprocessor, running at 168 MHz, its performance is much better than the APM autopilot system. In this thesis, the main Central Processing Unit (CPU) for the Pixhawk version 2.4.8 is STM32F427VI by STMicroelectronics, for the detailed specification refer to 3.2 [69]. In addition to the main controller, there is a failsafe controller on Pixhawk board. The failsafe controller is a 32 bit ARM Cortex M3 based STM32F1 series microprocessor. The main frequency is 72 MHz, which is still much faster than the AVR controller.

Also the software support of Ardupilot library ensures that the old version of code from APM can be easily transferred to the new hardware platform. In addition to Ardupilot library, the original PX4 library can be used. In fact, the Ardupilot library contains a part of PX4 library, mainly for the hardware drivers.

Unlike the AVR based APM board, Pixhawk runs with a Real Time Operation System (RTOS) called NuttX. It optimises the performance and is able to run multi threads.

Table 3.2: STM32F427VI Specification

Core	ARM 32-bit Cortex-M4 CPU with FPU
Frequencty	up to 180 MHz
Speed	1.25 DMIPS/MHz
Flash Memory	2 MB
RAM	256+4 KB of SRAM including 64 KB CCM data RAM
I2C	3
USARTs	4
SPIs	6
SAI	1
CAN	2
ADC	3 × 12 bit, 2.4 MSPS, up to 24 channels
DAC	2 × 12 bit

Sensors

Due to the higher performance of the main controller and the increased number of interfaces, Pixhawk can accommodate more sensors. Table 3.3 lists the on-board sensors of Pixhawk [70]. For instance, there are 2 sets of IMU on the Pixhawk board. In addition, Pixhawk can be externally connected to 2 GPS modules and 1 magnetometer.

Table 3.3: Pixhawk Onboard Sensors

1st IMU	ST Micro L3GD20H 16 bit gyroscope ST Micro LSM303D 14 bit accelerometer / magnetometer
2nd IMU	Invensense MPU 6000 3-axis accelerometer/gyroscope
Barometer	MEAS MS5611

Interfaces

In addition to the low level interfaces inherited from STM32F427, Pixhawk also supports most medium level and commercial level interfaces, such as Spektrum DSM/DSM2/DSM-X satellite compatible input interface, Futaba S.BUS compatible input and output interface, Pulse Position Modulation (PPM) sum signal input interface and Received Signal Strength Indicator (RSSI) (Pulse Width Modulation (PWM) or voltage) input interface [70].

Chapter 4

Design of the Proposed Controller

In this Chapter, two types of neural-network based adaptive controllers are designed using backstepping technique. As the basic of the controller derivation, the dynamic model of a quadrotor UAV is concerned firstly. Then, the adaptive controller is developed with four steps. It shows a good performance in simulation. However, the practical experiment results are not as good as expected. So, the 2nd approach for controller design is conducted, which consists of two steps. A better performance is observed from experimental tests. To avoid the singularity problem, the controller design is carried out on the model with unit quaternion representation.

4.1 Dynamics of a Quadrotor UAV

In this section, the dynamic model is presented. Because the error of the attitude in the unit quaternion representation is not a simple subtraction as in the Euler angle representation, the dynamics of the quaternion error is also introduced.

4.1.1 Modelling

The dynamics of a quadrotor consists of translational motion and rotational motion. After some comparisons among the models described in [9, 36, 37, 55, 56, 71–74], the following dynamic model is chosen in this thesis.

$$\dot{\mathbf{P}} = \mathbf{V} \tag{4.1}$$

$$\dot{\mathbf{V}} = g\mathbf{e}_3 - \frac{1}{m}T\mathbf{R}^T\mathbf{e_3} \tag{4.2}$$

$$\dot{Q} = \frac{1}{2}Q \odot Q_\omega \tag{4.3}$$

$$\dot{\omega} = \mathbf{I}_f^{-1}\left(-\omega \times (\mathbf{I}_f \cdot \omega) + \tau\right) \tag{4.4}$$

where $\mathbf{P}$ denotes the position, $\mathbf{V}$ represents the translational velocity, g denotes the gravity acceleration, $\mathbf{e}_3$ is the unit vector defined as $\mathbf{e}_3 = \begin{bmatrix} 0 & 0 & 1 \end{bmatrix}^T$, T is the system thrust, m denotes the mass, $\mathbf{R}$ and Q stand for the attitude in rotation matrix and unit quaternion representation respectively, $Q_\omega = \begin{bmatrix} 0 & \omega^T \end{bmatrix}^T$, $\omega = \begin{bmatrix} \omega_1 & \omega_2 & \omega_3 \end{bmatrix}^T$ denotes the angular velocity in the body fixed frame, $\mathbf{I_f}$ represents the moment of inertia, and τ denotes the torque in the body fixed frame. Note that (4.3) describes the dynamics of the attitude in unit quaternion representation, which can be modeled by the rotation matrix as follows:

$$\dot{\mathbf{R}}^T = \mathbf{R}^T S(\omega) \tag{4.5}$$

where $S(\omega)$ stands for the skew matrix for vector ω defined by

$$S(\omega) = \begin{bmatrix} 0 & -\omega_3 & \omega_2 \\ \omega_3 & 0 & -\omega_1 \\ -\omega_2 & \omega_1 & 0 \end{bmatrix} \tag{4.6}$$

The detailed derivation for (4.5) can be found in [75].

4.1.2 Dynamics for Quaternion Error

Let Q and Q_d denote the actual and desired attitudes in unit quaternion representation. Then, according to (2.26), the quaternion error between Q_d and Q is defined as

$$\begin{aligned} Q_e &= Q_d^{-1} \odot Q \\ &= \begin{bmatrix} q_{e0} \\ q_e \end{bmatrix} = \begin{bmatrix} q_{d0}q_0 + q_{d1}q_1 + q_{d2}q_2 + q_{d3}q_3 \\ q_{d1}q_0 - q_{d0}q_1 - q_{d3}q_2 + q_{d2}q_3 \\ q_{d2}q_0 + q_{d3}q_1 - q_{d0}q_2 - q_{d1}q_3 \\ q_{d3}q_0 - q_{d2}q_1 + q_{d1}q_2 - q_{d0}q_3 \end{bmatrix} \end{aligned} \tag{4.7}$$

According to [55]

$$\dot{Q}_e = \begin{bmatrix} -\frac{1}{2}q_e^T(\omega - \omega_d) \\ \frac{1}{2}\left(q_{e0}I_3(\omega - \omega_d) + S(q_e)(\omega + \omega_d)\right) \end{bmatrix} \tag{4.8}$$

4.2 Four Step Position Tracking Control with Neural-Network

Inspired by [36,37], where the backstepping controller design method was already successfully used in attitude control of a quadrotor system, it is natural to extend the backstepping design approach to the position tracking control problem. By backstepping technique, the research on position tracking control with Euler angle representation was conducted in [54]. In this section, an adaptive position tracking controller is proposed by using the backstepping method, together with the universal neural-network approximator.

Let x_d, y_d, z_d and x, y, z denote the coordinates of the desired and actual position in the inertial frame. Then, the position error is defined by the following equation.

$$\mathbf{e}_1 = \mathbf{P}_d - \mathbf{P} \tag{4.9}$$

where $\mathbf{P}_d = \begin{bmatrix} x_d & y_d & z_d \end{bmatrix}^T$ denotes the desired position, $\mathbf{P} = \begin{bmatrix} x & y & z \end{bmatrix}^T$ denotes the actual position.

Step 1. Position Tracking

Define a positive definite Lyapunov candidate

$$V_1 = \frac{1}{2} K_p \mathbf{e}_1^T \mathbf{e}_1 \tag{4.10}$$

where K_p is a positive parameter, which is introduced to adjust the amplitude of the control signals.

By differentiating (4.10), it yields

$$\dot{V}_1 = K_p \mathbf{e}_1^T \dot{\mathbf{e}}_1 \tag{4.11}$$

Substituting (4.9) into (4.11), it follows that

$$\dot{V}_1 = K_p \mathbf{e}_1^T \left(\dot{\mathbf{P}}_d - \dot{\mathbf{P}} \right) \tag{4.12}$$

It follows from (4.1) that $\dot{\mathbf{P}} = \mathbf{V}$. Hence, (4.12) can be rewritten as

$$\dot{V}_1 = K_p \mathbf{e}_1^T \left(\dot{\mathbf{P}}_d - \mathbf{V} \right) \tag{4.13}$$

$$= K_p \mathbf{e}_1^T \left(\dot{\mathbf{P}}_d - \mathbf{V} + \alpha_1 - \alpha_1 \right) \tag{4.14}$$

$$= K_p \mathbf{e}_1^T \left(\dot{\mathbf{P}}_d - \alpha_1 \right) + K_p \mathbf{e}_1^T \left(-\mathbf{V} + \alpha_1 \right) \tag{4.15}$$

where α_1 is a virtual velocity. α_1 can be chosen as

$$\alpha_1 = \mathbf{K}_1 \mathbf{e}_1 + \dot{\mathbf{P}}_d \tag{4.16}$$

so that $\dot{V}_1$ becomes

$$\dot{V}_1 = -K_p \mathbf{e}_1^T \mathbf{K}_1 \mathbf{e}_1 + K_p \mathbf{e}_1^T \left(-\mathbf{V} + \alpha_1 \right) \tag{4.17}$$

where $\mathbf{K}_1$ is a positive matrix which has to be tuned in order to achieve a satisfatory control performance. It is clear seen that $\dot{V}_1 = -K_p \mathbf{e}_1^T \mathbf{K}_1 \mathbf{e}_1$ is negative definite if $\mathbf{V} = \alpha_1$.

Step 2. Translational Velocity Tracking

The error between the virtual velocity and actual velocity can be defined as

$$\mathbf{e}_2 = \alpha_1 - \mathbf{V} \tag{4.18}$$

and the derivative of the error $\mathbf{e}_2$ satisfies

$$\dot{\mathbf{e}}_2 = \dot{\alpha}_1 - \dot{\mathbf{V}} \tag{4.19}$$

Define a Lyapunov function candidate

$$V_2 = V_1 + \frac{1}{2}\mathbf{e}_2^T\mathbf{e}_2 \tag{4.20}$$

Differentiating (4.20) gives

$$\dot{V}_2 = \dot{V}_1 + \mathbf{e}_2^T\dot{\mathbf{e}}_2 \tag{4.21}$$

By substituting (4.19) to (4.21), taking (4.17) and (4.18) into consideration, it follows that

$$\begin{aligned}
\dot{V}_2 &= \dot{V}_1 + \mathbf{e}_2^T\left(\dot{\alpha}_1 - \dot{\mathbf{V}}\right) \\
&= -K_p\mathbf{e}_1^T\mathbf{K}_1\mathbf{e}_1 + K_p\mathbf{e}_1^T\mathbf{e}_2 + \mathbf{e}_2^T\left(\dot{\alpha}_1 - \dot{\mathbf{V}}\right) \\
&= -K_p\mathbf{e}_1^T\mathbf{K}_1\mathbf{e}_1 + \mathbf{e}_2^T\left(\dot{\alpha}_1 - \dot{\mathbf{V}} + \mathbf{K_p}\mathbf{e}_1\right) \\
&= -K_p\mathbf{e}_1^T\mathbf{K}_1\mathbf{e}_1 + \mathbf{e}_2^T\left(\dot{\alpha}_1 - \dot{\mathbf{V}} + \mathbf{K_p}\mathbf{e}_1 - \mu_d + \mu_d\right) \\
&= -K_p\mathbf{e}_1^T\mathbf{K}_1\mathbf{e}_1 + \mathbf{e}_2^T\left(\dot{\alpha}_1 + \mathbf{K_p}\mathbf{e}_1 - \mu_d - \dot{\mathbf{V}} + \mu_d\right) \\
&= -K_p\mathbf{e}_1^T\mathbf{K}_1\mathbf{e}_1 + \mathbf{e}_2^T\left(\dot{\alpha}_1 + \mathbf{K_p}\mathbf{e}_1 - \mu_d\right) + \mathbf{e}_2^T\left(-\dot{\mathbf{V}} + \mu_d\right)
\end{aligned} \tag{4.22}$$

where μ_d represents the virtual acceleration, which can be set to

$$\mu_d = K_p\mathbf{e}_1 + \mathbf{K}_2\mathbf{e}_2 + \dot{\alpha}_1 \tag{4.23}$$

where $\mathbf{K}_2$ is a positive matrix which has to be tuned for a good control performance.

Replacing μ_d with (4.23) for the second term in (4.22) produces

$$\dot{V}_2 = -K_p\mathbf{e}_1^T\mathbf{K}_1\mathbf{e}_1 - \mathbf{e}_2^T\mathbf{K}_2\mathbf{e}_2 + \mathbf{e}_2^T\left(-\dot{\mathbf{V}} + \mu_d\right) \tag{4.24}$$

Let μ denote the actual acceleration. Then, it follows from (4.2) that $\dot{\mathbf{V}} = \mu$ and

$$\mu = g\mathbf{e}_3 - \frac{1}{m}T\mathbf{R}^T\mathbf{e}_3 \tag{4.25}$$

from which (4.24) can be rewritten as

$$\dot{V}_2 = -K_p\mathbf{e}_1^T\mathbf{K}_1\mathbf{e}_1 - \mathbf{e}_2^T\mathbf{K}_2\mathbf{e}_2 + \mathbf{e}_2^T\left(-\mu + \mu_d\right) \tag{4.26}$$

Define the acceleration error as

$$\tilde{\mu} = -\mu + \mu_d \tag{4.27}$$

Then, by substituting (4.27) into (4.26), it produces

$$\dot{V}_2 = -K_p\mathbf{e}_1^T\mathbf{K}_1\mathbf{e}_1 - \mathbf{e}_2^T\mathbf{K}_2\mathbf{e}_2 + \mathbf{e}_2^T\tilde{\mu} \tag{4.28}$$

According to (4.25), the acceleration μ is related to the attitude $\mathbf{R}$ or Q. Similarly, associated with the virtual acceleration μ_d, there is a virtual quaternion Q_d, which can be determined from the relation

$$\mu_d{=}g\mathbf{e}_3 - \frac{1}{m}T\mathbf{R}_d^T\mathbf{e}_3 \tag{4.29}$$

where $\mathbf{R}_d$ is the rotation matrix corresponding to Q_d and can be determined by

$$\mathbf{R}_d = \begin{bmatrix} -2q_{d2}^2 - 2q_{d3}^2 + 1 & 2q_{d0}q_{d3} + 2q_{d1}q_{d2} & 2q_{d1}q_{d3} - 2q_{d0}q_{d2} \\ 2q_{d1}q_{d2} - 2q_{d0}q_{d3} & -2q_{d1}^2 - 2q_{d3}^2 + 1 & 2q_{d0}q_{d1} + 2q_{d2}q_{d3} \\ 2q_{d0}q_{d2} + 2q_{d1}q_{d3} & 2q_{d2}q_{d3} - 2q_{d0}q_{d1} & -2q_{d1}^2 - 2q_{d2}^2 + 1 \end{bmatrix} \tag{4.30}$$

Replacing $\mathbf{R}_d$ in (4.29) results in

$$\mu_d{=}g\begin{bmatrix} 0 \\ 0 \\ 1 \end{bmatrix} - \frac{1}{m}T\begin{bmatrix} -2q_{d2}^2 - 2q_{d3}^2 + 1 & 2q_{d0}q_{d3} + 2q_{d1}q_{d2} & 2q_{d1}q_{d3} - 2q_{d0}q_{d2} \\ 2q_{d1}q_{d2} - 2q_{d0}q_{d3} & -2q_{d1}^2 - 2q_{d3}^2 + 1 & 2q_{d0}q_{d1} + 2q_{d2}q_{d3} \\ 2q_{d0}q_{d2} + 2q_{d1}q_{d3} & 2q_{d2}q_{d3} - 2q_{d0}q_{d1} & -2q_{d1}^2 - 2q_{d2}^2 + 1 \end{bmatrix}^T \begin{bmatrix} 0 \\ 0 \\ 1 \end{bmatrix}$$

which can be rewritten as

$$\begin{bmatrix} \mu_{d1} \\ \mu_{d2} \\ \mu_{d3} \end{bmatrix} = \begin{bmatrix} -\frac{T}{m}\left(2q_{d2}q_{d0} + 2q_{d3}q_{d1}\right) \\ -\frac{T}{m}\left(2q_{d2}q_{d3} - 2q_{d0}q_{d1}\right) \\ g + \frac{T}{m}\left(2q_{d2}^2 + 2q_{d1}^2 - 1\right) \end{bmatrix} \tag{4.31}$$

By setting $q_{d3} = 0$, according to Appendix C, the followings can be obtained.

$$\begin{aligned} q_{d0} &= \sqrt{\frac{1}{2}\left(1 - \left(\mu_{d3} - g\right)\frac{m}{T}\right)} \\ q_{d1} &= \frac{\mu_{d2}}{q_{d0}}\frac{m}{2T} \\ q_{d2} &= -\frac{\mu_{d1}}{q_{d0}}\frac{m}{2T} \\ q_{d3} &= 0 \end{aligned}$$

As a result, $\tilde{\mu} = -\mu + \mu_d$ can be expressed as $\tilde{\mu} = W^T\mathbf{q}_e$ [55], where W is given in Appendix A. Therefore, (4.28) can be rewritten as

$$\begin{aligned} \dot{V}_2 &= -K_p\mathbf{e}_1^T\mathbf{K}_1\mathbf{e}_1 - \mathbf{e}_2^T\mathbf{K}_2\mathbf{e}_2 + \mathbf{e}_2^T(W^T\mathbf{q}_e) \\ &= -K_p\mathbf{e}_1^T\mathbf{K}_1\mathbf{e}_1 - \mathbf{e}_2^T\mathbf{K}_2\mathbf{e}_2 + \mathbf{q}_e^TW\mathbf{e}_2 \end{aligned} \tag{4.32}$$

Step 3. Attitude Tracking

Define a Lyapunov candidate V_3 as follows:

$$V_3 = V_2 + \mathbf{q}_e^T\mathbf{q}_e + (q_{e0} - 1)^2 \tag{4.33}$$

Time derivative of (4.33) is

$$\dot{V}_3 = \dot{V}_2 + 2\mathbf{q}_e^T \dot{\mathbf{q}}_e + 2(q_{e0} - 1)\dot{q}_{e0} \tag{4.34}$$

Substituting (4.32) into (4.34) yields

$$\dot{V}_3 = -K_p \mathbf{e}_1^T \mathbf{K}_1 \mathbf{e}_1 - \mathbf{e}_2^T \mathbf{K}_2 \mathbf{e}_2 + \mathbf{q}_e^T W \mathbf{e}_2 + 2\dot{\mathbf{q}}_e^T \mathbf{q}_e + 2(q_{e0} - 1)\dot{q}_{e0} \tag{4.35}$$

By flipping the term $2\dot{\mathbf{q}}_e^T \mathbf{q}_e$ in (4.35), it follows that

$$\dot{V}_3 = -K_p \mathbf{e}_1^T \mathbf{K}_1 \mathbf{e}_1 - \mathbf{e}_2^T \mathbf{K}_2 \mathbf{e}_2 + \mathbf{q}_e^T W \mathbf{e}_2 + 2\mathbf{q}_e^T \dot{\mathbf{q}}_e + 2(q_{e0} - 1)\dot{q}_{e0} \tag{4.36}$$

The following equation can be obtained by substituting (4.8) into (4.36).

$$\begin{aligned} \dot{V}_3 = & -K_p \mathbf{e}_1^T \mathbf{K}_1 \mathbf{e}_1 - \mathbf{e}_2^T \mathbf{K}_2 \mathbf{e}_2 + \mathbf{q}_e^T W \mathbf{e}_2 \\ & + 2\mathbf{q}_e^T \left(\frac{1}{2} \left(q_{e0} \left(\omega - \omega_d \right) + S\left(\mathbf{q}_e \right) \left(\omega + \omega_d \right) \right) \right) + 2(q_{e0} - 1) \frac{1}{2} \mathbf{q}_e^T \left(\omega_d - \omega \right) \end{aligned} \tag{4.37}$$

where $\omega_d = M\left(\mu_d\right) \dot{\mu}_d$, for details refer to the Appendix D.

By simplifying the equation (4.37), it produces

$$\dot{V}_3 = -K_p \mathbf{e}_1^T \mathbf{K}_1 \mathbf{e}_1 - \mathbf{e}_2^T \mathbf{K}_2 \mathbf{e}_2 + \mathbf{q}_e^T W \mathbf{e}_2 + q_{e0} \mathbf{q}_e^T \left(\omega - \omega_d \right) + \mathbf{q}_e^T S\left(\mathbf{q}_e \right) \left(\omega + \omega_d \right) + (1 - q_{e0}) \mathbf{q}_e^T \left(\omega - \omega_d \right) \tag{4.38}$$

Combining the 4th term and the last term of (4.38) produces

$$\dot{V}_3 = -K_p \mathbf{e}_1^T \mathbf{K}_1 \mathbf{e}_1 - \mathbf{e}_2^T \mathbf{K}_2 \mathbf{e}_2 + \mathbf{q}_e^T W \mathbf{e}_2 + \mathbf{q}_e^T \left(\omega - \omega_d \right) + \mathbf{q}_e^T S\left(\mathbf{q}_e \right) \left(\omega + \omega_d \right) \tag{4.39}$$

According to Appendix B, $\mathbf{q}_e^T S\left(\mathbf{q}_e \right) \left(\omega + \omega_d \right) = 0$, which means that $\dot{V}_3$ can be expressed as

$$\dot{V}_3 = -K_p \mathbf{e}_1^T \mathbf{K}_1 \mathbf{e}_1 - \mathbf{e}_2^T \mathbf{K}_2 \mathbf{e}_2 + \mathbf{q}_e^T W \mathbf{e}_2 + \mathbf{q}_e^T \omega - \mathbf{q}_e^T \omega_d \tag{4.40}$$

By introducing ω_α as virtual control for angular velocity ω, (4.40) can be put into the following form.

$$\dot{V}_3 = -K_p \mathbf{e}_1^T \mathbf{K}_1 \mathbf{e}_1 - \mathbf{e}_2^T \mathbf{K}_2 \mathbf{e}_2 + \mathbf{q}_e^T \left(\omega - \omega_\alpha \right) + \mathbf{q}_e^T \omega_\alpha + \mathbf{q}_e^T W \mathbf{e}_2 - \mathbf{q}_e^T \omega_d \tag{4.41}$$

Define the angular velocity error ω_e as

$$\omega_e = \omega - \omega_\alpha \tag{4.42}$$

Then, by combining the last three terms in (4.41) and replacing $\omega - \omega_\alpha$ with ω_e in (4.42), the following can be easily verified.

$$\dot{V}_3 = -K_p \mathbf{e}_1^T \mathbf{K}_1 \mathbf{e}_1 - \mathbf{e}_2^T \mathbf{K}_2 \mathbf{e}_2 + \mathbf{q}_e^T \omega_e + \mathbf{q}_e^T \left(\omega_\alpha + W \mathbf{e}_2 - \omega_d \right) \tag{4.43}$$

Set

$$\omega_\alpha + W\mathbf{e}_2 - \omega_d = -\mathbf{K}_3\mathbf{q}_e$$

or

$$\omega_\alpha = -\mathbf{K}_3\mathbf{q}_e - W\mathbf{e}_2 + \omega_d \tag{4.44}$$

where $\mathbf{K}_3$ is a positive matrix to be tuned for a better control performance.

Then, (4.43) becomes

$$\dot{V}_3 = -K_p\mathbf{e}_1^T\mathbf{K}_1\mathbf{e}_1 - \mathbf{e}_2^T\mathbf{K}_2\mathbf{e}_2 - \mathbf{q}_e^T\mathbf{K}_3\mathbf{q}_e + \mathbf{q}_e^T\omega_e \tag{4.45}$$

Step 4. Angular Velocity Tracking

Define a Lyapunov candidate

$$V_4 = V_3 + \frac{1}{2}\omega_e^T\omega_e \tag{4.46}$$

Time derivative of (4.46) is

$$\dot{V}_4 = \dot{V}_3 + \omega_e^T\dot{\omega}_e \tag{4.47}$$

By substituting (4.45) into (4.47), the following can be obtained.

$$\dot{V}_4 = -K_p\mathbf{e}_1^T\mathbf{K}_1\mathbf{e}_1 - \mathbf{e}_2^T\mathbf{K}_2\mathbf{e}_2 - \mathbf{q}_e^T\mathbf{K}_3\mathbf{q}_e + \mathbf{q}_e^T\omega_e + \omega_e^T\dot{\omega}_e \tag{4.48}$$

By subsitituting the time derivative of (4.42) into (4.48), it yields

$$\dot{V}_4 = -K_p\mathbf{e}_1^T\mathbf{K}_1\mathbf{e}_1 - \mathbf{e}_2^T\mathbf{K}_2\mathbf{e}_2 - \mathbf{q}_e^T\mathbf{K}_3\mathbf{q}_e + \mathbf{q}_e^T\omega_e + \omega_e^T\left(\dot{\omega} - \dot{\omega}_\alpha\right) \tag{4.49}$$

It follows from (4.4) and (4.49) that

$$\begin{aligned}\dot{V}_4 &= -K_p\mathbf{e}_1^T\mathbf{K}_1\mathbf{e}_1 - \mathbf{e}_2^T\mathbf{K}_2\mathbf{e}_2 - \mathbf{q}_e^T\mathbf{K}_3\mathbf{q}_e + \omega_e^T\mathbf{q}_e + \omega_e^T\left[I_f^{-1}(-\omega\times(\mathbf{I}_f\cdot\omega)+\tau) - \dot{\omega}_\alpha\right] \\ &= -K_p\mathbf{e}_1^T\mathbf{K}_1\mathbf{e}_1 - \mathbf{e}_2^T\mathbf{K}_2\mathbf{e}_2 - \mathbf{q}_e^T\mathbf{K}_3\mathbf{q}_e + \omega_e^T\left\{\mathbf{q}_e - \dot{\omega}_\alpha + I_f^{-1}\left[-\omega\times(\mathbf{I}_f\cdot\omega)+\tau\right]\right\}\end{aligned} \tag{4.50}$$

In order to introduce the adaptive neural-network method, $I_f^{-1}\left[-\omega\times(\mathbf{I}_f\cdot\omega)+\tau\right]$ in (4.50) can be expanded as follows:

$$I_f^{-1}\left[-\omega\times(\mathbf{I}_f\cdot\omega)+\tau\right] = \begin{bmatrix} \frac{1}{I_x}\left(I_y - I_z\right)\omega_2\omega_3 + \frac{1}{I_x}\tau_1 \\ \frac{1}{I_y}\left(I_z - I_x\right)\omega_1\omega_3 + \frac{1}{I_y}\tau_2 \\ \frac{1}{I_z}\left(I_x - I_y\right)\omega_1\omega_2 + \frac{1}{I_z}\tau_3 \end{bmatrix} \tag{4.51}$$

By substituting (4.51) into (4.50), $\dot{V}_4$ becomes

$$\begin{aligned}
\dot{V}_4 &= -K_p \mathbf{e}_1^T \mathbf{K}_1 \mathbf{e}_1 - \mathbf{e}_2^T \mathbf{K}_2 \mathbf{e}_2 - \mathbf{q}_e^T \mathbf{K}_3 \mathbf{q}_e \\
&+ \omega_e^T \left(\begin{bmatrix} q_{e1} - \dot{\omega}_{\alpha 1} + \frac{1}{I_x}\left(I_y - I_z\right)\omega_2\omega_3 + \frac{1}{I_x}\tau_1 \\ q_{e2} - \dot{\omega}_{\alpha 2} + \frac{1}{I_y}\left(I_z - I_x\right)\omega_1\omega_3 + \frac{1}{I_y}\tau_2 \\ q_{e3} - \dot{\omega}_{\alpha 3} + \frac{1}{I_z}\left(I_x - I_y\right)\omega_1\omega_2 + \frac{1}{I_z}\tau_3 \end{bmatrix} \right) \\
&= -K_p \mathbf{e}_1^T \mathbf{K}_1 \mathbf{e}_1 - \mathbf{e}_2^T \mathbf{K}_2 \mathbf{e}_2 - \mathbf{q}_e^T \mathbf{K}_3 \mathbf{q}_e \\
&+ \omega_{e1} \left(q_{e1} - \dot{\omega}_{\alpha 1} + \frac{1}{I_x}\left(I_y - I_z\right)\omega_2\omega_3 + \frac{1}{I_x}\tau_1 \right) \\
&+ \omega_{e2} \left(q_{e2} - \dot{\omega}_{\alpha 2} + \frac{1}{I_y}\left(I_z - I_x\right)\omega_1\omega_3 + \frac{1}{I_y}\tau_2 \right) \\
&+ \omega_{e3} \left(q_{e3} - \dot{\omega}_{\alpha 3} + \frac{1}{I_z}\left(I_x - I_y\right)\omega_1\omega_2 + \frac{1}{I_z}\tau_3 \right)
\end{aligned} \tag{4.52}$$

It is assumed that I_x, I_y, and I_z are not known. In order to facilitate the estimation of these unknown variables, define

$$\begin{aligned}
\beta_1 &= \frac{1}{I_x} \\
\beta_2 &= \frac{1}{I_y} \\
\beta_3 &= \frac{1}{I_z}
\end{aligned} \tag{4.53}$$

It is also assumed that the following nonlinear terms are unknown.

$$\begin{aligned}
f_1 &= \left(\frac{I_y - I_z}{I_x} \right) \omega_2\omega_3 \\
f_2 &= \left(\frac{I_z - I_x}{I_y} \right) \omega_1\omega_3 \\
f_3 &= \left(\frac{I_x - I_y}{I_z} \right) \omega_1\omega_2
\end{aligned} \tag{4.54}$$

In order to estimate these unknown nonlinearities, three neural network universal approximators are used. The neural network universal approximators are shown as Fig. 4.1, Fig. 4.2 and Fig. 4.3. The number of neural cells can be adjusted. In this thesis, 9 cells are good enough for the expected performance. More cells increase the approximation accuracy, however, it increases computation burden too.

Mathematically, the nonlinear terms can be estimated by the neural networks as shown below.

$$\begin{aligned}
f_1 &= \varrho_1^T \xi_1\left(\omega_2, \omega_3\right) + \varepsilon_1 \\
f_2 &= \varrho_2^T \xi_2\left(\omega_1, \omega_3\right) + \varepsilon_2 \\
f_3 &= \varrho_3^T \xi_3\left(\omega_1, \omega_2\right) + \varepsilon_3
\end{aligned} \tag{4.55}$$

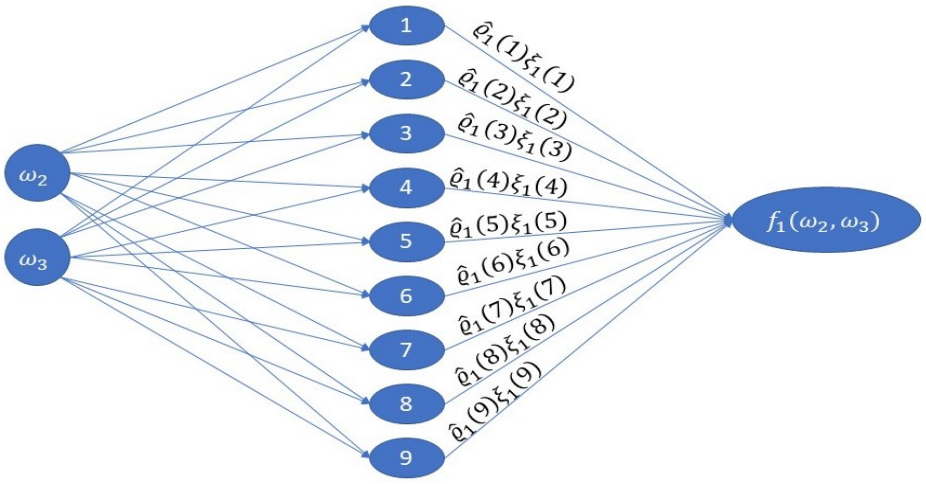

Figure 4.1: Neural Network in Roll Direction

where ξ_1, ξ_2, and ξ_3 are the vector-valued functions of the angular velocities, which are composed of the activation functions of the neural cells in the hidden layer. In this thesis, the activation functions are chosen as the trangular functions. ϱ_1, ϱ_2, and ϱ_3 are the vectors of parameters which represents the weights between the input layer and hidden layer. ϱ_1, ϱ_2, and ϱ_3 are assumed to be unknown and will be estimated online by adaptive laws designed later. ε_1, ε_2, and ε_3 are the estimation errors between the ture value for nonlinar terms and the output value by neural networks. According to the universal approximation theorem, ε_1, ε_2, and ε_3 can be made arbitrarily small, which are considered to be bounded. By using $\hat{\varrho}_1$, $\hat{\varrho}_2$, and $\hat{\varrho}_3$ to estimate ϱ_1, ϱ_2, and ϱ_3 and I_x, I_y, and I_z to estimate I_x, I_y, and I_z, the estimation errors can be used to define the following Lyapunov candidate.

$$\begin{aligned} V_5 = & \frac{1}{2}\left(\varrho_1 - \hat{\varrho}_1\right)^T \Gamma_1 \left(\varrho_1 - \hat{\varrho}_1\right) \\ & + \frac{1}{2}\left(\varrho_2 - \hat{\varrho}_2\right)^T \Gamma_2 \left(\varrho_2 - \hat{\varrho}_2\right) \\ & + \frac{1}{2}\left(\varrho_3 - \hat{\varrho}_3\right)^T \Gamma_3 \left(\varrho_3 - \hat{\varrho}_3\right) \\ & + \frac{1}{2}\lambda_1\beta_1\left(I_x - \hat{I}_x\right)^2 \\ & + \frac{1}{2}\lambda_2\beta_2\left(I_y - \hat{I}_y\right)^2 \\ & + \frac{1}{2}\lambda_3\beta_3\left(I_z - \hat{I}_z\right)^2 \end{aligned} \tag{4.56}$$

where Γ_1, Γ_2, and Γ_3 are positive definite matrices and λ_1, λ_2, and λ_3 are the positive parameters, which can be tuned to obtain a good performance.

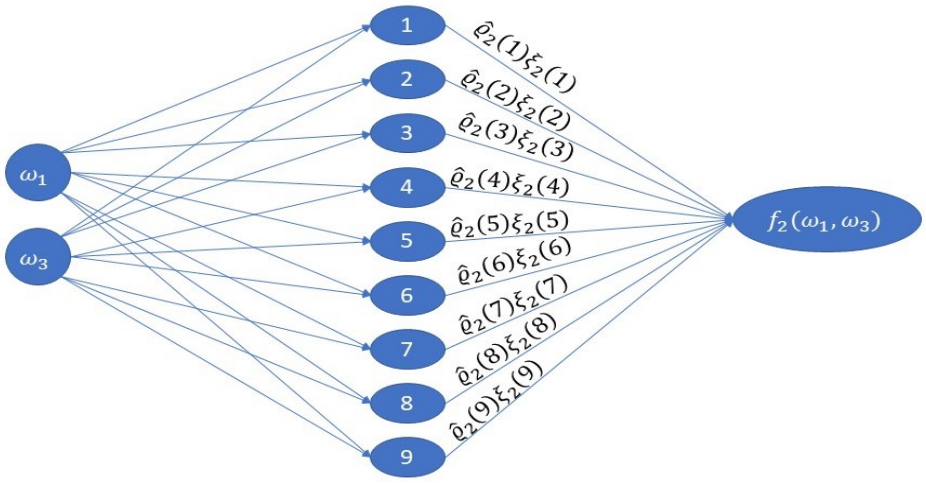

Figure 4.2: Neural Network in Pitch Direction

Time derivative of (4.56) is

$$\begin{aligned}\dot{V}_5 = &\left(\varrho_1 - \hat{\varrho}_1\right)^T \Gamma_1 \left(-\dot{\hat{\varrho}}_1\right) + \left(\varrho_2 - \hat{\varrho}_2\right)^T \Gamma_2 \left(-\dot{\hat{\varrho}}_2\right) + \left(\varrho_3 - \hat{\varrho}_3\right)^T \Gamma_3 \left(-\dot{\hat{\varrho}}_3\right) \\ &+ \lambda_1\beta_1 \left(I_x - \hat{I}_x\right)\left(-\dot{\hat{I}}_x\right) + \lambda_2\beta_2 \left(I_y - \hat{I}_y\right)\left(-\dot{\hat{I}}_y\right) + \lambda_3\beta_3 \left(I_z - \hat{I}_z\right)\left(-\dot{\hat{I}}_z\right)\end{aligned} \tag{4.57}$$

Now define $V = V_4 + V_5$. Then, it follows from (4.52) and (4.57) that

$$\begin{aligned}\dot{V} &= \dot{V}_4 + \dot{V}_5 \\ &= -K_p \mathbf{e}_1^T \mathbf{K}_1 \mathbf{e}_1 - \mathbf{e}_2^T \mathbf{K}_2 \mathbf{e}_2 - \mathbf{q}_e^T \mathbf{K}_3 \mathbf{q}_e \\ &+ \omega_{e1}\left(q_{e1} + \varrho_1\xi_1 + \varepsilon_1 + \beta_1\tau_1 - \dot{\omega}_{\alpha 1}\right) \\ &+ \omega_{e2}\left(q_{e2} + \varrho_2\xi_2 + \varepsilon_2 + \beta_2\tau_2 - \dot{\omega}_{\alpha 2}\right) \\ &+ \omega_{e3}\left(q_{e3} + \varrho_3\xi_3 + \varepsilon_3 + \beta_3\tau_3 - \dot{\omega}_{\alpha 3}\right) \\ &+ \left(\varrho_1 - \hat{\varrho}_1\right)^T \Gamma_1 \left(-\dot{\hat{\varrho}}_1\right) + \left(\varrho_2 - \hat{\varrho}_2\right)^T \Gamma_2 \left(-\dot{\hat{\varrho}}_2\right) + \left(\varrho_3 - \hat{\varrho}_3\right)^T \Gamma_3 \left(-\dot{\hat{\varrho}}_3\right) \\ &+ \lambda_1\beta_1 \left(I_x - \hat{I}_x\right)\left(-\dot{\hat{I}}_x\right) + \lambda_2\beta_2 \left(I_y - \hat{I}_y\right)\left(-\dot{\hat{I}}_y\right) + \lambda_3\beta_3 \left(I_z - \hat{I}_z\right)\left(-\dot{\hat{I}}_z\right)\end{aligned} \tag{4.58}$$

By replacing the ϱ with $\hat{\varrho}$ in the 2nd to 4th lines and adding some items in the 5th line, the

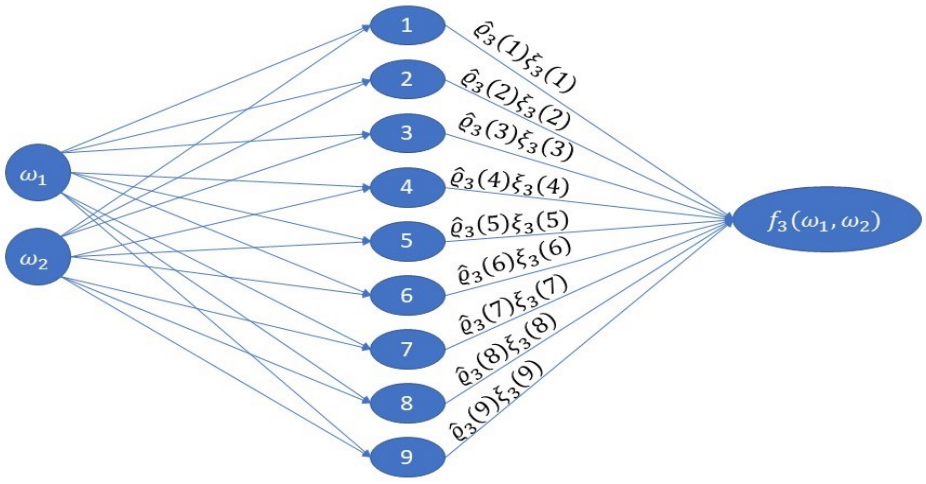

Figure 4.3: Neural Network in Yaw Direction

following can be easily obtained.

$$\begin{aligned}
\dot{V} = & -K_p \mathbf{e}_1^T \mathbf{K}_1 \mathbf{e}_1 - \mathbf{e}_2^T \mathbf{K}_2 \mathbf{e}_2 - \mathbf{q}_e^T \mathbf{K}_3 \mathbf{q}_e \\
& + \omega_{e1} \left(q_{e1} + \hat{\varrho}_1 \xi_1 + \varepsilon_1 + \beta_1 \tau_1 - \dot{\omega}_{\alpha 1} \right) \\
& + \omega_{e2} \left(q_{e2} + \hat{\varrho}_2 \xi_2 + \varepsilon_2 + \beta_2 \tau_2 - \dot{\omega}_{\alpha 2} \right) \\
& + \omega_{e3} \left(q_{e3} + \hat{\varrho}_3 \xi_3 + \varepsilon_3 + \beta_3 \tau_3 - \dot{\omega}_{\alpha 3} \right) \\
& + \left(\varrho_1 - \hat{\varrho}_1 \right)^T \Gamma_1 \left(\Gamma_1^{-1} \omega_{e1} \xi_1 - \dot{\hat{\varrho}}_1 \right) \\
& + \left(\varrho_2 - \hat{\varrho}_2 \right)^T \Gamma_2 \left(\Gamma_2^{-1} \omega_{e2} \xi_2 - \dot{\hat{\varrho}}_2 \right) \\
& + \left(\varrho_3 - \hat{\varrho}_3 \right)^T \Gamma_3 \left(\Gamma_3^{-1} \omega_{e3} \xi_3 - \dot{\hat{\varrho}}_3 \right) \\
& + \lambda_1 \beta_1 \left(I_x - \hat{I}_x \right) \left(-\dot{\hat{I}}_x \right) + \lambda_2 \beta_2 \left(I_y - \hat{I}_y \right) \left(-\dot{\hat{I}}_y \right) + \lambda_3 \beta_3 \left(I_z - \hat{I}_z \right) \left(-\dot{\hat{I}}_z \right)
\end{aligned} \tag{4.59}$$

Define

$$\begin{aligned}
u_1 &= \frac{\tau_1}{\hat{I}_x} \\
u_2 &= \frac{\tau_2}{\hat{I}_y} \\
u_3 &= \frac{\tau_3}{\hat{I}_z}
\end{aligned} \tag{4.60}$$

It can be verified that the followings are true

$$\begin{aligned}\beta_1\tau_1 &= u_1 - \beta_1(I_x - \hat{I}_x)u_1\\ \beta_2\tau_2 &= u_2 - \beta_2(I_y - \hat{I}_y)u_2\\ \beta_3\tau_3 &= u_3 - \beta_3(I_z - \hat{I}_z)u_3\end{aligned} \tag{4.61}$$

For example,

$$\begin{aligned}\beta_1\tau_1 &= \beta_1 u_1 \hat{I}_x\\ &= \beta_1 u_1 \left(\hat{I}_x - I_x + I_x\right)\\ &= \beta_1 u_1 I_x - \beta_1 u_1 \left(I_x - \hat{I}_x\right)\\ &= u_1 - \beta_1 \left(I_x - \hat{I}_x\right) u_1,\end{aligned} \tag{4.62}$$

By introducing the following adaptation laws for $\hat{\varrho}_1$, $\hat{\varrho}_2$, $\hat{\varrho}_3$,

$$\begin{aligned}\dot{\hat{\varrho}}_1 &= \Gamma_1^{-1}\omega_{1e}\xi_1 - \sigma_1\hat{\varrho}_1\\ \dot{\hat{\varrho}}_2 &= \Gamma_2^{-1}\omega_{2e}\xi_2 - \sigma_2\hat{\varrho}_2\\ \dot{\hat{\varrho}}_3 &= \Gamma_3^{-1}\omega_{3e}\xi_3 - \sigma_3\hat{\varrho}_3\end{aligned} \tag{4.63}$$

$\dot{V}$ becomes

$$\begin{aligned}\dot{V} = &-K_p\mathbf{e}_1^T\mathbf{K}_1\mathbf{e}_1 - \mathbf{e}_2^T\mathbf{K}_2\mathbf{e}_2 - \mathbf{q}_e^T\mathbf{K}_3\mathbf{q}_e\\ &+ \omega_{e1}\left(q_{e1} + \hat{\varrho}_1\xi_1 + u_1 - \beta_1(I_x - \hat{I}_x)u_1 - \dot{\omega}_{\alpha1}\right)\\ &+ \omega_{e2}\left(q_{e2} + \hat{\varrho}_2\xi_2 + u_2 - \beta_2(I_y - \hat{I}_y)u_2 - \dot{\omega}_{\alpha2}\right)\\ &+ \omega_{e3}\left(q_{e3} + \hat{\varrho}_3\xi_3 + u_3 - \beta_3(I_z - \hat{I}_z)u_3 - \dot{\omega}_{\alpha3}\right)\\ &+ \omega_{e1}\varepsilon_1 + \omega_{e2}\varepsilon_2 + \omega_{e3}\varepsilon_3\\ &+ \sigma_1\left(\varrho_1 - \hat{\varrho}_1\right)^T\Gamma_1\hat{\varrho}_1 + \sigma_2\left(\varrho_2 - \hat{\varrho}_2\right)^T\Gamma_2\hat{\varrho}_2 + \sigma_3\left(\varrho_3 - \hat{\varrho}_3\right)^T\Gamma_3\hat{\varrho}_3\\ &+ \lambda_1\beta_1\left(I_x - \hat{I}_x\right)\left(-\dot{\hat{I}}_x\right) + \lambda_2\beta_2\left(I_y - \hat{I}_y\right)\left(-\dot{\hat{I}}_y\right) + \lambda_3\beta_3\left(I_z - \hat{I}_z\right)\left(-\dot{\hat{I}}_z\right)\end{aligned} \tag{4.64}$$

where σ_1, σ_2, and σ_3 are the positive design parameters, which can be tuned to obtain a good adaptive performance.

By separating the terms related to moment of inertia from the 2nd line to 4th lines, it results in

$$\begin{aligned}\dot{V} = &-K_p\mathbf{e}_1^T\mathbf{K}_1\mathbf{e}_1 - \mathbf{e}_2^T\mathbf{K}_2\mathbf{e}_2 - \mathbf{q}_e^T\mathbf{K}_3\mathbf{q}_e\\ &+ \omega_{e1}\left(q_{e1} + \hat{\varrho}_1\xi_1 + u_1 - \dot{\omega}_{\alpha1}\right) + \omega_{e2}\left(q_{e2} + \hat{\varrho}_2\xi_2 + u_2 - \dot{\omega}_{\alpha2}\right)\\ &+ \omega_{e3}\left(q_{e3} + \hat{\varrho}_3\xi_3 + u_3 - \dot{\omega}_{\alpha3}\right)\\ &+ \omega_{e1}\varepsilon_1 + \omega_{e2}\varepsilon_2 + \omega_{e3}\varepsilon_3\\ &+ \sigma_1\left(\varrho_1 - \hat{\varrho}_1\right)^T\Gamma_1\hat{\varrho}_1 + \sigma_2\left(\varrho_2 - \hat{\varrho}_2\right)^T\Gamma_2\hat{\varrho}_2 + \sigma_3\left(\varrho_3 - \hat{\varrho}_3\right)^T\Gamma_3\hat{\varrho}_3\\ &- \lambda_1\beta_1\left(I_x - \hat{I}_x\right)\dot{\hat{I}}_x - \lambda_2\beta_2\left(I_y - \hat{I}_y\right)\dot{\hat{I}}_y - \lambda_3\beta_3\left(I_z - \hat{I}_z\right)\dot{\hat{I}}_z\\ &- \omega_{e1}\beta_1(I_x - \hat{I}_x)u_1 - \omega_{e2}\beta_2(I_y - \hat{I}_y)u_2 - \omega_{e3}\beta_3(I_z - \hat{I}_z)u_3\end{aligned} \tag{4.65}$$

By combining the last two lines, it follows that

$$\begin{aligned}\dot{V} = & -K_p \mathbf{e}_1^T \mathbf{K}_1 \mathbf{e}_1 - \mathbf{e}_2^T \mathbf{K}_2 \mathbf{e}_2 - \mathbf{q}_e^T \mathbf{K}_3 \mathbf{q}_e \\ & + \omega_{e1} \left(q_{e1} + \hat{\varrho}_1 \xi_1 + u_1 - \dot{\omega}_{\alpha 1} \right) \\ & + \omega_{e2} \left(q_{e2} + \hat{\varrho}_2 \xi_2 + u_2 - \dot{\omega}_{\alpha 2} \right) \\ & + \omega_{e3} \left(q_{e3} + \hat{\varrho}_3 \xi_3 + u_3 - \dot{\omega}_{\alpha 3} \right) \\ & + \omega_{e1} \varepsilon_1 + \omega_{e2} \varepsilon_2 + \omega_{e3} \varepsilon_3 \\ & + \sigma_1 \left(\varrho_1 - \hat{\varrho}_1 \right)^T \Gamma_1 \hat{\varrho}_1 + \sigma_2 \left(\varrho_2 - \hat{\varrho}_2 \right)^T \Gamma_2 \hat{\varrho}_2 + \sigma_3 \left(\varrho_3 - \hat{\varrho}_3 \right)^T \Gamma_3 \hat{\varrho}_3 \\ & - \beta_1 \left(I_x - \hat{I}_x \right) \left(\lambda_1 \dot{\hat{I}}_x + \omega_{e1} u_1 \right) - \beta_2 \left(I_y - \hat{I}_y \right) \left(\lambda_2 \dot{\hat{I}}_y + \omega_{e2} u_2 \right) \\ & - \beta_3 \left(I_z - \hat{I}_z \right) \left(\lambda_3 \dot{\hat{I}}_z + \omega_{e3} u_3 \right) \end{aligned} \tag{4.66}$$

Set the following adaptation laws for $\hat{I}_x$, $\hat{I}_y$, $\hat{I}_z$

$$\begin{aligned} \dot{\hat{I}}_x &= -\omega_{e1} u_1 / \lambda_1 - \nu_1 \hat{I}_x \\ \dot{\hat{I}}_y &= -\omega_{e2} u_2 / \lambda_2 - \nu_2 \hat{I}_y \\ \dot{\hat{I}}_z &= -\omega_{e3} u_3 / \lambda_3 - \nu_3 \hat{I}_z \end{aligned} \tag{4.67}$$

where ν_1, ν_2, and ν_3 are the positive design parameters. They can be tuned to obtain a good adaptive performance.

Substituting (4.67) into (4.66) produces

$$\begin{aligned}\dot{V} = & -K_p \mathbf{e}_1^T \mathbf{K}_1 \mathbf{e}_1 - \mathbf{e}_2^T \mathbf{K}_2 \mathbf{e}_2 - \mathbf{q}_e^T \mathbf{K}_3 \mathbf{q}_e \\ & + \omega_{e1} \left(q_{e1} + \hat{\varrho}_1 \xi_1 + u_1 - \dot{\omega}_{\alpha 1} \right) \\ & + \omega_{e2} \left(q_{e2} + \hat{\varrho}_2 \xi_2 + u_2 - \dot{\omega}_{\alpha 2} \right) \\ & + \omega_{e3} \left(q_{e3} + \hat{\varrho}_3 \xi_3 + u_3 - \dot{\omega}_{\alpha 3} \right) \\ & + \omega_{e1} \varepsilon_1 + \omega_{e2} \varepsilon_2 + \omega_{e3} \varepsilon_3 \\ & + \sigma_1 \left(\varrho_1 - \hat{\varrho}_1 \right)^T \Gamma_1 \hat{\varrho}_1 + \sigma_2 \left(\varrho_2 - \hat{\varrho}_2 \right)^T \Gamma_2 \hat{\varrho}_2 + \sigma_3 \left(\varrho_3 - \hat{\varrho}_3 \right)^T \Gamma_3 \hat{\varrho}_3 \\ & + \lambda_1 \nu_1 \beta_1 \left(I_x - \hat{I}_x \right) \hat{I}_x + \lambda_2 \nu_2 \beta_2 \left(I_y - \hat{I}_y \right) \hat{I}_y + \lambda_3 \nu_3 \beta_3 \left(I_z - \hat{I}_z \right) \hat{I}_z \end{aligned} \tag{4.68}$$

Due to the relation

$$\sigma_i \left(\varrho_i - \hat{\varrho}_i \right)^T \Gamma_i \hat{\varrho}_i = -\sigma_i \left(\varrho_i - \hat{\varrho}_i \right)^T \Gamma_i \left(\varrho_i - \hat{\varrho}_i \right) + \sigma_i \left(\varrho_i - \hat{\varrho}_i \right)^T \Gamma_i \varrho_i \tag{4.69}$$

for $i = 1, 2, 3$, $\dot{V}$ becomes

$$\begin{aligned}
\dot{V} = & -K_p \mathbf{e}_1^T \mathbf{K}_1 \mathbf{e}_1 - \mathbf{e}_2^T \mathbf{K}_2 \mathbf{e}_2 - \mathbf{q}_e^T \mathbf{K}_3 \mathbf{q}_e \\
& + \omega_{e1} \left(q_{e1} + \hat{\varrho}_1 \xi_1 + u_1 - \dot{\omega}_{\alpha 1} \right) \\
& + \omega_{e2} \left(q_{e2} + \hat{\varrho}_2 \xi_2 + u_2 - \dot{\omega}_{\alpha 2} \right) \\
& + \omega_{e3} \left(q_{e3} + \hat{\varrho}_3 \xi_3 + u_3 - \dot{\omega}_{\alpha 3} \right) \\
& + \omega_{e1} \varepsilon_1 + \omega_{e2} \varepsilon_2 + \omega_{e3} \varepsilon_3 \\
& - \sigma_1 \left(\varrho_1 - \hat{\varrho}_1 \right)^T \Gamma_1 \left(\varrho_1 - \hat{\varrho}_1 \right) + \sigma_1 \left(\varrho_1 - \hat{\varrho}_1 \right)^T \Gamma_1 \varrho_1 \\
& - \sigma_2 \left(\varrho_2 - \hat{\varrho}_2 \right)^T \Gamma_2 \left(\varrho_2 - \hat{\varrho}_2 \right) + \sigma_2 \left(\varrho_2 - \hat{\varrho}_2 \right)^T \Gamma_2 \varrho_2 \\
& - \sigma_3 \left(\varrho_3 - \hat{\varrho}_3 \right)^T \Gamma_3 \left(\varrho_3 - \hat{\varrho}_3 \right) + \sigma_3 \left(\varrho_3 - \hat{\varrho}_3 \right)^T \Gamma_3 \varrho_3 \\
& + \lambda_1 \nu_1 \beta_1 \left(I_x - \hat{I}_x \right) \hat{I}_x + \lambda_2 \nu_2 \beta_2 \left(I_y - \hat{I}_y \right) \hat{I}_y + \lambda_3 \nu_3 \beta_3 \left(I_z - \hat{I}_z \right) \hat{I}_z
\end{aligned} \tag{4.70}$$

By using Young's inequality $xy \leq \frac{1}{2}x^2 + \frac{1}{2}y^2$ and $x^T \Gamma y \leq \frac{1}{2}x^T \Gamma x + \frac{1}{2}y^T \Gamma y$, the following relationships can be determined.

$$\begin{aligned}
\omega_{e1} \varepsilon_1 &\leq \frac{1}{2}\omega_{e1}^2 + \frac{1}{2}\varepsilon_1^2 \\
\omega_{e2} \varepsilon_2 &\leq \frac{1}{2}\omega_{e2}^2 + \frac{1}{2}\varepsilon_2^2 \\
\omega_{e3} \varepsilon_3 &\leq \frac{1}{2}\omega_{e3}^2 + \frac{1}{2}\varepsilon_3^2
\end{aligned} \tag{4.71}$$

$$\begin{aligned}
\left(I_x - \hat{I}_x \right) I_x &\leq \frac{1}{2} \left(I_x - \hat{I}_x \right)^2 + \frac{1}{2} I_x^2 \\
\left(I_y - \hat{I}_y \right) I_y &\leq \frac{1}{2} \left(I_y - \hat{I}_y \right)^2 + \frac{1}{2} I_y^2 \\
\left(I_z - \hat{I}_z \right) I_z &\leq \frac{1}{2} \left(I_z - \hat{I}_z \right)^2 + \frac{1}{2} I_z^2
\end{aligned} \tag{4.72}$$

$$\begin{aligned}
\left(\varrho_1 - \hat{\varrho}_1 \right)^T \Gamma_1 \varrho_1 &\leq \frac{1}{2} \left(\varrho_1 - \hat{\varrho}_1 \right)^T \Gamma_1 \left(\varrho_1 - \hat{\varrho}_1 \right) + \frac{1}{2} \varrho_1^T \Gamma_1 \varrho_1 \\
\left(\varrho_2 - \hat{\varrho}_2 \right)^T \Gamma_2 \varrho_2 &\leq \frac{1}{2} \left(\varrho_2 - \hat{\varrho}_2 \right)^T \Gamma_2 \left(\varrho_2 - \hat{\varrho}_2 \right) + \frac{1}{2} \varrho_2^T \Gamma_2 \varrho_2 \\
\left(\varrho_3 - \hat{\varrho}_3 \right)^T \Gamma_3 \varrho_3 &\leq \frac{1}{2} \left(\varrho_3 - \hat{\varrho}_3 \right)^T \Gamma_3 \left(\varrho_3 - \hat{\varrho}_3 \right) + \frac{1}{2} \varrho_3^T \Gamma_3 \varrho_3
\end{aligned} \tag{4.73}$$

As a result, It can be easily proved that $\dot{V}$ can be expressed as

$$\begin{aligned}
\dot{V} \leq & -K_p \mathbf{e}_1^T \mathbf{K}_1 \mathbf{e}_1 - \mathbf{e}_2^T \mathbf{K}_2 \mathbf{e}_2 - \mathbf{q}_e^T \mathbf{K}_3 \mathbf{q}_e \\
& + \omega_{e1} \left(\frac{1}{2}\omega_{e1} + q_{e1} + \hat{\varrho}_1 \xi_1 + u_1 - \dot{\omega}_{\alpha 1} \right) \\
& + \omega_{e2} \left(\frac{1}{2}\omega_{e2} + q_{e2} + \hat{\varrho}_2 \xi_2 + u_2 - \dot{\omega}_{\alpha 2} \right) \\
& + \omega_{e3} \left(\frac{1}{2}\omega_{e3} + q_{e3} + \hat{\varrho}_3 \xi_3 + u_3 - \dot{\omega}_{\alpha 3} \right) \\
& + \frac{1}{2}\varepsilon_1^2 + \frac{1}{2}\varepsilon_2^2 + \frac{1}{2}\varepsilon_3^2 + \frac{1}{2}\varrho_1^T \Gamma_1 \varrho_1 + \frac{1}{2}\varrho_2^T \Gamma_2 \varrho_2 + \frac{1}{2}\varrho_3^T \Gamma_3 \varrho_3 \\
& - \frac{1}{2}\sigma_1 \left(\varrho_1 - \hat{\varrho}_1 \right)^T \Gamma_1 \left(\varrho_1 - \hat{\varrho}_1 \right) - \frac{1}{2}\sigma_2 \left(\varrho_2 - \hat{\varrho}_2 \right)^T \Gamma_2 \left(\varrho_2 - \hat{\varrho}_2 \right) \\
& - \frac{1}{2}\sigma_3 \left(\varrho_3 - \hat{\varrho}_3 \right)^T \Gamma_3 \left(\varrho_3 - \hat{\varrho}_3 \right) \\
& + \frac{1}{2}\lambda_1 \nu_1 \beta_1 \left(I_x - \hat{I}_x \right)^2 + \frac{1}{2}\lambda_1 \nu_1 \beta_1 I_x^2 \\
& + \frac{1}{2}\lambda_2 \nu_2 \beta_2 \left(I_y - \hat{I}_y \right)^2 + \frac{1}{2}\lambda_2 \nu_2 \beta_2 I_y^2 \\
& + \frac{1}{2}\lambda_3 \nu_3 \beta_3 \left(I_z - \hat{I}_z \right)^2 + \frac{1}{2}\lambda_3 \nu_3 \beta_3 I_z^2 \\
& - \lambda_1 \nu_1 \beta_1 \left(I_x - \hat{I}_x \right)^2 - \lambda_2 \nu_2 \beta_2 \left(I_y - \hat{I}_y \right)^2 - \lambda_3 \nu_3 \beta_3 \left(I_z - \hat{I}_z \right)^2
\end{aligned} \tag{4.74}$$

By combining the items related with moment of inertia in the last 4 lines, it yields

$$\begin{aligned}
\dot{V} \leq & -K_p \mathbf{e}_1^T \mathbf{K}_1 \mathbf{e}_1 - \mathbf{e}_2^T \mathbf{K}_2 \mathbf{e}_2 - \mathbf{q}_e^T \mathbf{K}_3 \mathbf{q}_e \\
& + \omega_{e1} \left(\frac{1}{2}\omega_{e1} + q_{e1} + \hat{\varrho}_1 \xi_1 + u_1 - \dot{\omega}_{\alpha 1} \right) \\
& + \omega_{e2} \left(\frac{1}{2}\omega_{e2} + q_{e2} + \hat{\varrho}_2 \xi_2 + u_2 - \dot{\omega}_{\alpha 2} \right) \\
& + \omega_{e3} \left(\frac{1}{2}\omega_{e3} + q_{e3} + \hat{\varrho}_3 \xi_3 + u_3 - \dot{\omega}_{\alpha 3} \right) \\
& + \frac{1}{2}\varepsilon_1^2 + \frac{1}{2}\varepsilon_2^2 + \frac{1}{2}\varepsilon_3^2 + \frac{1}{2}\varrho_1^T \Gamma_1 \varrho_1 + \frac{1}{2}\varrho_2^T \Gamma_2 \varrho_2 + \frac{1}{2}\varrho_3^T \Gamma_3 \varrho_3 \\
& - \frac{1}{2}\sigma_1 \left(\varrho_1 - \hat{\varrho}_1 \right)^T \Gamma_1 \left(\varrho_1 - \hat{\varrho}_1 \right) - \frac{1}{2}\sigma_2 \left(\varrho_2 - \hat{\varrho}_2 \right)^T \Gamma_2 \left(\varrho_2 - \hat{\varrho}_2 \right) \\
& - \frac{1}{2}\sigma_3 \left(\varrho_3 - \hat{\varrho}_3 \right)^T \Gamma_3 \left(\varrho_3 - \hat{\varrho}_3 \right) \\
& - \frac{1}{2}\lambda_1 \nu_1 \beta_1 \left(I_x - \hat{I}_x \right)^2 - \frac{1}{2}\lambda_2 \nu_2 \beta_2 \left(I_y - \hat{I}_y \right)^2 - \frac{1}{2}\lambda_3 \nu_3 \beta_3 \left(I_z - \hat{I}_z \right)^2 \\
& + \frac{1}{2}\lambda_1 \nu_1 \beta_1 I_x^2 + \frac{1}{2}\lambda_2 \nu_2 \beta_2 I_y^2 + \frac{1}{2}\lambda_3 \nu_3 \beta_3 I_z^2
\end{aligned} \tag{4.75}$$

Set the following

$$\begin{bmatrix} -k_{4x}\omega_{e1} \\ -k_{4y}\omega_{e2} \\ -k_{4z}\omega_{e3} \end{bmatrix} = \begin{bmatrix} \frac{1}{2}\omega_{e1} + q_{e1} + \hat{\varrho}_1\xi_1 + u_1 - \dot{\omega}_{\alpha 1} \\ \frac{1}{2}\omega_{e2} + q_{e2} + \hat{\varrho}_2\xi_2 + u_2 - \dot{\omega}_{\alpha 2} \\ \frac{1}{2}\omega_{e3} + q_{e3} + \hat{\varrho}_3\xi_3 + u_3 - \dot{\omega}_{\alpha 3} \end{bmatrix} \tag{4.76}$$

$$= \begin{bmatrix} \frac{1}{2}\omega_{e1} + q_{e1} + \hat{\varrho}_1\xi_1 + \frac{\tau_1}{\hat{I}_x} - \dot{\omega}_{\alpha 1} \\ \frac{1}{2}\omega_{e2} + q_{e2} + \hat{\varrho}_2\xi_2 + \frac{\tau_2}{\hat{I}_y} - \dot{\omega}_{\alpha 2} \\ \frac{1}{2}\omega_{e3} + q_{e3} + \hat{\varrho}_3\xi_3 + \frac{\tau_3}{\hat{I}_z} - \dot{\omega}_{\alpha 3} \end{bmatrix} \tag{4.77}$$

then, the control law can be obtained as

$$\begin{bmatrix} \tau_1 \\ \tau_2 \\ \tau_3 \end{bmatrix} = \begin{bmatrix} \hat{I}_x\left(-k_{4x}\omega_{e1} - \frac{1}{2}\omega_{e1} - q_{e1} + \dot{\omega}_{\alpha 1} - \hat{\varrho}_1\xi_1\right) \\ \hat{I}_y\left(-k_{4y}\omega_{e2} - \frac{1}{2}\omega_{e2} - q_{e2} + \dot{\omega}_{\alpha 2} - \hat{\varrho}_2\xi_2\right) \\ \hat{I}_z\left(-k_{4z}\omega_{e3} - \frac{1}{2}\omega_{e3} - q_{e3} + \dot{\omega}_{\alpha 3} - \hat{\varrho}_3\xi_3\right) \end{bmatrix} \tag{4.78}$$

with k_{4x}, k_{4y}, and k_{4z} denoting control gains. With these torques, (4.75) becomes

$$\begin{aligned} \dot{V} \leq & -K_p\mathbf{e}_1^T\mathbf{K}_1\mathbf{e}_1 - \mathbf{e}_2^T\mathbf{K}_2\mathbf{e}_2 - \mathbf{q}_e^T\mathbf{K}_3\mathbf{q}_e - k_{4x}\omega_{e1}^2 - k_{4y}\omega_{e2}^2 - k_{4z}\omega_{e3}^2 \\ & - \frac{1}{2}\sigma_1\left(\varrho_1 - \hat{\varrho}_1\right)^T\Gamma_1\left(\varrho_1 - \hat{\varrho}_1\right) - \frac{1}{2}\sigma_2\left(\varrho_2 - \hat{\varrho}_2\right)^T\Gamma_2\left(\varrho_2 - \hat{\varrho}_2\right) - \frac{1}{2}\sigma_3\left(\varrho_3 - \hat{\varrho}_3\right)^T\Gamma_3\left(\varrho_3 - \hat{\varrho}_3\right) \\ & + \frac{1}{2}\varepsilon_1^2 + \frac{1}{2}\varepsilon_2^2 + \frac{1}{2}\varepsilon_3^2 + \frac{1}{2}\varrho_1^T\Gamma_1\varrho_1 + \frac{1}{2}\varrho_2^T\Gamma_2\varrho_2 + \frac{1}{2}\varrho_3^T\Gamma_3\varrho_3 \\ & - \frac{1}{2}\lambda_1\nu_1\beta_1\left(I_x - \hat{I}_x\right)^2 - \frac{1}{2}\lambda_2\nu_2\beta_2\left(I_y - \hat{I}_y\right)^2 - \frac{1}{2}\lambda_3\nu_3\beta_3\left(I_z - \hat{I}_z\right)^2 \\ & + \frac{1}{2}\lambda_1\nu_1\beta_1 I_x^2 + \frac{1}{2}\lambda_2\nu_2\beta_2 I_y^2 + \frac{1}{2}\lambda_3\nu_3\beta_3 I_z^2 \end{aligned} \tag{4.79}$$

By exchanging the 3rd line and 4th line and rewriting the last three terms in the 1st line as matrix form, the following can be expressed.

$$\begin{aligned} \dot{V} \leq & -K_p\mathbf{e}_1^T\mathbf{K}_1\mathbf{e}_1 - \mathbf{e}_2^T\mathbf{K}_2\mathbf{e}_2 - \mathbf{q}_e^T\mathbf{K}_3\mathbf{q}_e - \omega_e^T\mathbf{K}_4\omega_e \\ & - \frac{1}{2}\sigma_1\left(\varrho_1 - \hat{\varrho}_1\right)^T\Gamma_1\left(\varrho_1 - \hat{\varrho}_1\right) - \frac{1}{2}\sigma_2\left(\varrho_2 - \hat{\varrho}_2\right)^T\Gamma_2\left(\varrho_2 - \hat{\varrho}_2\right) - \frac{1}{2}\sigma_3\left(\varrho_3 - \hat{\varrho}_3\right)^T\Gamma_3\left(\varrho_3 - \hat{\varrho}_3\right) \\ & - \frac{1}{2}\lambda_1\nu_1\beta_1\left(I_x - \hat{I}_x\right)^2 - \frac{1}{2}\lambda_2\nu_2\beta_2\left(I_y - \hat{I}_y\right)^2 - \frac{1}{2}\lambda_3\nu_3\beta_3\left(I_z - \hat{I}_z\right)^2 \\ & + \frac{1}{2}\varepsilon_1^2 + \frac{1}{2}\varepsilon_2^2 + \frac{1}{2}\varepsilon_3^2 + \frac{1}{2}\lambda_1\nu_1\beta_1 I_x^2 + \frac{1}{2}\lambda_2\nu_2\beta_2 I_y^2 + \frac{1}{2}\lambda_3\nu_3\beta_3 I_z^2 \\ & + \frac{1}{2}\varrho_1^T\Gamma_1\varrho_1 + \frac{1}{2}\varrho_2^T\Gamma_2\varrho_2 + \frac{1}{2}\varrho_3^T\Gamma_3\varrho_3 \end{aligned} \tag{4.80}$$

where $\mathbf{K}_4 = diag(k_{4x}, k_{4y}, k_{4z})$.

$$\begin{aligned}\dot{V} \leq & -K_p \mathbf{e}_1^T \mathbf{K}_1 \mathbf{e}_1 - \mathbf{e}_2^T \mathbf{K}_2 \mathbf{e}_2 - \mathbf{q}_e^T \mathbf{K}_3 \mathbf{q}_e - c(q_{e0}-1)^2 - \omega_e^T \mathbf{K}_4 \omega_e \\ & - \frac{1}{2}\sigma_1 \left(\varrho_1 - \hat{\varrho}_1\right)^T \Gamma_1 \left(\varrho_1 - \hat{\varrho}_1\right) - \frac{1}{2}\sigma_2 \left(\varrho_2 - \hat{\varrho}_2\right)^T \Gamma_2 \left(\varrho_2 - \hat{\varrho}_2\right) - \frac{1}{2}\sigma_3 \left(\varrho_3 - \hat{\varrho}_3\right)^T \Gamma_3 \left(\varrho_3 - \hat{\varrho}_3\right) \\ & - \frac{1}{2}\lambda_1\nu_1\beta_1 \left(I_x - \hat{I}_x\right)^2 - \frac{1}{2}\lambda_2\nu_2\beta_2 \left(I_y - \hat{I}_y\right)^2 - \frac{1}{2}\lambda_3\nu_3\beta_3 \left(I_z - \hat{I}_z\right)^2 \\ & + \frac{1}{2}\varepsilon_1^2 + \frac{1}{2}\varepsilon_2^2 + \frac{1}{2}\varepsilon_3^2 + \frac{1}{2}\lambda_1\nu_1\beta_1 I_x^2 + \frac{1}{2}\lambda_2\nu_2\beta_2 I_y^2 + \frac{1}{2}\lambda_3\nu_3\beta_3 I_z^2 \\ & + \frac{1}{2}\varrho_1^T\Gamma_1\varrho_1 + \frac{1}{2}\varrho_2^T\Gamma_2\varrho_2 + \frac{1}{2}\varrho_3^T\Gamma_3\varrho_3 + c(q_{e0}-1)^2 \end{aligned} \tag{4.81}$$

where c is a positive constant which can be chosen arbitrarily small.

Finally, it can be proved that V satisfies the following condition

$$\dot{V} \leq -aV + b \tag{4.82}$$

which implies that all the terms in V are bounded [76], that is, all the error terms are bounded, where

$$\begin{aligned} a &= \min\{2\bar{K}_1,\, 2\bar{K}_2,\, \bar{K}_3,\, c,\, 2\bar{K}_4,\, \sigma_1,\, \sigma_2,\, \sigma_3,\, \nu_1,\, \nu_2,\, \nu_3\} \\ b &= \frac{1}{2}\bar{\varepsilon}_1^2 + \frac{1}{2}\bar{\varepsilon}_2^2 + \frac{1}{2}\bar{\varepsilon}_3^2 + \frac{1}{2}\lambda_1\nu_1\beta_1 I_x^2 + \frac{1}{2}\lambda_2\nu_2\beta_2 I_y^2 + \frac{1}{2}\lambda_3\nu_3\beta_3 I_z^2 \\ &\quad + \frac{1}{2}\varrho_1^T\Gamma_1\varrho_1 + \frac{1}{2}\varrho_2^T\Gamma_2\varrho_2 + \frac{1}{2}\varrho_3^T\Gamma_3\varrho_3 + \bar{C} \end{aligned}$$

with $\bar{\varepsilon}_1$, $\bar{\varepsilon}_2$, and $\bar{\varepsilon}_3$ being the upper bounds of ε_1, ε_2, and ε_3, $\bar{K}_1$, $\bar{K}_2$, $\bar{K}_3$, and $\bar{K}_4$ being the minimum eigenvalues of K_1, K_2, K_3, and K_4 and $\bar{C}$ being the upper bound of $c(q_{e0}-1)^2$, respectively.

Using the property of a unit quaternion in (2.23) gives

$$q_{e0}^2 + q_{e1}^2 + q_{e2}^2 + q_{e3}^2 = 1$$

By using the fact that $q_{e1}^2 + q_{e2}^2 + q_{e3}^2 \geq 0$, it can be obtained that

$$q_{e0}^2 \leq 1$$

$$-1 \leq q_{e0} \leq 1$$

$$-2 \leq q_{e0} - 1 \leq 0$$

$$0 \leq (q_{e0}-1)^2 \leq 4$$

Finally it results in

$$\bar{C} = 4c$$

A block diagram for the designed system with a four step controller is shown in Fig. 4.4.

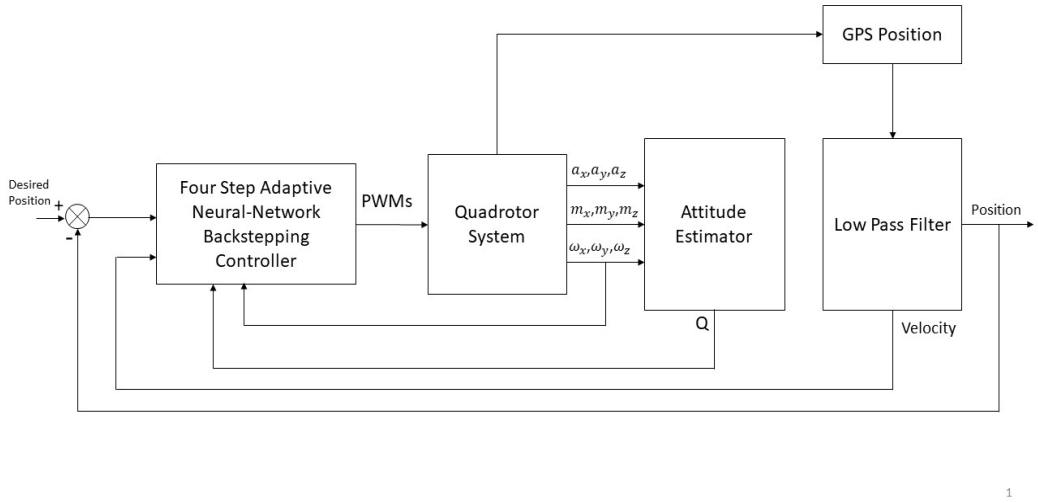

Figure 4.4: Block Diagram of the System with Four Step Controller

4.2.1 Simulation Results

The simulation is carried out by using Matlab. By using the ODE function, the differential equations of the dynamic model are solved. The triangular activation functions for the neural-network are used. The center of the activation function is -0.2 for cells 1-3, 0 for cells 4-6, 0.2 for cells 7-9. The width for all the activation functions is 0.06. The initial weight for each neural is 0. There are no load and the simulation is carried out in an ideal environment without wind and turbulence. With the design parameters $K_p = 0.5$, $K_1 = I_3$, $K_2 = 7I_3$, $K_3 = 600I_3$, $K_4 = 500I_3$, $\sigma_1 = \sigma_2 = \sigma_3 = 0.5$, $\Gamma_1 = \Gamma_2 = \Gamma_3 = 20I_9$, $\lambda_1 = \lambda_2 = \lambda_3 = 1$, $\nu_1 = \nu_2 = \nu_3 = 0.005$, $c = 1$, a good control performance can be observed from simulation results as shown in Fig. 4.5, Fig. 4.6, Fig. 4.7, Fig. 4.8 and Fig. 4.9. I_3 is the 3×3 identity matrix and I_9 is the 9×9 identity matrix.

4.2.2 Experimental Results

For the safety, the experiments were carried out by semi-automatic mode. For the same reason, the altitude control is not implemented in the experiments. The quadrotor is vertically controlled by a human operator. The desired velocities are determined by using the signals from the RC system and the corresponding coordinates of the desired position are calculated by integrating the desired velocities. The activation functions for the neural-network are the same as the simulation. Due to the difference in loop time between the Personal Computer (PC) and the microprocessor, the optimal design parameter is not the same as the simulation. With the parameters $K_p = 0.5$, $K_1 = 0.01I_3$, $K_2 = 0.001I_3$, $K_3 = diag(220, 260, 8)$, $K_4 = diag(10.5, 12, 600)$, $\sigma_1 = \sigma_2 = \sigma_3 = 0.0001$, $\Gamma_1 = \Gamma_2 = \Gamma_3 = 0.001I_9$, $\lambda_1 = \lambda_2 = \lambda_3 = 1$, $\nu_1 = \nu_2 = \nu_3 = 1$, $c = 1$, the real performance of the controller is poor but the system is still

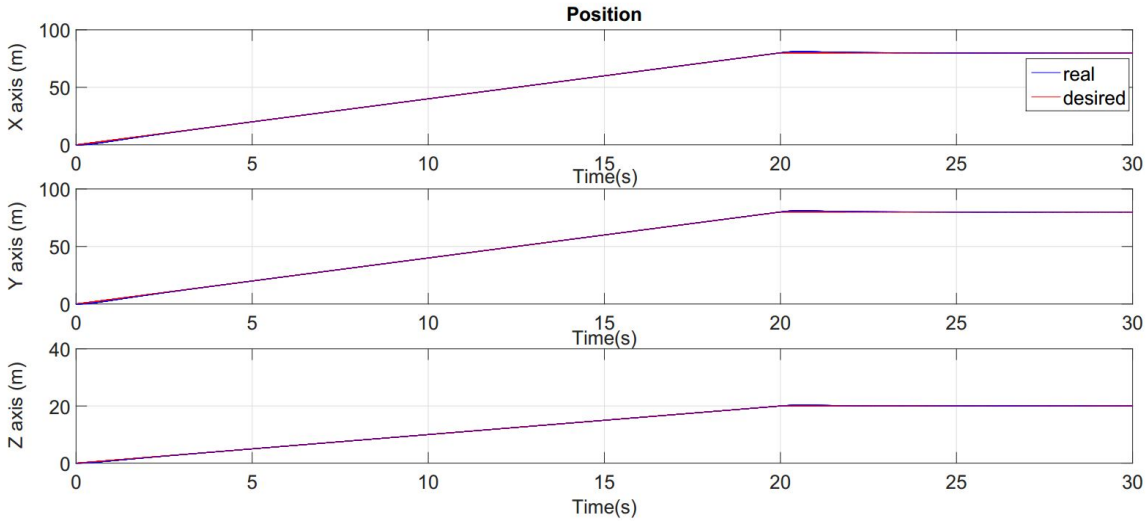

Figure 4.5: Simulation Results for Positions

converged, as shown in Fig. 4.10 and Fig. 4.11. These parameters are able to be used in the simulation as well. The flight test was carried out in a relative ideal weather with no loads. However, there are still gust of winds at about 100 s and 800 s. The desired position was reset at about 850 s to avoid the unexpected collision. Then, the system regain the control and the gust of wind disappeared.

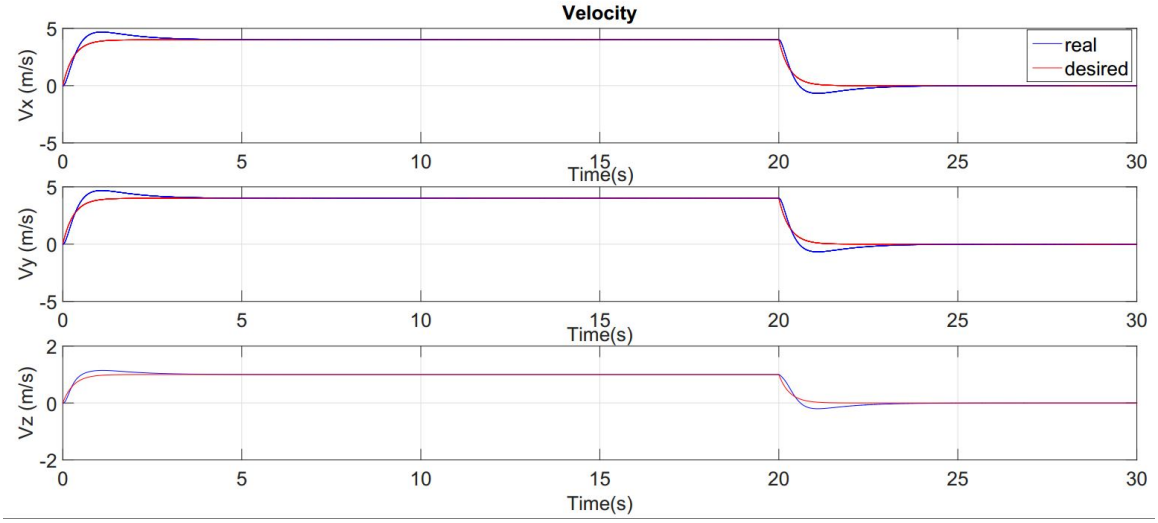

Figure 4.6: Simulation Results for Velocities

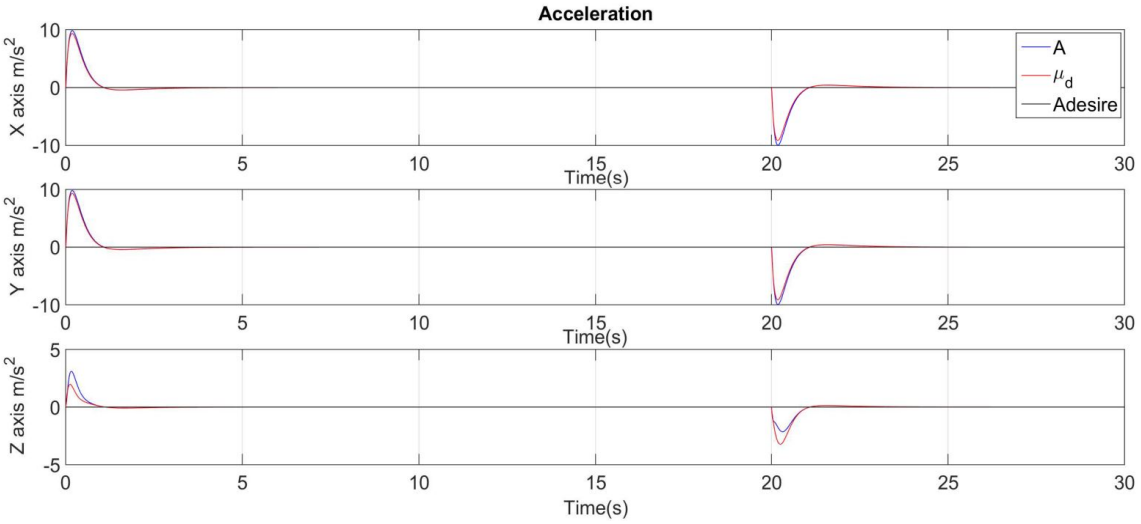

Figure 4.7: Simulation Results for Accelerations

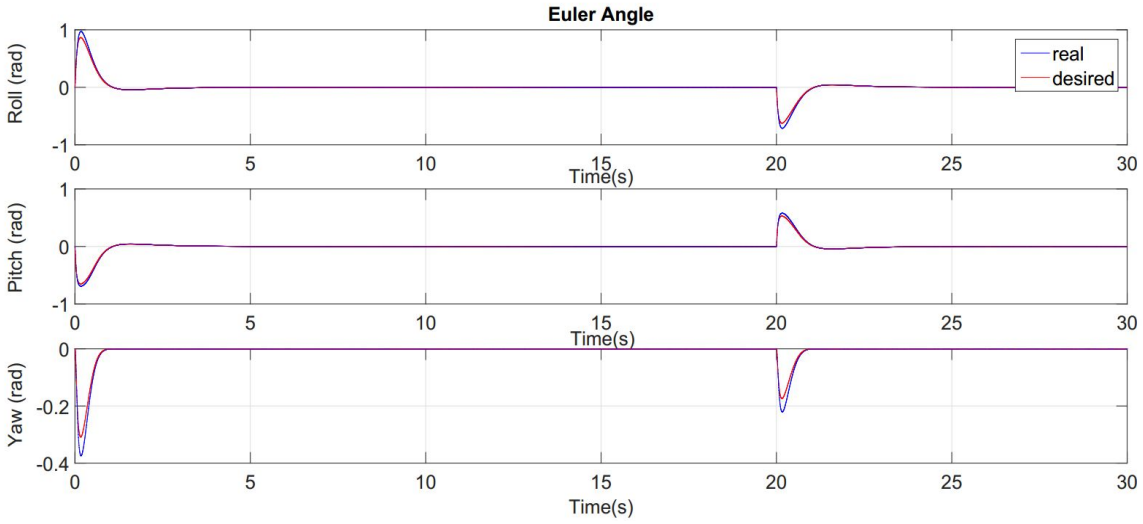

Figure 4.8: Simulation Results for Euler Angles

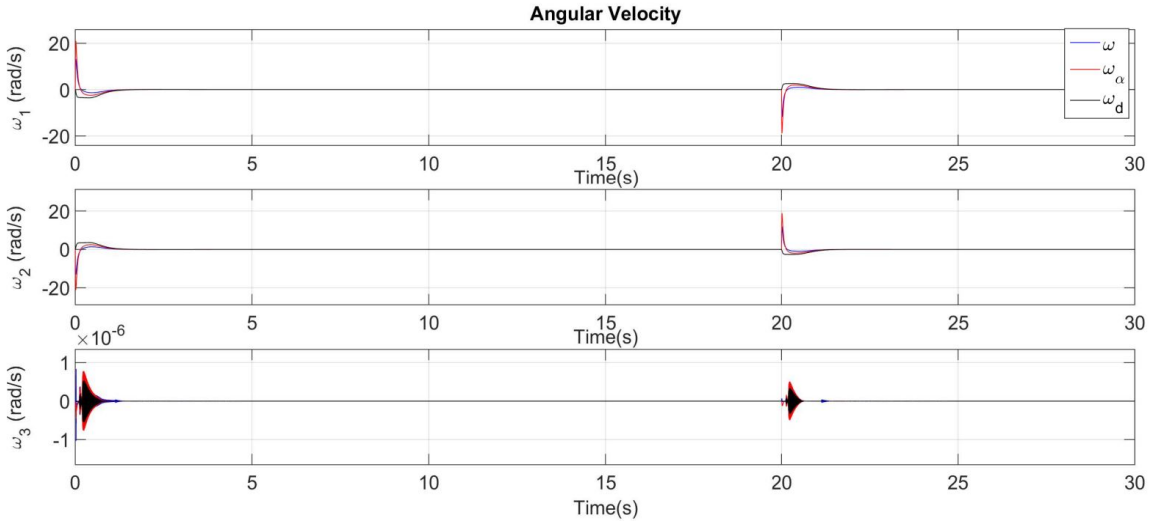

Figure 4.9: Simulation Results for Angular Velocities

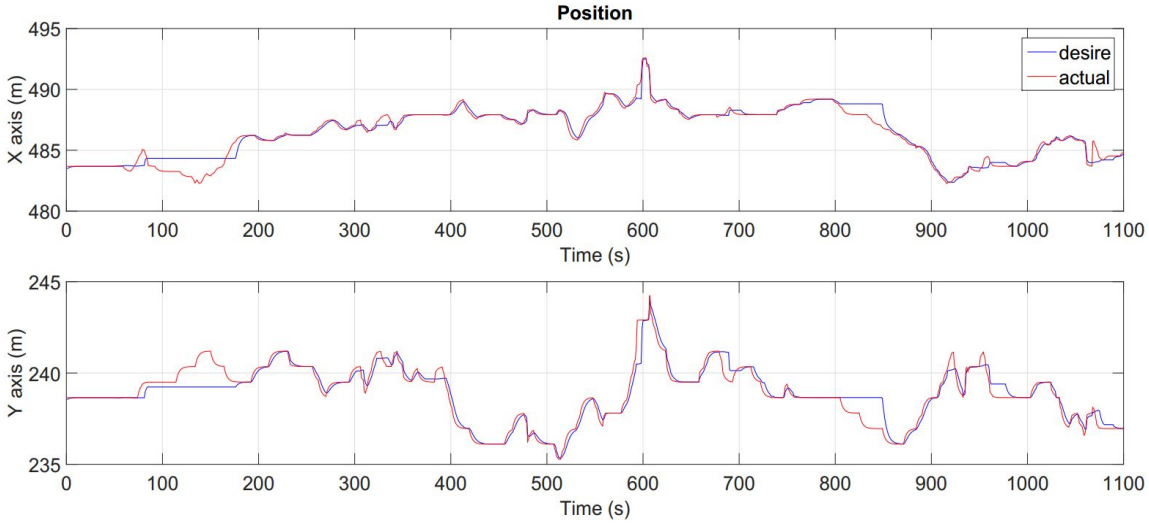

Figure 4.10: Experimental Results for Position Tracking

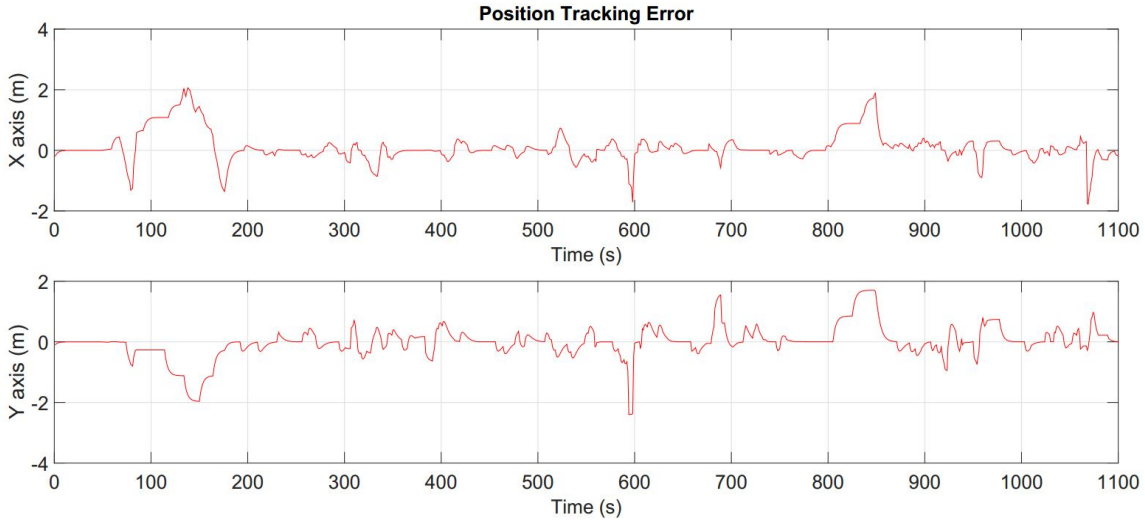

Figure 4.11: Experimental Results for Position Tracking Errors

4.3 Two Step Position Tracking Controller Design

In addition to the four step controller developed in the previous section, a two step position tracking controller is also developed. The controller design consists of two steps.

The position error is defined in (4.9).

The velocity error is defined as

$$\mathbf{e}_2 = \mathbf{V}_d - \mathbf{V} \tag{4.83}$$

where $\mathbf{V}_d = \dot{\mathbf{P}}_d = \begin{bmatrix} v_{dx} & v_{dy} & v_{dz} \end{bmatrix}^T$ denotes the desired translational velocity and $\mathbf{V} = \dot{\mathbf{P}} = \begin{bmatrix} v_x & v_y & v_z \end{bmatrix}^T$ denotes the actual translational velocity.

It is obvious that

$$\dot{\mathbf{e}}_1 = \mathbf{e}_2 \tag{4.84}$$

Inspired by [55], a function h is defined as

$$h\left(\mathbf{x},\varepsilon_1,\varepsilon_2\right) = \Delta\left(\mathbf{x},\varepsilon_1,\varepsilon_2\right)\mathbf{x} \tag{4.85}$$

with

$$\Delta\left(\mathbf{x},\varepsilon_1,\varepsilon_2\right) = \left(\varepsilon_1 + \varepsilon_2 \mathbf{x}^T\mathbf{x}\right)^{-\frac{1}{2}} \tag{4.86}$$

where ε_1 is a positive constant, ε_2 is a positive constant and $\mathbf{x}$ is a column vector.

Step 1. Position and Velocity Tracking

Set a positive definite Lyapunov candidate

$$V_1 = k_1\left[\left(\varepsilon_1 + \varepsilon_2 \mathbf{e}_1^T\mathbf{e}_1\right)^{\frac{1}{2}} - \varepsilon_1^{\frac{1}{2}}\right] + \frac{1}{2}\mathbf{e}_2^T\Gamma_{e_2}\mathbf{e}_2 \tag{4.87}$$

where k_1 is a positive parameter and Γ_{e_2} is a positive definite matrix which can be tuned to obtain a good performance.

The time derivative of (4.87) is given by

$$\dot{V}_1 = k_1\varepsilon_2\left(\varepsilon_1 + \varepsilon_2\mathbf{e}_1^T\mathbf{e}_1\right)^{-\frac{1}{2}}\dot{\mathbf{e}}_1^T\mathbf{e}_1 + \mathbf{e}_2^T\Gamma_{e_2}\dot{\mathbf{e}}_2 \tag{4.88}$$

By substituting the time derivative of (4.83) and (**??**) into (4.88), it results in

$$\dot{V}_1 = k_1\varepsilon_2\left(\varepsilon_1 + \varepsilon_2\mathbf{e}_1^T\mathbf{e}_1\right)^{-\frac{1}{2}}\dot{\mathbf{e}}_1^T\mathbf{e}_1 + \mathbf{e}_2^T\Gamma_{e_2}\left(\ddot{\mathbf{P}}_d - \ddot{\mathbf{P}}\right) \tag{4.89}$$

$$= k_1\varepsilon_2\left(\varepsilon_1 + \varepsilon_2\mathbf{e}_1^T\mathbf{e}_1\right)^{-\frac{1}{2}}\mathbf{e}_2^T\mathbf{e}_1 + \mathbf{e}_2^T\Gamma_{e_2}\left(\ddot{\mathbf{P}}_d - \dot{\mathbf{V}}\right) \tag{4.90}$$

The following can be produced by combining the two terms and introducing a virtual acceleration μ_d.

$$\dot{V}_1 = \mathbf{e}_2^T \left[k_1 \varepsilon_2 \left(\varepsilon_1 + \varepsilon_2 \mathbf{e}_1^T \mathbf{e}_1 \right)^{-\frac{1}{2}} \mathbf{e}_1 + \Gamma_{e_2} \left(\ddot{\mathbf{P}}_d - \dot{\mathbf{V}} + \mu_d - \mu_d \right) \right] \tag{4.91}$$

$$= \mathbf{e}_2^T \left[k_1 \varepsilon_2 \left(\varepsilon_1 + \varepsilon_2 \mathbf{e}_1^T \mathbf{e}_1 \right)^{-\frac{1}{2}} \mathbf{e}_1 + \Gamma_{e_2} \left(\ddot{\mathbf{P}}_d - \mu_d \right) + \Gamma_{e_2} \left(-\dot{\mathbf{V}} + \mu_d \right) \right] \tag{4.92}$$

Set

$$k_1 \varepsilon_2 \left(\varepsilon_1 + \varepsilon_2 \mathbf{e}_1^T \mathbf{e}_1 \right)^{-\frac{1}{2}} \mathbf{e}_1 + \Gamma_{e_2} \left(\ddot{\mathbf{P}}_d - \mu_d \right) = -\mathbf{K}_2 h \left(\mathbf{e}_2, \varepsilon_3, \varepsilon_4 \right)$$

from which, μ_d can be determined as

$$\begin{aligned} \mu_d &= \ddot{\mathbf{P}}_d + \Gamma_{e_2}^{-1} \left[k_1 \varepsilon_2 \left(\varepsilon_1 + \varepsilon_2 \mathbf{e}_1^T \mathbf{e}_1 \right)^{-\frac{1}{2}} \mathbf{e}_1 + \mathbf{K}_2 h \left(\mathbf{e}_2, \varepsilon_3, \varepsilon_4 \right) \right] \\ &= \dot{\mathbf{V}}_d + \Gamma_{e_2}^{-1} \left[k_1 \varepsilon_2 h \left(\mathbf{e}_1, \varepsilon_1, \varepsilon_2 \right) + \mathbf{K}_2 h \left(\mathbf{e}_2, \varepsilon_3, \varepsilon_4 \right) \right] \end{aligned} \tag{4.93}$$

where $\mathbf{K}_2$ is a diagonal gain matrix, ε_3 and ε_4 are two positive constants.

To avoid the singularity problem when extracting the desire attitude Q_d in Appendix C, the following assumption must be satisfied [55].

Assumption 1. *$\mu_d \notin L$ with $L = \{\mu_d \in R_{3\times 1}; \mu_d = \begin{bmatrix} 0 & 0 & \mu_{d3} \end{bmatrix}^T; \mu_{d3} \in (g - s, \infty)\}$, where s is an arbitrarily small positive constant.*

Set $\tilde{\mu} = -\mu + \mu_d$. It follows from Appendix A that $\tilde{\mu} = W^T \mathbf{q}_e$ [55]. Due to $\mu = \dot{\mathbf{V}}$, $\dot{V}_1$ can be rewritten as

$$\begin{aligned} \dot{V}_1 &= -\mathbf{e}_2^T \mathbf{K}_2 h \left(\mathbf{e}_2, \varepsilon_3, \varepsilon_4 \right) + \mathbf{e}_2^T \Gamma_{e_2} \left(-\dot{\mathbf{V}} + \mu_d \right) \\ &= -\mathbf{e}_2^T \mathbf{K}_2 h \left(\mathbf{e}_2, \varepsilon_3, \varepsilon_4 \right) + \mathbf{e}_2^T \Gamma_{e_2} \tilde{\mu} \\ &= -\mathbf{e}_2^T \mathbf{K}_2 h \left(\mathbf{e}_2, \varepsilon_3, \varepsilon_4 \right) + \mathbf{e}_2^T \Gamma_{e_2} \mathbf{W}^T \mathbf{q}_e \end{aligned} \tag{4.94}$$

Step 2. Attitude and Angular Velocity Tracking

The angular velocity error is defined as

$$\omega_e = \omega - \omega_\alpha \tag{4.95}$$

where ω_α denotes a virtual angular velocity, which will be determined later.

Then, taking the time derivative of (4.95) produces

$$\dot{\omega}_e = \dot{\omega} - \dot{\omega}_\alpha \tag{4.96}$$

A positive definite Lyapunov function candidate can be chosen as

$$V_2 = V_1 + \mathbf{q}_e^T \mathbf{q}_e + (q_{e0} - 1)^2 + \frac{1}{2}\omega_e^T \omega_e \tag{4.97}$$

The time derivative of (4.97) is given by

$$\dot{V}_2 = \dot{V}_1 + 2\mathbf{q}_e^T \dot{\mathbf{q}}_e + 2(q_{e0} - 1)\dot{q}_{e0} + \omega_e^T \dot{\omega}_e \tag{4.98}$$

By substituting (4.94) into (4.98), the following can be obtained.

$$\dot{V}_2 = -\mathbf{e}_2^T \mathbf{K}_2 h\left(\mathbf{e}_2, \varepsilon_3, \varepsilon_4\right) + \mathbf{e}_2^T \Gamma_{e_2} \mathbf{W}^T \mathbf{q}_e + 2\mathbf{q}_e^T \dot{\mathbf{q}}_e + 2\left(q_{e0} - 1\right)\dot{q}_{e0} + \omega_e^T \dot{\omega}_e \tag{4.99}$$

By substituting (4.96) into (4.99) and rewriting $\mathbf{e}_2^T \Gamma_{e_2} \mathbf{W}^T \mathbf{q}_e$ as $\mathbf{q}_e^T \mathbf{W} \Gamma_{e_2}^T \mathbf{e}_2$, $\dot{V}_2$ can be written as

$$\dot{V}_2 = -\mathbf{e}_2^T \mathbf{K}_2 h\left(\mathbf{e}_2, \varepsilon_3, \varepsilon_4\right) + \mathbf{q}_e^T \mathbf{W} \Gamma_{e_2}^T \mathbf{e}_2 + 2\mathbf{q}_e^T \dot{\mathbf{q}}_e + 2\left(q_{e0} - 1\right)\dot{q}_{e0} + \omega_e^T \left(\dot{\omega} - \dot{\omega}_\alpha\right) \tag{4.100}$$

By substituting (4.8) and (4.4) into (4.100), it follows from (4.100) that

$$\begin{aligned}
\dot{V}_2 &= -\mathbf{e}_2^T \mathbf{K}_2 h\left(\mathbf{e}_2, \varepsilon_3, \varepsilon_4\right) + \mathbf{q}_e^T \mathbf{W} \Gamma_{e_2}^T \mathbf{e}_2 + \mathbf{q}_e^T \left(q_{e0}\left(\omega - \omega_d\right) + S\left(\mathbf{q}_e\right)\left(\omega + \omega_d\right)\right) \\
&\quad + \left(q_{e0} - 1\right)\mathbf{q}_e^T \left(\omega_d - \omega\right) + \omega_e^T \left(\mathbf{I}_f^{-1}\left(-\omega \times \left(\mathbf{I}_f \cdot \omega\right) + \tau\right) - \dot{\omega}_\alpha\right) \\
&= -\mathbf{e}_2^T \mathbf{K}_2 h\left(\mathbf{e}_2, \varepsilon_3, \varepsilon_4\right) + \mathbf{q}_e^T \mathbf{W} \Gamma_{e_2}^T \mathbf{e}_2 + q_{e0}\mathbf{q}_e^T \left(\omega - \omega_d\right) + \mathbf{q}_e^T S\left(\mathbf{q}_e\right)\left(\omega + \omega_d\right) \\
&\quad + (1 - q_{e0})\mathbf{q}_e^T \left(\omega - \omega_d\right) + \omega_e^T \left(\mathbf{I}_f^{-1}\left(-\omega \times \left(\mathbf{I}_f \cdot \omega\right) + \tau\right) - \dot{\omega}_\alpha\right)
\end{aligned} \tag{4.101}$$

where ω_d denotes the desired angular velocity associated with Q_d, for details refer to Appendix D. The expression of ω_d is shown as

$$\omega_d = M(\mu_d)\dot{\mu}_d \tag{4.102}$$

where the expression of $M(\mu_d)$ is given by (D.14).

By combining the 3rd term and the 5th term in (4.101), using the fact that the 4th term equals to zero (for details refers to Appendix B), the $\dot{V}_2$ becomes

$$\begin{aligned}
\dot{V}_2 &= -\mathbf{e}_2^T \mathbf{K}_2 h\left(\mathbf{e}_2, \varepsilon_3, \varepsilon_4\right) + \mathbf{q}_e^T \mathbf{W} \Gamma_{e_2}^T \mathbf{e}_2 + \mathbf{q}_e^T \left(\omega - \omega_d\right) \\
&\quad + \omega_e^T \left(\mathbf{I}_f^{-1}\left(-\omega \times \left(\mathbf{I}_f \cdot \omega\right) + \tau\right) - \dot{\omega}_\alpha\right) \\
&= -\mathbf{e}_2^T \mathbf{K}_2 h\left(\mathbf{e}_2, \varepsilon_3, \varepsilon_4\right) + \mathbf{q}_e^T \left(\mathbf{W} \Gamma_{e_2}^T \mathbf{e}_2 + \left(\omega - \omega_d\right)\right) \\
&\quad + \omega_e^T \left(\mathbf{I}_f^{-1}\left(-\omega \times \left(\mathbf{I}_f \cdot \omega\right) + \tau\right) - \dot{\omega}_\alpha\right)
\end{aligned} \tag{4.103}$$

Due to (4.95), $\omega = \omega_e + \omega_\alpha$. By replacing ω with $\omega_e + \omega_\alpha$, $\dot{V}_2$ can be written as

$$\begin{aligned}
\dot{V}_2 &= -\mathbf{e}_2^T \mathbf{K}_2 h\left(\mathbf{e}_2, \varepsilon_3, \varepsilon_4\right) + \mathbf{q}_e^T \left(\mathbf{W} \Gamma_{e_2}^T \mathbf{e}_2 + \left(\omega_e + \omega_\alpha - \omega_d\right)\right) \\
&\quad + \omega_e^T \left(\mathbf{I}_f^{-1}\left(-\omega \times \left(\mathbf{I}_f \cdot \omega\right) + \tau\right) - \dot{\omega}_\alpha\right) \\
&= -\mathbf{e}_2^T \mathbf{K}_2 h\left(\mathbf{e}_2, \varepsilon_3, \varepsilon_4\right) + \mathbf{q}_e^T \left(\mathbf{W} \Gamma_{e_2}^T \mathbf{e}_2 + \omega_e + \omega_\alpha - \omega_d\right) \\
&\quad + \omega_e^T \left(\mathbf{I}_f^{-1}\left(-\omega \times \left(\mathbf{I}_f \cdot \omega\right) + \tau\right) - \dot{\omega}_\alpha\right)
\end{aligned} \tag{4.104}$$

By taking out ω_e from the 2nd term in (4.104), (4.104) can be rewritten as

$$\begin{aligned}\dot{V}_2 &= -\mathbf{e}_2^T\mathbf{K}_2 h\left(\mathbf{e}_2,\varepsilon_3,\varepsilon_4\right)+\mathbf{q}_e^T\left(\mathbf{W}\Gamma_{e_2}^T\mathbf{e}_2-\omega_d+\omega_\alpha\right)\\&+\mathbf{q}_e^T\omega_e+\omega_e^T\left(\mathbf{I}_f^{-1}\left(-\omega\times\left(\mathbf{I}_f\cdot\omega\right)+\tau\right)-\dot{\omega}_\alpha\right)\\&=-\mathbf{e}_2^T\mathbf{K}_2 h\left(\mathbf{e}_2,\varepsilon_3,\varepsilon_4\right)+\mathbf{q}_e^T\left(\mathbf{W}\Gamma_{e_2}^T\mathbf{e}_2-\omega_d+\omega_\alpha\right)\\&+\omega_e^T\left(\mathbf{q}_e+\mathbf{I}_f^{-1}\left(-\omega\times\left(\mathbf{I}_f\cdot\omega\right)+\tau\right)-\dot{\omega}_\alpha\right)\end{aligned}\tag{4.105}$$

Set

$$\omega_\alpha=-\mathbf{W}\Gamma_{e_2}^T\mathbf{e}_2-\mathbf{K}_q\mathbf{q}_e+\omega_d\tag{4.106}$$

then, $\dot{V}_2$ becomes

$$\begin{aligned}\dot{V}_2&=-\mathbf{e}_2^T\mathbf{K}_2 h\left(\mathbf{e}_2,\varepsilon_3,\varepsilon_4\right)-\mathbf{q}_e^T\mathbf{K}_q\mathbf{q}_e+\omega_e^T\left\{\mathbf{q}_e+\mathbf{I}_f^{-1}\left[-\omega\times\left(\mathbf{I}_f\cdot\omega\right)+\tau\right]-\dot{\omega}_\alpha\right\}\\&=-\mathbf{e}_2^T\mathbf{K}_2 h\left(\mathbf{e}_2,\varepsilon_3,\varepsilon_4\right)-\mathbf{q}_e^T\mathbf{K}_q\mathbf{q}_e+\omega_e^T\left\{\mathbf{q}_e-\dot{\omega}_\alpha+\mathbf{I}_f^{-1}\left[-\omega\times\left(\mathbf{I}_f\cdot\omega\right)+\tau\right]\right\}\end{aligned}\tag{4.107}$$

By substituting (4.51) into (4.107), it produces

$$\begin{aligned}\dot{V}_2&=-\mathbf{e}_2^T\mathbf{K}_2 h\left(\mathbf{e}_2,\varepsilon_3,\varepsilon_4\right)\text{-}\mathbf{q}_e^T\mathbf{K}_q\mathbf{q}_e\\&+\omega_e^T\left(\begin{bmatrix}q_{e1}-\dot{\omega}_{\alpha1}+\frac{1}{I_x}\left(I_y-I_z\right)\omega_2\omega_3+\frac{1}{I_x}\tau_1\\q_{e2}-\dot{\omega}_{\alpha2}+\frac{1}{I_y}\left(I_z-I_x\right)\omega_1\omega_3+\frac{1}{I_y}\tau_2\\q_{e3}-\dot{\omega}_{\alpha3}+\frac{1}{I_z}\left(I_x-I_y\right)\omega_1\omega_2+\frac{1}{I_z}\tau_3\end{bmatrix}\right)\end{aligned}\tag{4.108}$$

$$\begin{aligned}&=-\mathbf{e}_2^T\mathbf{K}_2 h\left(\mathbf{e}_2,\varepsilon_3,\varepsilon_4\right)-\mathbf{q}_e^T\mathbf{K}_q\mathbf{q}_e\\&+\omega_{e1}\left(q_{e1}-\dot{\omega}_{\alpha1}+\frac{1}{I_x}\left(I_y-I_z\right)\omega_2\omega_3+\frac{1}{I_x}\tau_1\right)\\&+\omega_{e2}\left(q_{e2}-\dot{\omega}_{\alpha2}+\frac{1}{I_y}\left(I_z-I_x\right)\omega_1\omega_3+\frac{1}{I_y}\tau_2\right)\\&+\omega_{e3}\left(q_{e3}-\dot{\omega}_{\alpha3}+\frac{1}{I_z}\left(I_x-I_y\right)\omega_1\omega_2+\frac{1}{I_z}\tau_3\right)\end{aligned}\tag{4.109}$$

Assume that $\frac{1}{I_x}\left(I_y-I_z\right)$, $\frac{1}{I_y}\left(I_z-I_x\right)$, and$\frac{1}{I_z}\left(I_x-I_y\right)$ are unknown. Define

$$\begin{aligned}V_6&=\frac{1}{2}\gamma_1\left(\delta_1-\hat{\delta}_1\right)^2\\&+\frac{1}{2}\gamma_1\left(\delta_2-\hat{\delta}_2\right)^2\\&+\frac{1}{2}\gamma_1\left(\delta_3-\hat{\delta}_3\right)^2\\&+\frac{1}{2}\lambda_1\beta_1\left(I_x-\hat{I}_x\right)^2\\&+\frac{1}{2}\lambda_2\beta_2\left(I_y-\hat{I}_y\right)^2\\&+\frac{1}{2}\lambda_3\beta_3\left(I_z-\hat{I}_z\right)^2\end{aligned}\tag{4.110}$$

where γ_1, γ_2, γ_3, λ_1, λ_2, and λ_3 are positive design parameters, $\delta_1 = \frac{1}{I_x}(I_y - I_z)$, $\delta_2 = \frac{1}{I_y}(I_z - I_x)$, $\delta_3 = \frac{1}{I_z}(I_x - I_y)$, and $\hat{\delta}_1$, $\hat{\delta}_2$, and $\hat{\delta}_3$ are the estimates of δ_1, δ_2, and δ_3, respectively.

By defining the same symbols as in (4.53) and defining the Lyapunov candidate V_6 as shown in (4.110), the time derivative of $V = V_2 + V_6$ is given by

$$\begin{aligned}
\dot{V} &= \dot{V}_2 + \dot{V}_6 \\
&= -\mathbf{e}_2^T \mathbf{K}_2 h(\mathbf{e}_2, \varepsilon_3, \varepsilon_4) - \mathbf{q}_e^T \mathbf{K}_q \mathbf{q}_e \\
&+ \omega_{e1}(q_{e1} - \dot{\omega}_{\alpha 1} + \delta_1 \omega_2 \omega_3 + \beta_1 \tau_1) \\
&+ \omega_{e2}(q_{e2} - \dot{\omega}_{\alpha 2} + \delta_2 \omega_1 \omega_3 + \beta_2 \tau_2) \\
&+ \omega_{e3}(q_{e3} - \dot{\omega}_{\alpha 3} + \delta_3 \omega_1 \omega_2 + \beta_3 \tau_3) \\
&+ \gamma_1 \left(\delta_1 - \hat{\delta}_1\right)\left(-\dot{\hat{\delta}}_1\right) + \gamma_2 \left(\delta_2 - \hat{\delta}_2\right)\left(-\dot{\hat{\delta}}_2\right) + \gamma_3 \left(\delta_3 - \hat{\delta}_3\right)\left(-\dot{\hat{\delta}}_3\right) \\
&+ \lambda_1 \beta_1 \left(I_x - \hat{I}_x\right)\left(-\dot{\hat{I}}_x\right) + \lambda_2 \beta_2 \left(I_y - \hat{I}_y\right)\left(-\dot{\hat{I}}_y\right) + \lambda_3 \beta_3 \left(I_z - \hat{I}_z\right)\left(-\dot{\hat{I}}_z\right)
\end{aligned} \tag{4.111}$$

To introduce the approximation in the controller, by replacing the δ_1, δ_2, and δ_3 with $\hat{\delta}_1$, $\hat{\delta}_2$, and $\hat{\delta}_3$ in the 2nd to 4th lines and adding some items in the 5th line in (4.111) to eliminate the change, it can be shown that

$$\begin{aligned}
\dot{V} &= -\mathbf{e}_2^T \mathbf{K}_2 h(\mathbf{e}_2, \varepsilon_3, \varepsilon_4) - \mathbf{q}_e^T \mathbf{K}_q \mathbf{q}_e \\
&+ \omega_{e1}\left(q_{e1} - \dot{\omega}_{\alpha 1} + \hat{\delta}_1 \omega_2 \omega_3 + \beta_1 \tau_1\right) \\
&+ \omega_{e2}\left(q_{e2} - \dot{\omega}_{\alpha 2} + \hat{\delta}_2 \omega_1 \omega_3 + \beta_2 \tau_2\right) \\
&+ \omega_{e3}\left(q_{e3} - \dot{\omega}_{\alpha 3} + \hat{\delta}_3 \omega_1 \omega_2 + \beta_3 \tau_3\right) \\
&+ \gamma_1 \left(\delta_1 - \hat{\delta}_1\right)\left(-\dot{\hat{\delta}}_1 + \gamma_1^{-1} \omega_{e1} \omega_2 \omega_3\right) \\
&+ \gamma_2 \left(\delta_2 - \hat{\delta}_2\right)\left(-\dot{\hat{\delta}}_2 + \gamma_2^{-1} \omega_{e2} \omega_1 \omega_3\right) \\
&+ \gamma_3 \left(\delta_3 - \hat{\delta}_3\right)\left(-\dot{\hat{\delta}}_3 + \gamma_3^{-1} \omega_{e3} \omega_1 \omega_2\right) \\
&+ \lambda_1 \beta_1 \left(I_x - \hat{I}_x\right)\left(-\dot{\hat{I}}_x\right) + \lambda_2 \beta_2 \left(I_y - \hat{I}_y\right)\left(-\dot{\hat{I}}_y\right) + \lambda_3 \beta_3 \left(I_z - \hat{I}_z\right)\left(-\dot{\hat{I}}_z\right)
\end{aligned} \tag{4.112}$$

Define

$$\begin{aligned}
u_1 &= \frac{\tau_1}{\hat{I}_x} \\
u_2 &= \frac{\tau_2}{\hat{I}_y} \\
u_3 &= \frac{\tau_3}{\hat{I}_z}
\end{aligned} \tag{4.113}$$

It can be verified that the followings are true

$$\begin{aligned}\beta_1\tau_1 &= u_1 - \beta_1(I_x - \hat{I}_x)u_1\\ \beta_2\tau_2 &= u_2 - \beta_2(I_y - \hat{I}_y)u_2\\ \beta_3\tau_3 &= u_3 - \beta_3(I_z - \hat{I}_z)u_3\end{aligned} \tag{4.114}$$

By introducing the following adaptation laws for $\hat{\varrho}_1$, $\hat{\varrho}_2$, and $\hat{\varrho}_3$

$$\begin{aligned}\dot{\hat{\delta}}_1 &= \gamma_1^{-1}\omega_{e1}\omega_2\omega_3\\ \dot{\hat{\delta}}_2 &= \gamma_2^{-1}\omega_{e2}\omega_1\omega_3\\ \dot{\hat{\delta}}_3 &= \gamma_3^{-1}\omega_{e3}\omega_1\omega_2\end{aligned} \tag{4.115}$$

$\dot{V}$ becomes

$$\begin{aligned}\dot{V} = &-\mathbf{e}_2^T\mathbf{K}_2 h\left(\mathbf{e}_2, \varepsilon_3, \varepsilon_4\right) - \mathbf{q}_e^T\mathbf{K}_q\mathbf{q}_e\\ &+ \omega_{e1}\left(q_{e1} + \hat{\delta}_1\omega_2\omega_3 + u_1 - \beta_1(I_x - \hat{I}_x)u_1 - \dot{\omega}_{\alpha 1}\right)\\ &+ \omega_{e2}\left(q_{e2} + \hat{\delta}_2\omega_1\omega_3 + u_2 - \beta_2(I_y - \hat{I}_y)u_2 - \dot{\omega}_{\alpha 2}\right)\\ &+ \omega_{e3}\left(q_{e3} + \hat{\delta}_3\omega_1\omega_2 + u_3 - \beta_3(I_z - \hat{I}_z)u_3 - \dot{\omega}_{\alpha 3}\right)\\ &+ \lambda_1\beta_1\left(I_x - \hat{I}_x\right)\left(-\dot{\hat{I}}_x\right) + \lambda_2\beta_2\left(I_y - \hat{I}_y\right)\left(-\dot{\hat{I}}_y\right) + \lambda_3\beta_3\left(I_z - \hat{I}_z\right)\left(-\dot{\hat{I}}_z\right)\end{aligned} \tag{4.116}$$

By separating the terms related to moment of inertia from the 2nd to 4th lines in (4.116), it results in

$$\begin{aligned}\dot{V} = &-\mathbf{e}_2^T\mathbf{K}_2 h\left(\mathbf{e}_2, \varepsilon_3, \varepsilon_4\right) - \mathbf{q}_e^T\mathbf{K}_q\mathbf{q}_e\\ &+ \omega_{e1}\left(q_{e1} + \hat{\delta}_1\omega_2\omega_3 + u_1 - \dot{\omega}_{\alpha 1}\right)\\ &+ \omega_{e2}\left(q_{e2} + \hat{\delta}_2\omega_1\omega_3 + u_2 - \dot{\omega}_{\alpha 2}\right)\\ &+ \omega_{e3}\left(q_{e3} + \hat{\delta}_3\omega_1\omega_2 + u_3 - \dot{\omega}_{\alpha 3}\right)\\ &- \lambda_1\beta_1\left(I_x - \hat{I}_x\right)\dot{\hat{I}}_x - \lambda_2\beta_2\left(I_y - \hat{I}_y\right)\dot{\hat{I}}_y - \lambda_3\beta_3\left(I_z - \hat{I}_z\right)\dot{\hat{I}}_z\\ &- \omega_{e1}\beta_1(I_x - \hat{I}_x)u_1 - \omega_{e2}\beta_2(I_y - \hat{I}_y)u_2 - \omega_{e3}\beta_3(I_z - \hat{I}_z)u_3\end{aligned} \tag{4.117}$$

By combining the last two lines in (4.117), it follows that

$$\begin{aligned}\dot{V} = &-\mathbf{e}_2^T\mathbf{K}_2 h\left(\mathbf{e}_2, \varepsilon_3, \varepsilon_4\right) - \mathbf{q}_e^T\mathbf{K}_q\mathbf{q}_e \\ &+ \omega_{e1}\left(q_{e1} + \hat{\delta}_1\omega_2\omega_3 + u_1 - \dot{\omega}_{\alpha 1}\right) \\ &+ \omega_{e2}\left(q_{e2} + \hat{\delta}_2\omega_1\omega_3 + u_2 - \dot{\omega}_{\alpha 2}\right) \\ &+ \omega_{e3}\left(q_{e3} + \hat{\delta}_3\omega_1\omega_2 + u_3 - \dot{\omega}_{\alpha 3}\right) \\ &- \beta_1\left(I_x - \hat{I}_x\right)\left(\lambda_1\dot{\hat{I}}_x + \omega_{e1}u_1\right) \\ &- \beta_2\left(I_y - \hat{I}_y\right)\left(\lambda_2\dot{\hat{I}}_y + \omega_{e2}u_2\right) \\ &- \beta_3\left(I_z - \hat{I}_z\right)\left(\lambda_3\dot{\hat{I}}_z + \omega_{e3}u_3\right)\end{aligned} \tag{4.118}$$

Set the following adaptation laws for $\hat{I}_x$, $\hat{I}_y$, $\hat{I}_z$

$$\begin{aligned}\dot{\hat{I}}_x &= -\omega_{e1}u_1/\lambda_1 \\ \dot{\hat{I}}_y &= -\omega_{e2}u_2/\lambda_2 \\ \dot{\hat{I}}_z &= -\omega_{e3}u_3/\lambda_3\end{aligned} \tag{4.119}$$

Then, substituting (4.119) into (4.118) gives

$$\begin{aligned}\dot{V} = &-\mathbf{e}_2^T\mathbf{K}_2 h\left(\mathbf{e}_2, \varepsilon_3, \varepsilon_4\right) - \mathbf{q}_e^T\mathbf{K}_q\mathbf{q}_e \\ &+ \omega_{e1}\left(q_{e1} + \hat{\delta}_1\omega_2\omega_3 + u_1 - \dot{\omega}_{\alpha 1}\right) \\ &+ \omega_{e2}\left(q_{e2} + \hat{\delta}_2\omega_1\omega_3 + u_2 - \dot{\omega}_{\alpha 2}\right) \\ &+ \omega_{e3}\left(q_{e3} + \hat{\delta}_3\omega_1\omega_2 + u_3 - \dot{\omega}_{\alpha 3}\right)\end{aligned} \tag{4.120}$$

Set the following

$$\begin{aligned}\begin{bmatrix} -k_{ux}\omega_{e1} \\ -k_{uy}\omega_{e2} \\ -k_{uz}\omega_{e3}\end{bmatrix} &= \begin{bmatrix} \frac{1}{2}\omega_{e1} + q_{e1} + \hat{\delta}_1\omega_2\omega_3 + u_1 - \dot{\omega}_{\alpha 1} \\ \frac{1}{2}\omega_{e2} + q_{e2} + \hat{\delta}_2\omega_1\omega_3 + u_2 - \dot{\omega}_{\alpha 2} \\ \frac{1}{2}\omega_{e3} + q_{e3} + \hat{\delta}_3\omega_1\omega_2 + u_3 - \dot{\omega}_{\alpha 3}\end{bmatrix} \\ &= \begin{bmatrix} \frac{1}{2}\omega_{e1} + q_{e1} + \hat{\delta}_1\omega_2\omega_3 + \frac{\tau_1}{\hat{I}_x} - \dot{\omega}_{\alpha 1} \\ \frac{1}{2}\omega_{e2} + q_{e2} + \hat{\delta}_2\omega_1\omega_3 + \frac{\tau_2}{\hat{I}_y} - \dot{\omega}_{\alpha 2} \\ \frac{1}{2}\omega_{e3} + q_{e3} + \hat{\delta}_3\omega_1\omega_2 + \frac{\tau_3}{\hat{I}_z} - \dot{\omega}_{\alpha 3}\end{bmatrix}\end{aligned} \tag{4.121}$$

where k_{ux}, k_{uy}, and k_{uz} denote the design parameters.

Then, the control law can be solved as

$$\begin{bmatrix} \tau_1 \\ \tau_2 \\ \tau_3\end{bmatrix} = \begin{bmatrix} \hat{I}_x\left(-k_{ux}\omega_{e1} - \frac{1}{2}\omega_{e1} - q_{e1} + \dot{\omega}_{\alpha 1} - \hat{\delta}_1\omega_2\omega_3\right) \\ \hat{I}_y\left(-k_{uy}\omega_{e2} - \frac{1}{2}\omega_{e2} - q_{e2} + \dot{\omega}_{\alpha 2} - \hat{\delta}_2\omega_1\omega_3\right) \\ \hat{I}_z\left(-k_{uz}\omega_{e3} - \frac{1}{2}\omega_{e3} - q_{e3} + \dot{\omega}_{\alpha 3} - \hat{\delta}_3\omega_1\omega_2\right)\end{bmatrix} \tag{4.122}$$

Replacing u_1, u_2, and u_3 with $\frac{\tau_1}{\hat{I}_x}$, $\frac{\tau_2}{\hat{I}_y}$, and $\frac{\tau_3}{\hat{I}_z}$ in (4.120) and taking (4.122) into consideration yield

$$\dot{V} = -\mathbf{e}_2^T \mathbf{K}_2 h\left(\mathbf{e}_2, \varepsilon_3, \varepsilon_4\right) - \mathbf{q}_e^T \mathbf{K}_q \mathbf{q}_e - k_{ux}\omega_{e1}^2 - k_{uy}\omega_{e2}^2 - k_{uz}\omega_{e3}^2 \tag{4.123}$$

By replacing the 3rd to 5th terms in (4.123) with a matrix representation, the following can be obtained.

$$\dot{V} = -\mathbf{e}_2^T \mathbf{K}_2 h\left(\mathbf{e}_2, \varepsilon_3, \varepsilon_4\right) - \mathbf{q}_e^T \mathbf{K}_q \mathbf{q}_e - \omega_e^T \mathbf{K}_u \omega_e \leq 0 \tag{4.124}$$

where $\mathbf{K}_u = diag(k_{ux}, k_{uy}, k_{uz})$.

A block diagram for the designed system is shown in Fig. 4.12.

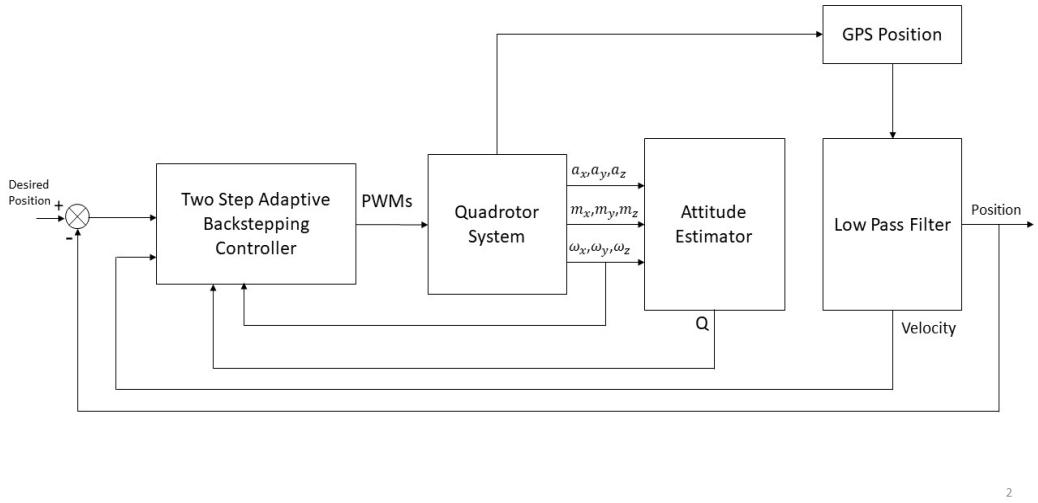

Figure 4.12: Block Diagram of the System with Two Step Controller

4.3.1 Stability Analysis

With the virtual acceleration μ_d in (4.93), $\dot{\mathbf{e}}_2$ can be expressed as

$$\begin{aligned}
\dot{\mathbf{e}}_2 &= \ddot{\mathbf{P}}_d - \dot{\mathbf{V}} = \ddot{\mathbf{P}}_d - \left(\mu_d - \mu_d + \mu\right) = \ddot{\mathbf{P}}_d - \left(\mu_d - \tilde{\mu}\right) \\
&= \ddot{\mathbf{P}}_d - \left(\ddot{\mathbf{P}}_d + \Gamma_{e_2}^{-1}\left[k_1 \varepsilon_2 h\left(\mathbf{e}_1, \varepsilon_1, \varepsilon_2\right) + \mathbf{K}_2 h\left(\mathbf{e}_2, \varepsilon_3, \varepsilon_4\right)\right] - \tilde{\mu}\right) \\
&= -\Gamma_{e_2}^{-1} k_1 \varepsilon_2 h\left(\mathbf{e}_1, \varepsilon_1, \varepsilon_2\right) - \mathbf{\Gamma}_{\mathbf{e_2}}^{-\mathbf{1}} \mathbf{K}_2 h\left(\mathbf{e}_2, \varepsilon_3, \varepsilon_4\right) + \tilde{\mu} \\
&= -\Gamma_{e_2}^{-1} k_1 \varepsilon_2 h\left(\mathbf{e}_1, \varepsilon_1, \varepsilon_2\right) - \mathbf{\Gamma}_{\mathbf{e_2}}^{-\mathbf{1}} \mathbf{K}_2 h\left(\mathbf{e}_2, \varepsilon_3, \varepsilon_4\right) + W^T \mathbf{q}_e
\end{aligned} \tag{4.125}$$

By differentiating (4.125), $\ddot{\mathbf{e}}_2$ is given by

$$\ddot{\mathbf{e}}_2 = -\Gamma_{e_2}^{-1} k_1 \frac{\partial h\left(\mathbf{e}_1, \varepsilon_1, \varepsilon_2\right)}{\partial \mathbf{e}_1} \dot{\mathbf{e}}_1 - \mathbf{\Gamma}_{\mathbf{e_2}}^{-\mathbf{1}} \mathbf{K}_2 \frac{\partial h\left(\mathbf{e}_2, \varepsilon_3, \varepsilon_4\right)}{\partial \mathbf{e}_2} \dot{\mathbf{e}}_2 + \dot{W}^T \mathbf{q}_e + W^T \dot{\mathbf{q}}_e \tag{4.126}$$

With the control law in (4.122), the dynamic equation for ω_e can be given by

$$\begin{aligned}\dot{\omega}_e &= \dot{\omega} - \dot{\omega}_\alpha = \mathbf{I}_f^{-1}\left[-\omega \times (\mathbf{I}_f \cdot \omega) + \tau\right] - \dot{\omega}_\alpha \\ &= \begin{bmatrix} \frac{1}{I_x}(I_y - I_z)\,\omega_2\omega_3 + \frac{1}{I_x}\tau_1 - \dot{\omega}_{\alpha 1} \\ \frac{1}{I_y}(I_z - I_x)\,\omega_1\omega_3 + \frac{1}{I_y}\tau_2 - \dot{\omega}_{\alpha 2} \\ \frac{1}{I_z}(I_x - I_y)\,\omega_1\omega_2 + \frac{1}{I_z}\tau_3 - \dot{\omega}_{\alpha 3} \end{bmatrix} \\ &= \begin{bmatrix} \frac{1}{I_x}(I_y - I_z)\,\omega_2\omega_3 + \frac{\hat{I}_x}{I_x}\left(-k_{ux}\omega_{e1} - \frac{1}{2}\omega_{e1} - q_{e1} + \dot{\omega}_{\alpha 1} - \hat{\delta}_1\omega_2\omega_3\right) - \dot{\omega}_{\alpha 1} \\ \frac{1}{I_y}(I_z - I_x)\,\omega_1\omega_3 + \frac{\hat{I}_y}{I_y}\left(-k_{uy}\omega_{e2} - \frac{1}{2}\omega_{e2} - q_{e2} + \dot{\omega}_{\alpha 2} - \hat{\delta}_2\omega_1\omega_3\right) - \dot{\omega}_{\alpha 2} \\ \frac{1}{I_z}(I_x - I_y)\,\omega_1\omega_2 + \frac{\hat{I}_z}{I_z}\left(-k_{uz}\omega_{e3} - \frac{1}{2}\omega_{e3} - q_{e3} + \dot{\omega}_{\alpha 3} - \hat{\delta}_3\omega_1\omega_2\right) - \dot{\omega}_{\alpha 3} \end{bmatrix} \end{aligned} \tag{4.127}$$

By taking the time derivative of (4.106), it gives

$$\dot{\omega}_\alpha = -\dot{\mathbf{W}}\Gamma_{e_2}^T\mathbf{e}_2 - \mathbf{W}\Gamma_{e_2}^T\dot{\mathbf{e}}_2 - \mathbf{K}_q\dot{\mathbf{q}}_e + \dot{\omega}_d \tag{4.128}$$

According to (A.22), $\dot{W}$ can be given as

$$\dot{W} = 2\frac{\dot{T}}{m}\bar{k}^T + 2\frac{T}{m}\dot{\bar{k}}^T \tag{4.129}$$

where $\bar{k}^T$ is shown in (A.19). By differentiating $\bar{k}$ in (A.19), $\dot{\bar{k}}$ can be expressed as

$$\dot{\bar{k}} = \begin{bmatrix} \dot{k}_{11} & \dot{k}_{12} & \dot{k}_{13} \\ \dot{k}_{21} & \dot{k}_{22} & \dot{k}_{23} \\ \dot{k}_{31} & \dot{k}_{32} & \dot{k}_{33} \end{bmatrix} \tag{4.130}$$

where

$$\begin{aligned}\dot{k}_{11} &= 2\dot{q}_{e1}(q_0q_2 + q_1q_3) + 2q_{e1}(\dot{q}_0q_2 + q_0\dot{q}_2 + \dot{q}_1q_3 + q_1\dot{q}_3) \\ &+ 2\dot{q}_{e0}(q_0q_3 - q_1q_2) + 2q_{e0}(\dot{q}_0q_3 + q_0\dot{q}_3 - \dot{q}_1q_2 - q_1\dot{q}_2)\end{aligned}$$

$$\begin{aligned}\dot{k}_{12} &= 2\dot{q}_{e2}(q_0q_2 + q_1q_3) + 2q_{e2}(\dot{q}_0q_2 + q_0\dot{q}_2 + \dot{q}_1q_3 + q_1\dot{q}_3) \\ &+ \dot{q}_{e0}\left(1 - 2q_2^2 - 2q_3^2\right) + q_{e0}(-4q_2\dot{q}_2 - 4q_3\dot{q}_3)\end{aligned}$$

$$\begin{aligned}\dot{k}_{13} &= \dot{q}_{e1}\left(1 - 2q_0^2 - 2q_1^2\right) + q_{e1}(-4q_0\dot{q}_0 - 4q_1\dot{q}_1) \\ &+ 2\dot{q}_{e2}(q_0q_3 - q_1q_2) + 2q_{e2}(\dot{q}_0q_3 + q_0\dot{q}_3 - \dot{q}_1q_2 - q_1\dot{q}_2)\end{aligned}$$

$$\begin{aligned}\dot{k}_{21} &= \dot{q}_{e0}\left(1 - 2q_0^2 - 2q_2^2\right) + q_{e0}(-4q_0\dot{q}_0 - 4q_2\dot{q}_2) \\ &+ 2\dot{q}_{e1}(q_2q_3 - q_0q_1) + 2q_{e1}(\dot{q}_2q_3 + q_2\dot{q}_3 - \dot{q}_0q_1 - q_0\dot{q}_1)\end{aligned}$$

$$\begin{aligned}\dot{k}_{22} &= 2\dot{q}_{e2}(-q_0q_1 + q_2q_3) + 2q_{e2}(-\dot{q}_0q_1 - q_0\dot{q}_1 + \dot{q}_2q_3 + q_2\dot{q}_3) \\ &+ 2\dot{q}_{e0}(q_0q_3 + q_1q_2) + 2q_{e0}(\dot{q}_0q_3 + q_0\dot{q}_3 + \dot{q}_1q_2 + q_1\dot{q}_2)\end{aligned}$$

$$\begin{aligned}\dot{k}_{23} &= \dot{q}_{e2}\left(1 - 2q_0^2 - 2q_2^2\right) + q_{e2}(-4q_0\dot{q}_0 - 4q_2\dot{q}_2) \\ &+ 2\dot{q}_{e1}(-q_0q_3 - q_1q_2) + 2\left(-\dot{q}_0q_3 - q_0\dot{q}_3 - \dot{q}_1q_2 - q_1\dot{q}_2\right)q_{e1}\end{aligned}$$

$$\begin{aligned}\dot{k}_{31} &= \dot{q}_{e1}\left(1 - 2q_1^2 - 2q_2^2\right) + q_{e1}(-4q_1\dot{q}_1 - 4q_2\dot{q}_2) \\ &+ 2\dot{q}_{e0}(-q_0q_1 - q_2q_3) + 2q_{e0}(-\dot{q}_0q_1 - q_0\dot{q}_1 - \dot{q}_2q_3 - q_2\dot{q}_3)\end{aligned}$$

$$\dot{k}_{32} = \dot{q}_{e2}\left(1-2q_1^2-2q_2^2\right)+q_{e2}\left(-4q_1\dot{q}_1-4q_2\dot{q}_2\right)$$
$$+2\dot{q}_{e0}\left(q_1q_3-q_0q_2\right)+2q_{e0}\left(\dot{q}_1q_3+q_1\dot{q}_3-\dot{q}_0q_2-q_0\dot{q}_2\right)$$

$$k_{33} = 2\dot{q}_{e1}\left(-q_1q_3+q_0q_2\right)+2q_{e1}\left(-\dot{q}_1q_3-q_1\dot{q}_3+\dot{q}_0q_2+q_0\dot{q}_2\right)$$
$$+2\dot{q}_{e2}\left(-q_2q_3-q_0q_1\right)+2q_{e2}\left(-\dot{q}_2q_3-q_2\dot{q}_3-\dot{q}_0q_1-q_0\dot{q}_1\right)$$

It follows form (D.2) that $T = m\left\|\mu_d - g\mathbf{e}_3\right\|$ and its time derivative is given by

$$\begin{aligned}\dot{T} &= \frac{1}{2}m\left(\left(\mu_d-g\mathbf{e}_3\right)^T\left(\mu_d-g\mathbf{e}_3\right)\right)^{-\frac{1}{2}}\left(\dot{\mu}_d^T\left(\mu_d-g\mathbf{e}_3\right)+\left(\mu_d-g\mathbf{e}_3\right)^T\dot{\mu}_d\right)\\ &= m\left(\left(\mu_d-g\mathbf{e}_3\right)^T\left(\mu_d-g\mathbf{e}_3\right)\right)^{-\frac{1}{2}}\dot{\mu}_d^T\left(\mu_d-g\mathbf{e}_3\right)\end{aligned}$$

By differentiating (4.93), the following can be derived.

$$\dot{\mu}_d = \ddot{\mathbf{V}}_d+\Gamma_{e_2}^{-1}k_1\varepsilon_2\frac{\partial h\left(\mathbf{e}_1,\varepsilon_1,\varepsilon_2\right)}{\partial\mathbf{e}_1}\mathbf{e}_2+\Gamma_{e_2}^{-1}\mathbf{K}_2\frac{\partial h\left(\mathbf{e}_2,\varepsilon_3,\varepsilon_4\right)}{\partial\mathbf{e}_2}\dot{\mathbf{e}}_2 \tag{4.131}$$

As a component of (4.128), ω_d can be expressed as

$$\dot{\omega}_d = \left(\frac{\partial M(\mu_d)}{\partial\mu_{d1}}\dot{\mu}_{d1}+\frac{\partial M(\mu_d)}{\partial\mu_{d2}}\dot{\mu}_{d2}+\frac{\partial M(\mu_d)}{\partial\mu_{d3}}\dot{\mu}_{d3}\right)\dot{\mu}_d+M(\mu_d)\ddot{\mu}_d \tag{4.132}$$

where $\ddot{\mu}_d$ is derived by differentiating (4.131).

$$\begin{aligned}\ddot{\mu}_d &= \dddot{\mathbf{V}}_d+\Gamma_{e_2}^{-1}k_1\varepsilon_2\left(\frac{\partial\frac{\partial h(\mathbf{e}_1,\varepsilon_1,\varepsilon_2)}{\partial\mathbf{e}_1}\mathbf{e}_2}{\partial\mathbf{e}_1}\dot{\mathbf{e}}_1+\frac{\partial h\left(\mathbf{e}_1,\varepsilon_1,\varepsilon_2\right)}{\partial\mathbf{e}_1}\dot{\mathbf{e}}_2\right)\\ &+\Gamma_{e_2}^{-1}\mathbf{K}_2\left(\frac{\partial\frac{\partial h(\mathbf{e}_2,\varepsilon_3,\varepsilon_4)}{\partial\mathbf{e}_2}\dot{\mathbf{e}}_2}{\partial\mathbf{e}_2}\dot{\mathbf{e}}_2+\frac{\partial h\left(\mathbf{e}_2,\varepsilon_3,\varepsilon_4\right)}{\partial\mathbf{e}_2}\ddot{\mathbf{e}}_2\right)\\ &= \dddot{\mathbf{V}}_d+\Gamma_{e_2}^{-1}k_1\varepsilon_2\left(\sum_{j=1}^{3}\sum_{i=1}^{3}\frac{\partial^2h\left(\mathbf{e}_1,\varepsilon_1,\varepsilon_2\right)}{\partial e_{1j}\partial e_{1i}}e_{2i}e_{2j}+\frac{\partial h\left(\mathbf{e}_1,\varepsilon_1,\varepsilon_2\right)}{\partial\mathbf{e}_1}\dot{\mathbf{e}}_2\right)\\ &+\Gamma_{e_2}^{-1}\mathbf{K}_2\left(\sum_{j=1}^{3}\sum_{i=1}^{3}\frac{\partial^2h\left(\mathbf{e}_2,\varepsilon_3,\varepsilon_4\right)}{\partial e_{2j}\partial e_{2i}}\dot{e}_{2i}\dot{e}_{2j}+\frac{\partial h\left(\mathbf{e}_2,\varepsilon_3,\varepsilon_4\right)}{\partial\mathbf{e}_2}\ddot{\mathbf{e}}_2\right)\end{aligned} \tag{4.133}$$

The following assumption for $\mathbf{V}_d$ is made for the subsequent stability analysis.

Assumption 2. *$\mathbf{V}_d(t)$, $\mathbf{V}_d^{(1)}(t)$, $\mathbf{V}_d^{(2)}(t)$, and $\mathbf{V}_d^{(3)}(t)$ are bounded.*

It can be verified that the function $h(\mathbf{x},\varepsilon_1,\varepsilon_2)$ has the following properties [77].

P1: $h\left(\mathbf{0},\varepsilon_1,\varepsilon_2\right)=\mathbf{0}$ and $\mathbf{x}^Th(\mathbf{x},\varepsilon_1,\varepsilon_2)>0$ for $\mathbf{x}\neq\mathbf{0}$,

P2: $\left\|h(\mathbf{x},\varepsilon_1,\varepsilon_2)\right\|\leq\frac{1}{\sqrt{\varepsilon_2}}$ for $\forall\mathbf{x}\in R^{3\times1}$.

P3: All the components in the function $\frac{\partial h(\mathbf{x},\varepsilon_1,\varepsilon_2)}{\partial \mathbf{x}}$ and $\frac{\partial^2 h(\mathbf{x},\varepsilon_1,\varepsilon_2)}{\partial \mathbf{x}^2}$ are bounded for $\mathbf{x} \in R^{3\times 1}$. For details refer to Appendix F.

Then, the following result will be used later in this section.

Lemma 1. [77] Define a second order system

$$\ddot{\mathbf{x}} = -k_p h(\mathbf{x},\varepsilon_1,\varepsilon_2) - k_d h(\dot{\mathbf{x}},\varepsilon_1,\varepsilon_2) + \epsilon$$

where $\mathbf{x} \in R^{3\times 1}$ and k_p and k_d are strictly positive scalars. If ϵ is globally bounded and $\epsilon \to 0$, then $\mathbf{x}$ and $\dot{\mathbf{x}}$ are globally bounded, $\mathbf{x} \to 0$, and $\dot{\mathbf{x}} \to 0$.

According to (4.124), $\mathbf{e}_2$, $\mathbf{q}_e$, ω_e, $\delta_1 - \hat{\delta}_1$, $\delta_2 - \hat{\delta}_2$, and $\delta_3 - \hat{\delta}_3$, and $I_x - \hat{I}_x$, $I_y - \hat{I}_y$, and $I_z - \hat{I}_z$ are bounded. Then, $\hat{\delta}_1$, $\hat{\delta}_2$, and $\hat{\delta}_3$ and $\hat{I}_x$, $\hat{I}_y$, and $\hat{I}_z$ are bounded since δ_1, δ_2, and δ_3 and I_x, I_y, and I_z are constants.

The virtual linear acceleration μ_d in (4.93) is bounded by using Assumption 2 and the bounded property of $h(\mathbf{x},\varepsilon_1,\varepsilon_2)$. Since the system thrust $T = m\,\|\mu_d - g\mathbf{e}_3\|$, T is bounded. Therefore, W is bounded in view of (A.22). Note that $\bar{k}$ is a function of Q and Q_e which are naturally bounded. Consequently, $\dot{\mathbf{e}}_2$ is bounded in view of (4.125). In addition, according to Assumption 2, the bounded property of function $\frac{\partial h(\mathbf{x},\varepsilon_1,\varepsilon_2)}{\partial \mathbf{x}}$ and the boundedness of $\mathbf{e}_2$ and $\dot{\mathbf{e}}_2$, $\dot{\mu}_d$ is bounded. The boundedness of ω_d can be concluded from the boundedness of μ_d and $\dot{\mu}_d$ in view of (4.102). Then, it can be verified that ω_α is bounded in view of (4.106) and ω is bounded since ω_e and ω_α are bounded in (4.95). Because ω, ω_d and $\mathbf{q}_e$ are bounded, $\dot{\mathbf{q}}_e$ is bounded in view of (4.8). $\dot{Q}$ is a function of Q and ω as shown in (4.3). $\dot{Q}_e$ is a function of Q_e, ω and ω_d as shown in (4.8). Because Q, Q_e, ω and ω_d are bounded, $\dot{Q}$ and $\dot{Q}_e$ are bounded. According to (4.130), $\dot{\bar{k}}$ is a function of $\dot{Q}$, Q, $\dot{Q}_e$ and Q_e which are bounded, so $\dot{\bar{k}}$ is bounded. $\dot{T}$ is a function of $\dot{\mu}_d$ and since $\dot{\mu}_d$ is bounded, $\dot{T}$ is bounded. $\dot{W}$ is bounded since T, $\dot{T}$, $\bar{k}$, and $\dot{\bar{k}}$ are bounded in (4.129). $\ddot{\mathbf{e}}_2$ is bounded due to the boundedness of $\dot{\mathbf{e}}_1$, $\dot{\mathbf{e}}_2$, $\dot{W}$, W, $\dot{\mathbf{q}}_e$, and $\mathbf{q}_e$ with respect to (4.126). $\ddot{\mu}_d$ is bounded since Assumption 2, property **P3** of $h(\mathbf{x},\varepsilon_1,\varepsilon_2)$ and the boundedness of $\mathbf{e}_1$, $\mathbf{e}_2$, $\dot{\mathbf{e}}_2$, and $\ddot{\mathbf{e}}_2$ in view of (4.133). It can be verified that $\dot{\omega}_d$ is bounded since μ_d, $\dot{\mu}_d$, and $\ddot{\mu}_d$ are bounded in view of (4.132), where the boundedness of $\frac{\partial M(\mu_d)}{\partial \mu_{dk}}$ with $k = 1,2,3$ is verified in Appendix E. By taking the time derivative of (4.106), it can be verified that $\dot{\omega}_\alpha$ is bounded because $\dot{\mathbf{e}}_2$, $\dot{\mathbf{q}}_e$, and $\dot{\omega}_d$ are bounded. Then, $\dot{\omega}_e$ is bounded due to the boundedness of ω_e, ω, $\mathbf{q}_e$, $\dot{\omega}_\alpha$ in view of (4.127)

By differentiating (4.124), $\ddot{V}$ can be expressed as

$$\ddot{V} = -\dot{\mathbf{e}}_2^T \mathbf{K}_2 h\left(\mathbf{e}_2,\varepsilon_3,\varepsilon_4\right) - \mathbf{e}_2^T \mathbf{K}_2 \frac{\partial h\left(\mathbf{e}_2,\varepsilon_3,\varepsilon_4\right)}{\partial \mathbf{e}_2}\dot{\mathbf{e}}_2 - 2\mathbf{q}_e^T \mathbf{K}_q \dot{\mathbf{q}}_e - 2\omega_e^T \mathbf{K}_u \dot{\omega}_e \tag{4.134}$$

As a result, $\ddot{V}$ is bounded as shown in (4.134). By invoking Barbalat lemma, it can be concluded that $\mathbf{e}_2 \to 0$, $\mathbf{q}_e \to 0$, and $\omega_e \to 0$.

Since $\dot{\mathbf{e}}_1 = \mathbf{e}_2$, (4.125) can be rewritten as

$$\ddot{\mathbf{e}}_1 = -\Gamma_{e_2}^{-1} k_1 h\left(\mathbf{e}_1,\varepsilon_1,\varepsilon_2\right) - \boldsymbol{\Gamma}_{\mathbf{e_2}}^{-\mathbf{1}} \mathbf{K}_2 h\left(\dot{\mathbf{e}}_1,\varepsilon_3,\varepsilon_4\right) + W^T \mathbf{q}_e \tag{4.135}$$

In addition, by using the Lemma 1 with respect to (4.135), it can be concluded that the position error $\mathbf{e}_1 \to 0$ because $W^T\mathbf{q}_e$ is globally bounded and $W^T\mathbf{q}_e \to 0$.

4.3.2 Simulation Results

The simulation is carried out by using Matlab. The physical parameters are measured from the real quadrotor platform. It is assumed that the actual values of the moment of inertia fall within the range of ± 0.01 around the estimated values determined in Section 2.1. The optimal parameters are tuned as $\varepsilon_1 = 0.001$, $\varepsilon_2 = 0.5I_3$, $\varepsilon_3 = 0.001$, $\varepsilon_4 = 0.5I_3$, $K_1 = I_3$, $K_2 = 8I_3$, $K_q = 200I_3$, $K_u = 30I_3$, $\gamma_1 = \gamma_2 = \gamma_3 = 0.5$, $\Gamma_{e_2} = I_3$, $\lambda_1 = \lambda_2 = \lambda_3 = 0.1$. There are no load and the simulation is carried out in an ideal environment without wind and turbulence. The result of the simulation is shown as in Fig. 4.13, Fig. 4.14, Fig. 4.15, Fig. 4.16 and Fig. 4.17. From these figures, it can be concluded that the performance of this two step controller is similar to the performance of the four step controller designed in Section 4.2.

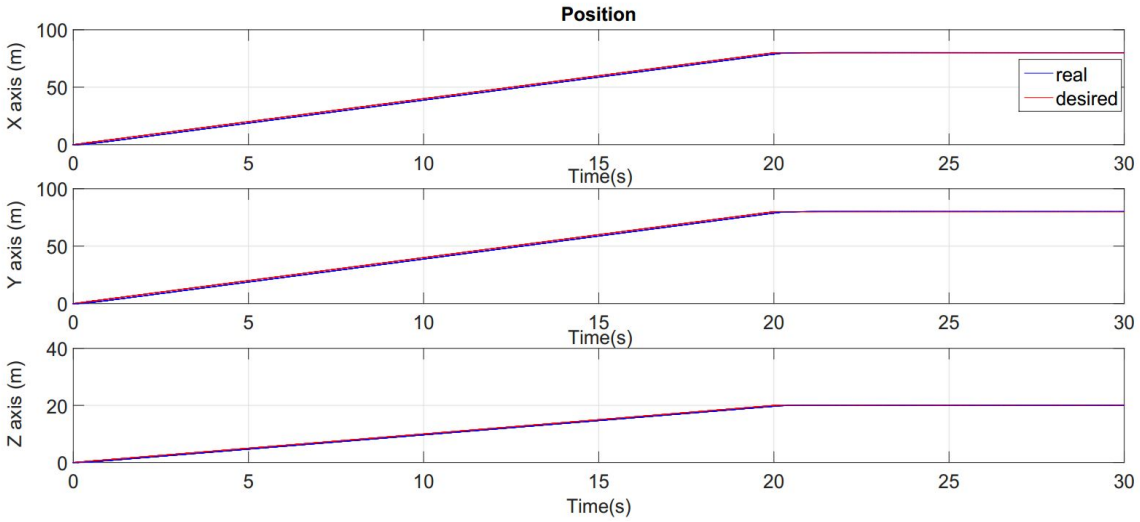

Figure 4.13: Simulation Results for Position Tracking

4.3.3 Experimental Results

The experiment were carried out by the same method as the four step controller. The flight test was carried out in a relative ideal weather with no loads. The optimized parameters are different from the simulation. They have been chosen as $\varepsilon_1 = 0.001$, $\varepsilon_2 = 0.5I_3$, $\varepsilon_3 = 0.001$, $\varepsilon_4 = 0.5I_3$, $K_1 = 0.5I_3$, $K_2 = 0.0001I_3$, $K_q = diag(240, 260, 8)$, $K_u = diag(16, 17, 600)$, $\gamma_1 = \gamma_2 = \gamma_3 = 0.0001$. $\Gamma_{e_2} = I_3$, $\lambda_1 = \lambda_2 = \lambda_3 = 0.1$. The possible reason is the loop time difference between the PC and the flight controller. The test time is shorter than that of the four step controller. However, 250 s is long enough to prove the convergence of the system. If the system has problems, it won't maintain stable in 10 s. The tracking error is smaller

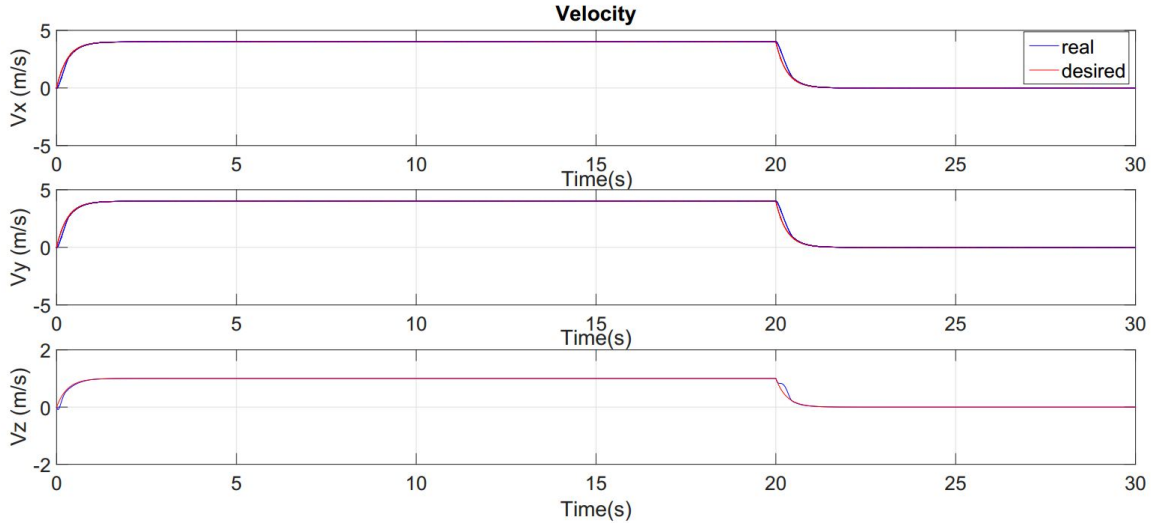

Figure 4.14: Simulation Results for Velocities

than the four step controller and the controller in [54]. The overall performance is smooth and stable.

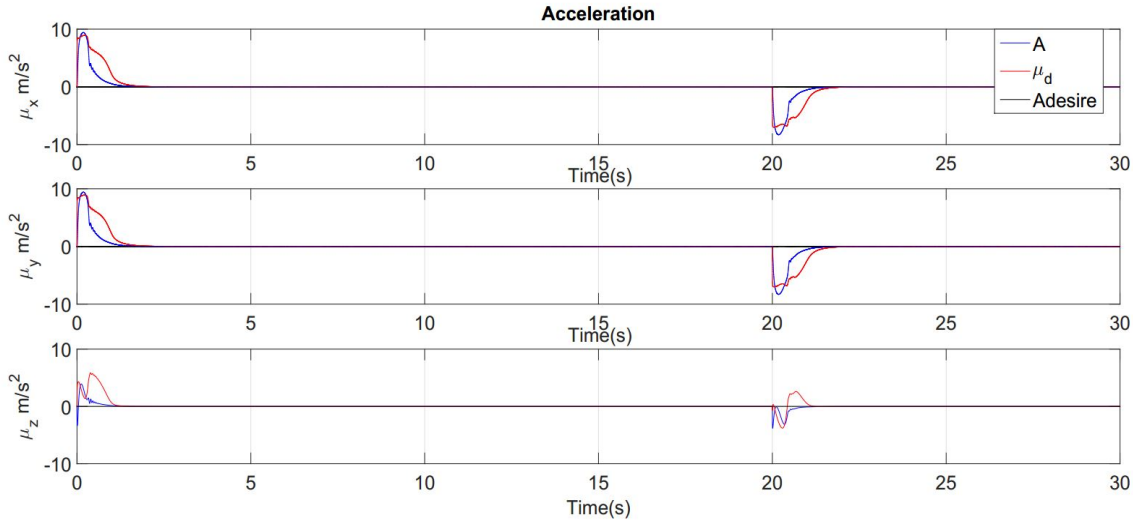

Figure 4.15: Simulation Results for Accelerations

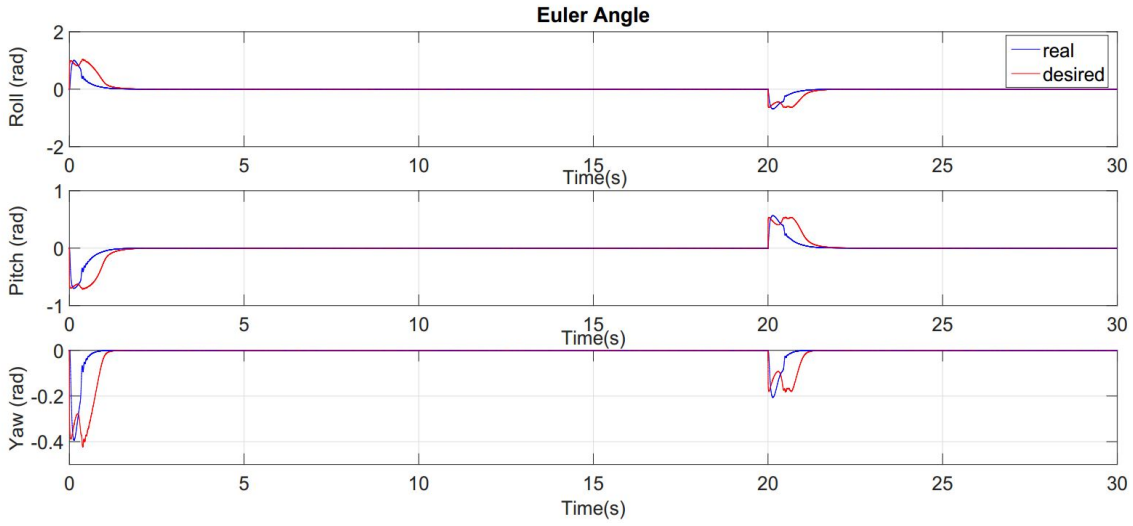

Figure 4.16: Simulation Results for Attitude in Euler Angles

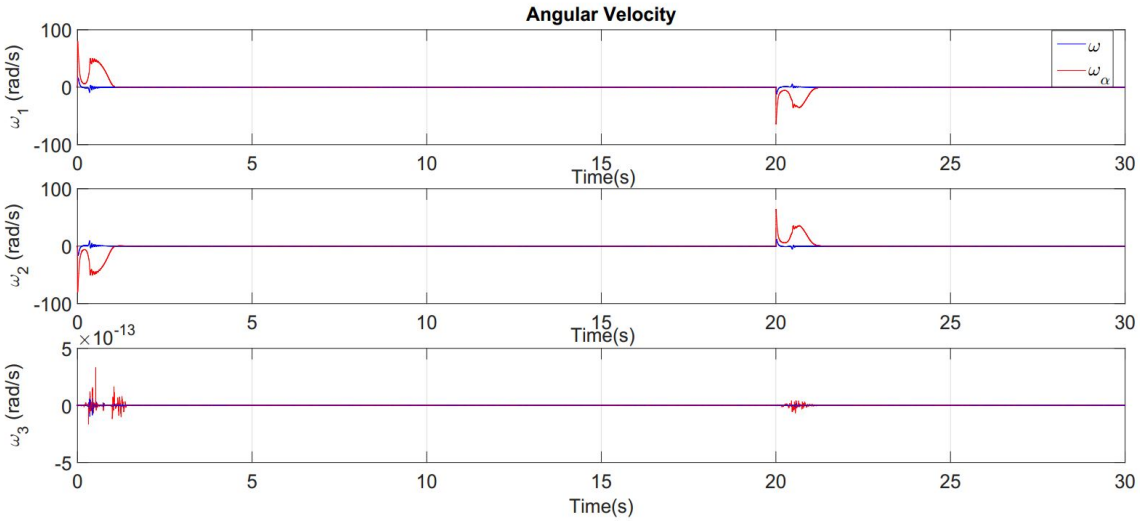

Figure 4.17: Simulation Results for Angular Velocities

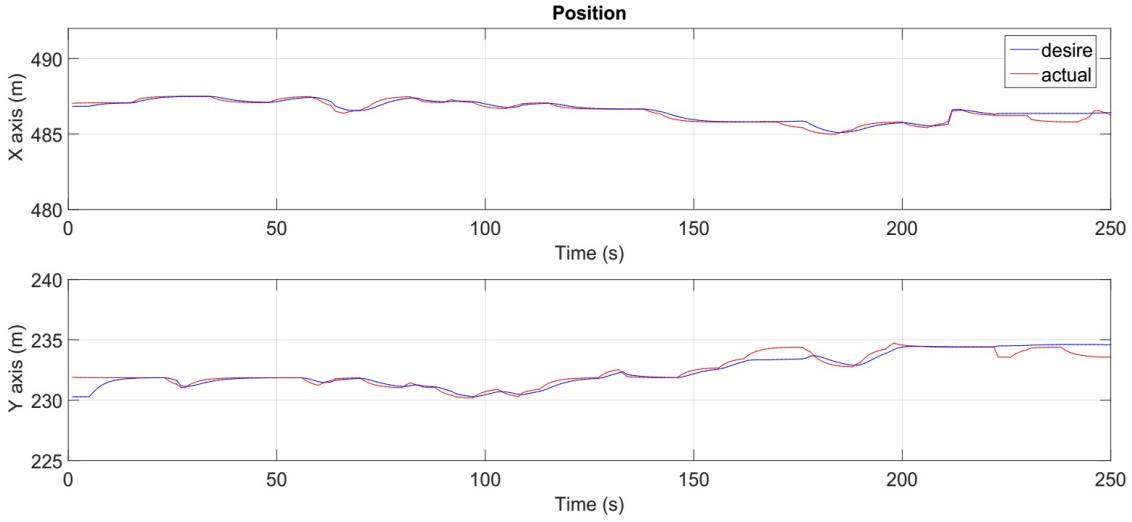

Figure 4.18: Experimental Results for Position Tracking

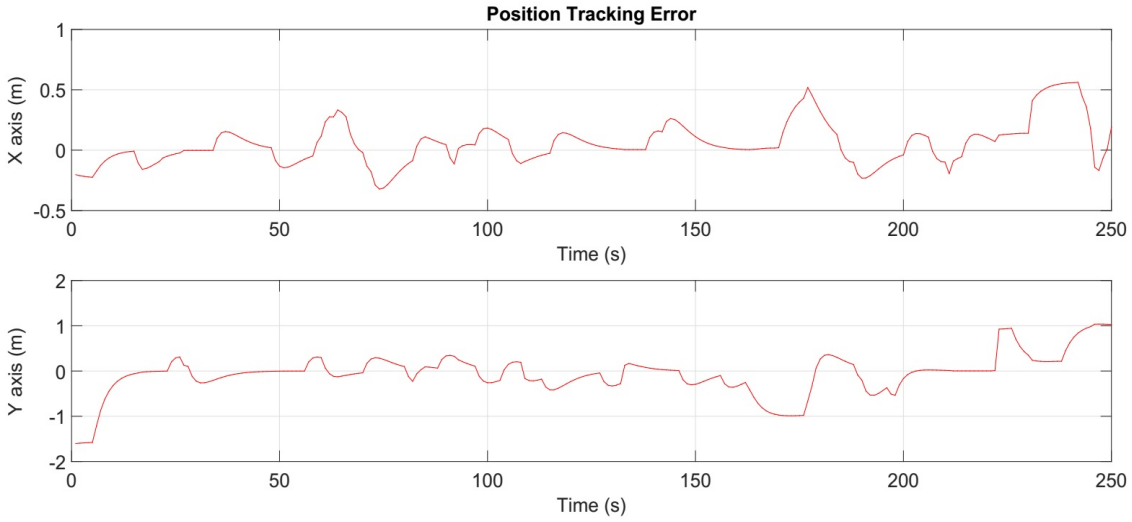

Figure 4.19: Experimental Results for Position Tracking Errors

4.4 Adaptive Performance

To verify the adaptive performance of the proposed controllers, simulations with the change of the moment of inertia were conducted.

4.4.1 Four Step Controller

The simulation is carried out with the moment of inertia changing from $I_x = 6.47 \times 10^{-3}, I_y = 6.47 \times 10^{-3}, I_z = 12.75 \times 10^{-3}$ to $I_x = 2, I_y = 2, I_z = 2$.

As showed in Fig. 4.20, Fig. 4.21, Fig. 4.22, Fig. 4.23, and Fig. 4.24, without the adaptive neural-network method, the system oscillate seriously after the moment of inertia changed. Although the position performance for x and y axis is well, there is a significant offset for z axis. Moreover, the oscillation amplitude of velocity, acceleration, attitude and angular velocity are out of reasonable values.

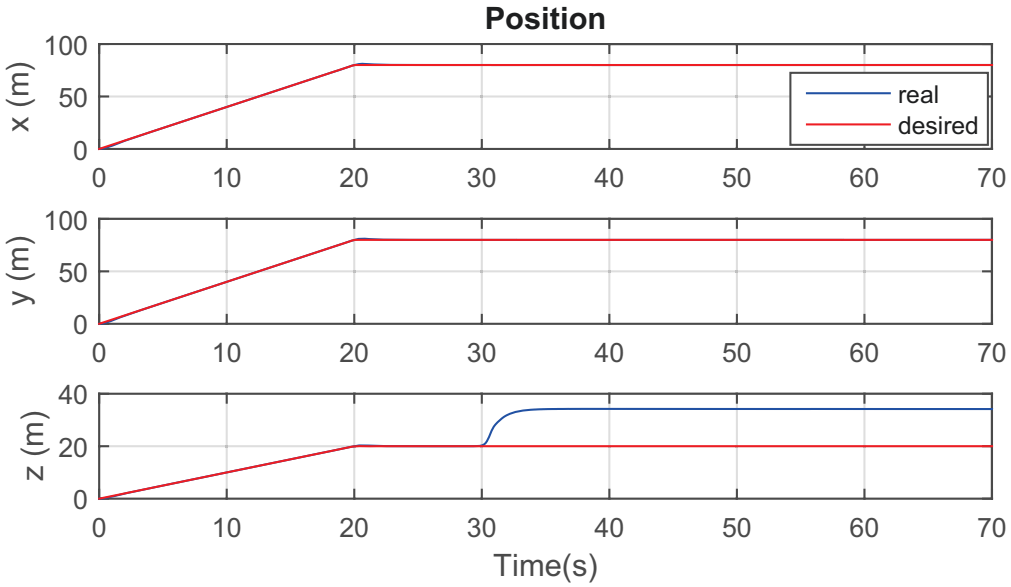

Figure 4.20: Simulation Results for Positions without Adaptive Method

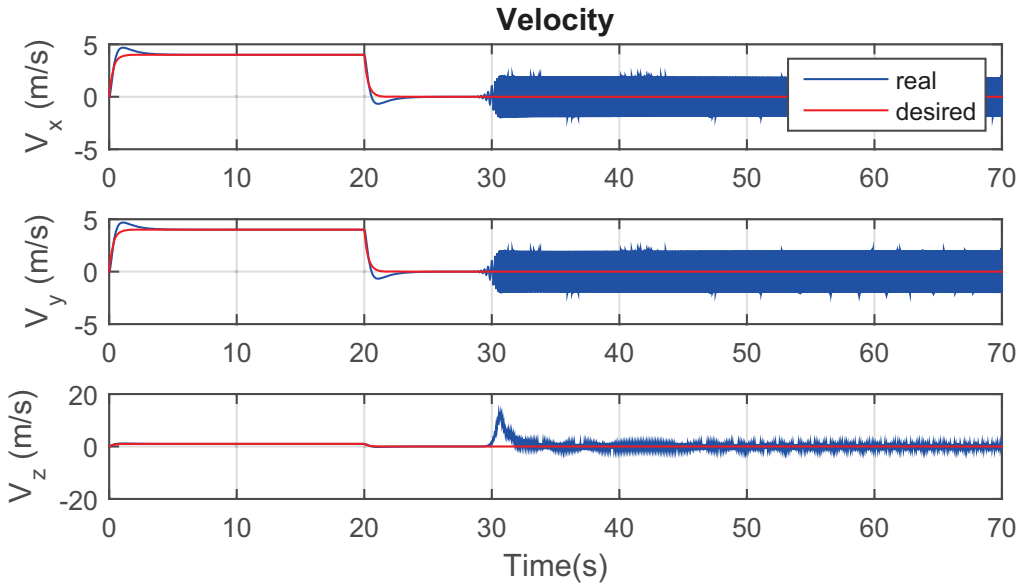

Figure 4.21: Simulation Results for Velocities without Adaptive Method

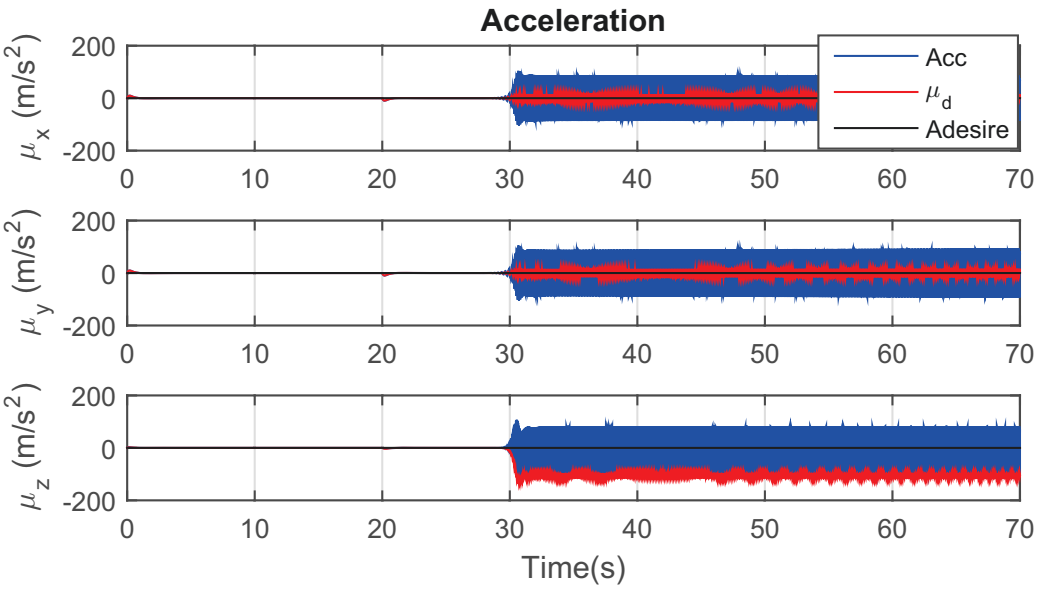

Figure 4.22: Simulation Results for Accelerations without Adaptive Method

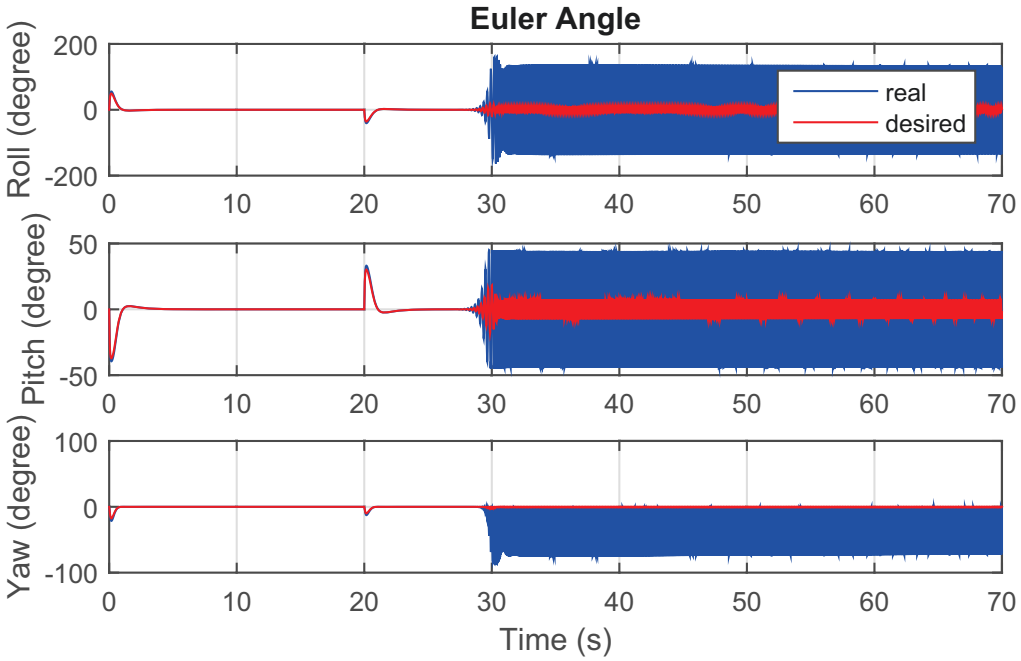

Figure 4.23: Simulation Results for Euler Angles without Adaptive Method

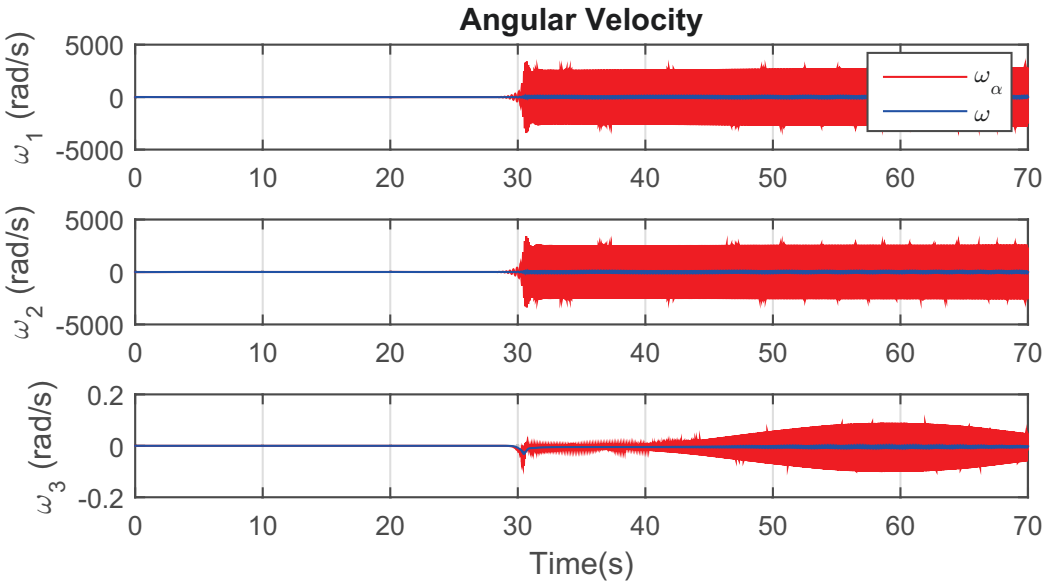

Figure 4.24: Simulation Results for Angular Velocities without Adaptive Method

As showed in Fig. 4.25, Fig. 4.26, Fig. 4.27, Fig. 4.28, and Fig. 4.29, with the adaptive neural-network method, the system is able to converge. The other conditions and parameters are all the same with the simulation in Chapter 4.

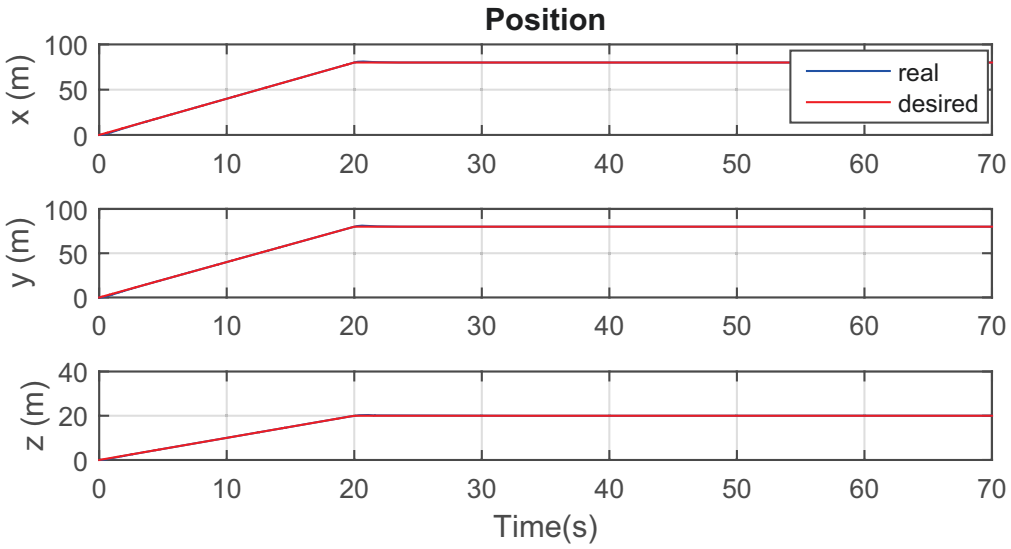

Figure 4.25: Simulation Results for Positions with Adaptive Method

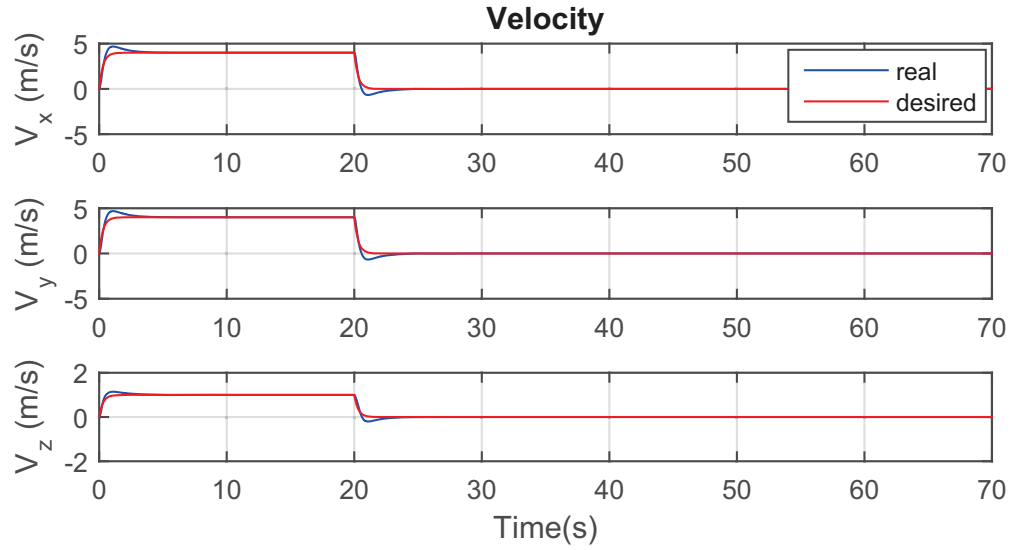

Figure 4.26: Simulation Results for Velocities with Adaptive Method

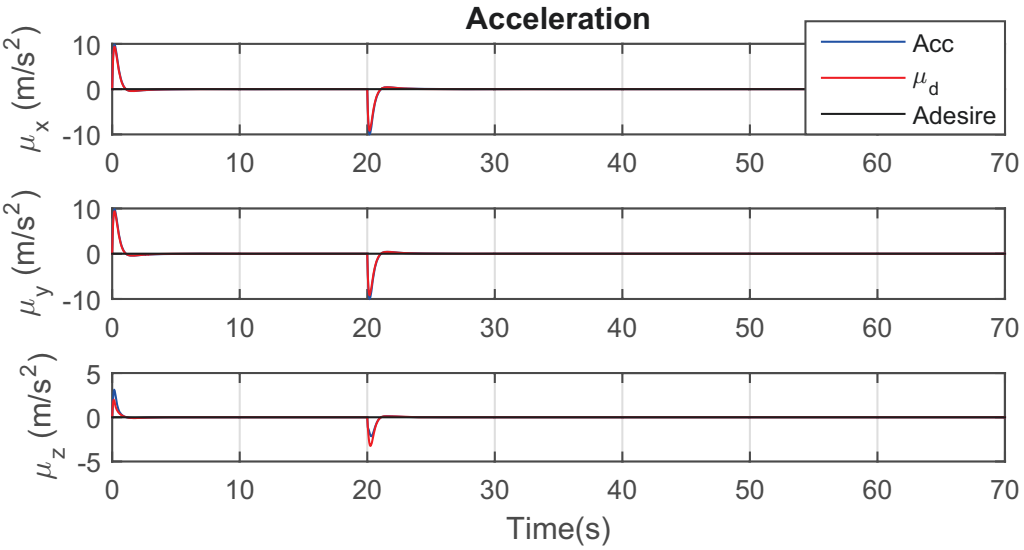

Figure 4.27: Simulation Results for Accelerations with Adaptive Method

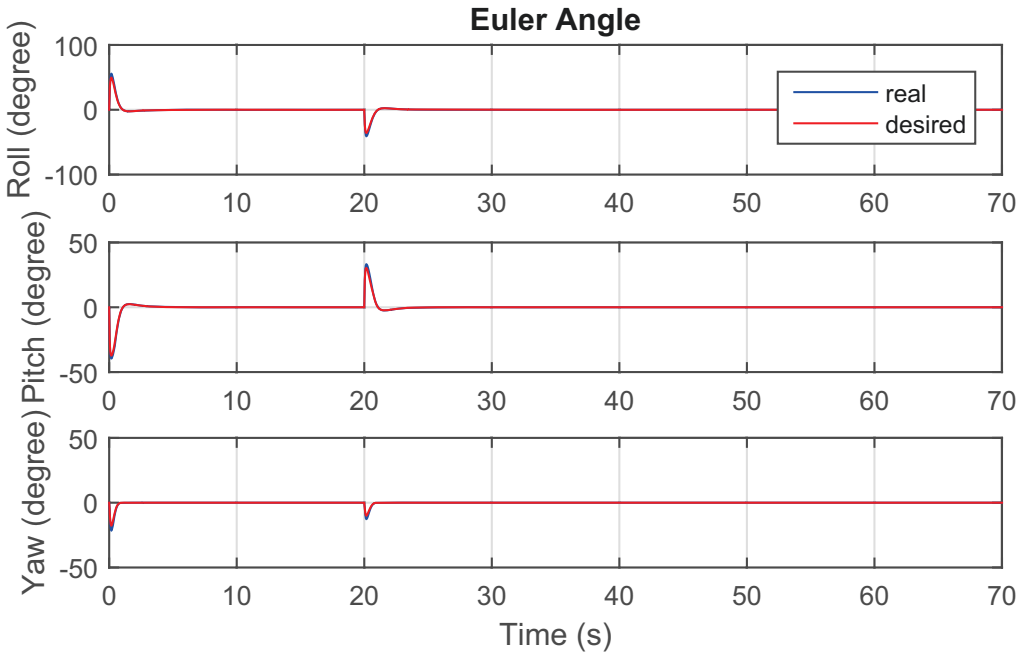

Figure 4.28: Simulation Results for Euler Angles with Adaptive Method

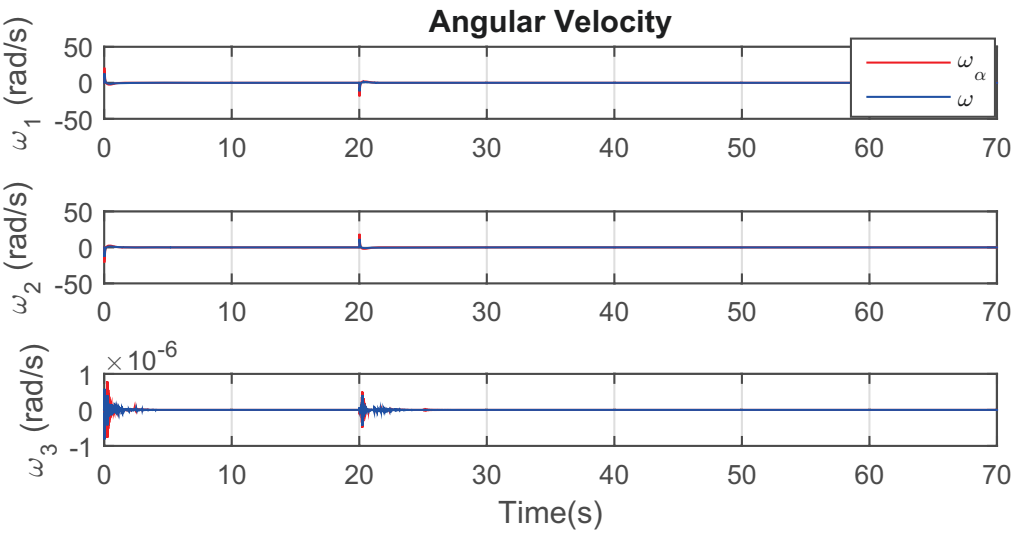

Figure 4.29: Simulation Results for Angular Velocities with Adaptive Method

4.4.2 Two Step Controller

The simulation is carried out with the moment of inertia changing from $I_x = 6.47 \times 10^{-3}, I_y = 6.47 \times 10^{-3}, I_z = 12.75 \times 10^{-3}$ to $I_x = 0.07, I_y = 0.07, I_z = 0.12$

As showed in Fig. 4.30, Fig. 4.31, Fig. 4.32, Fig. 4.33, and Fig. 4.34, without the adaptive method, the system loses control seriously after the moment of inertia changed.

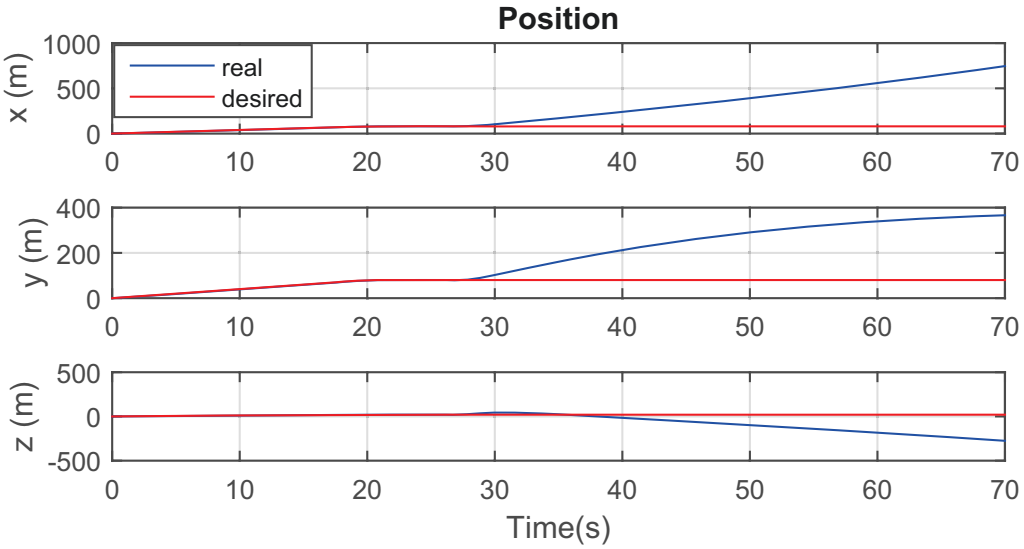

Figure 4.30: Simulation Results for Positions without Adaptive Method

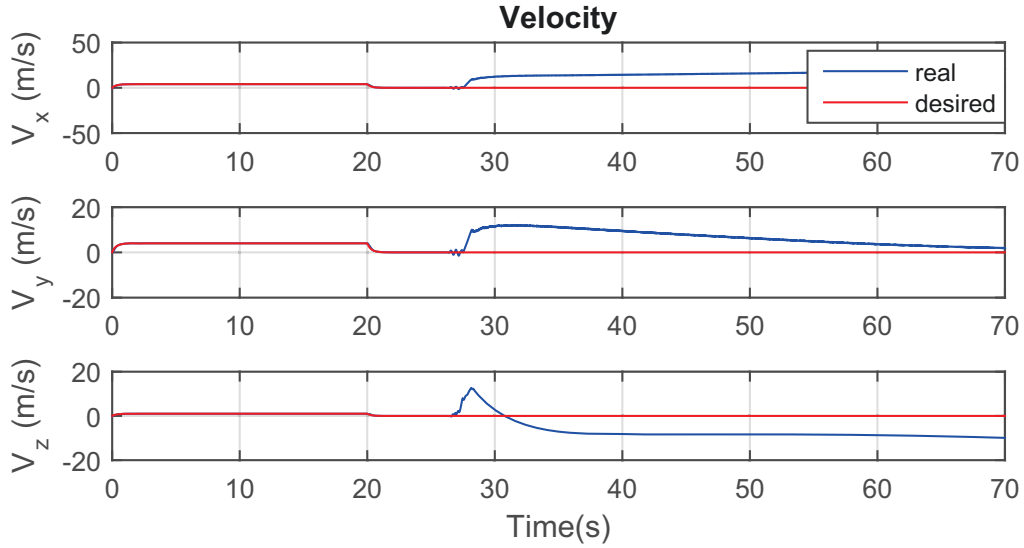

Figure 4.31: Simulation Results for Velocities without Adaptive Method

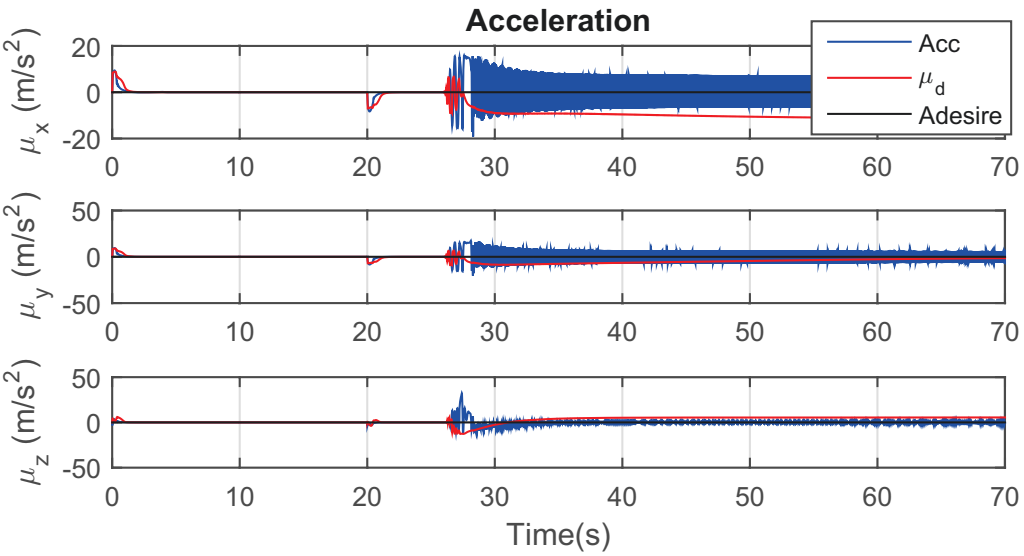

Figure 4.32: Simulation Results for Accelerations without Adaptive Method

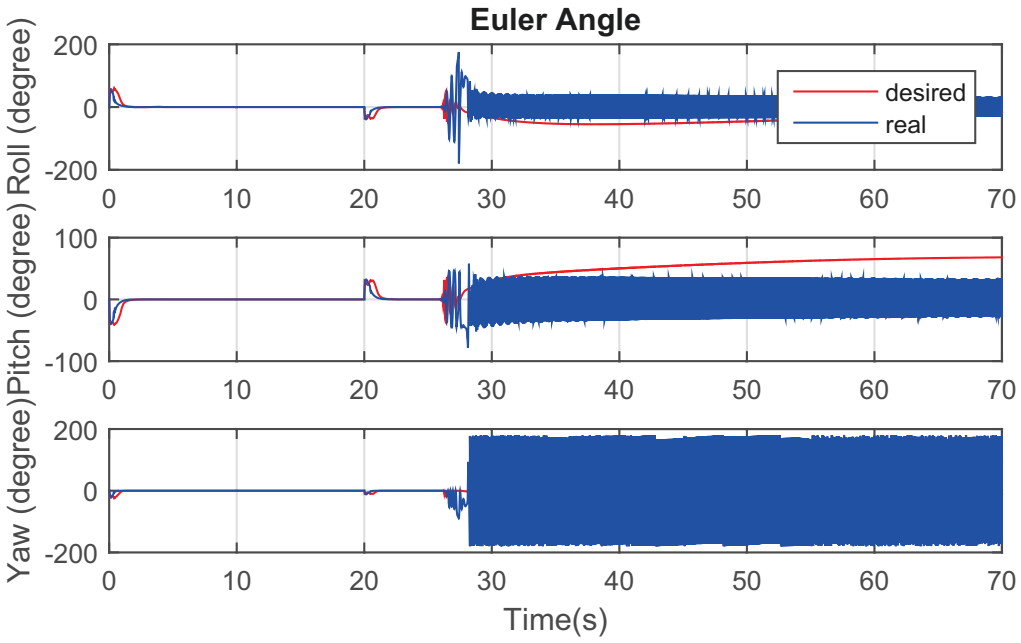

Figure 4.33: Simulation Results for Euler Angles without Adaptive Method

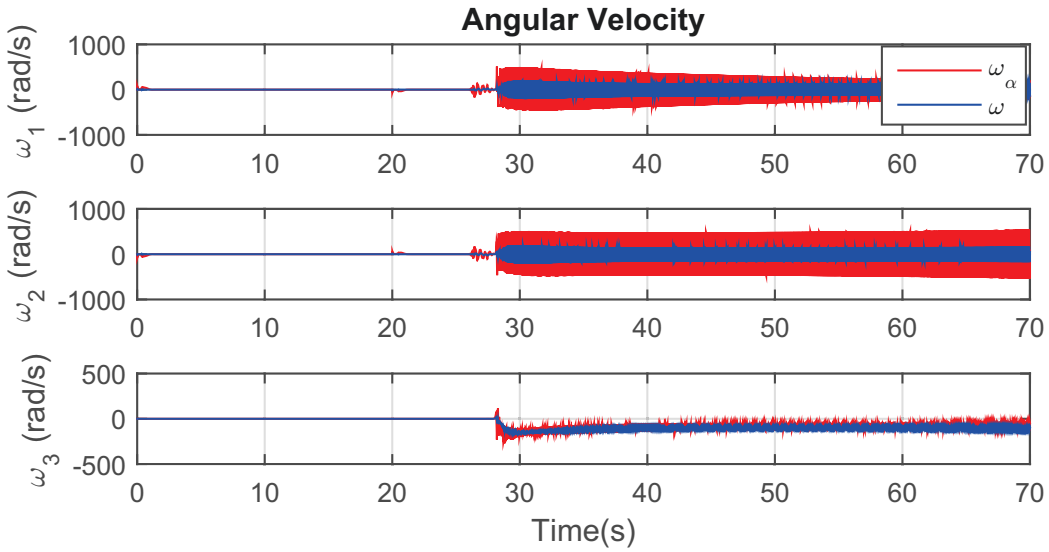

Figure 4.34: Simulation Results for Angular Velocities without Adaptive Method

As showed in Fig. 4.35, Fig. 4.36, Fig. 4.37, Fig. 4.38, and Fig. 4.39, with the adaptive method, the system is able to converge. The other conditions and parameters are all the same with the simulation in Chapter 4.

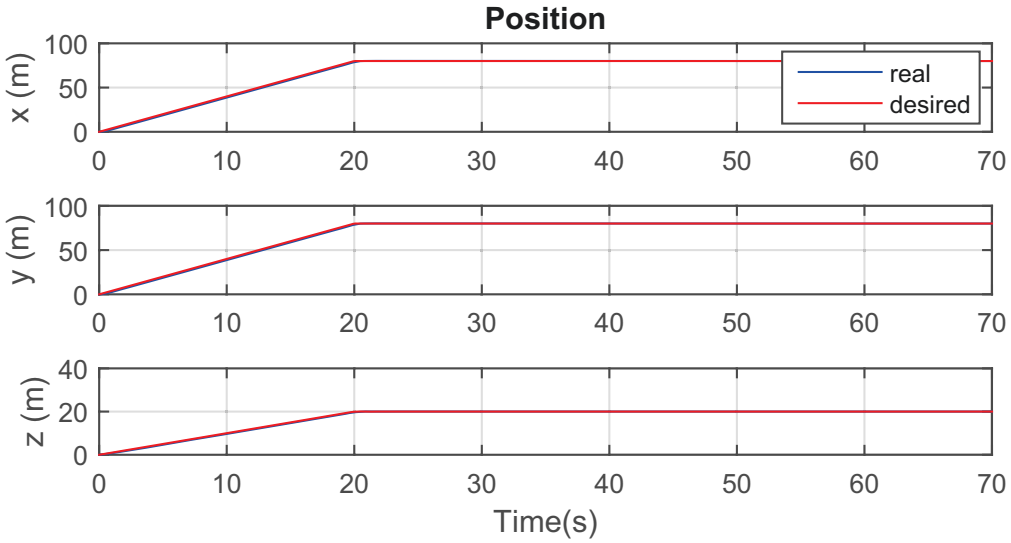

Figure 4.35: Simulation Results for Positions with Adaptive Method

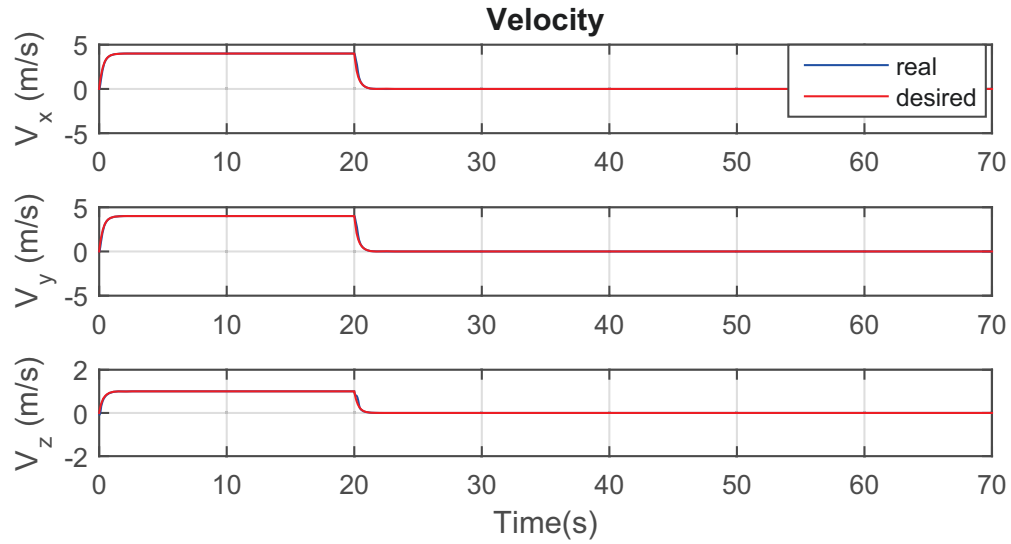

Figure 4.36: Simulation Results for Velocities with Adaptive Method

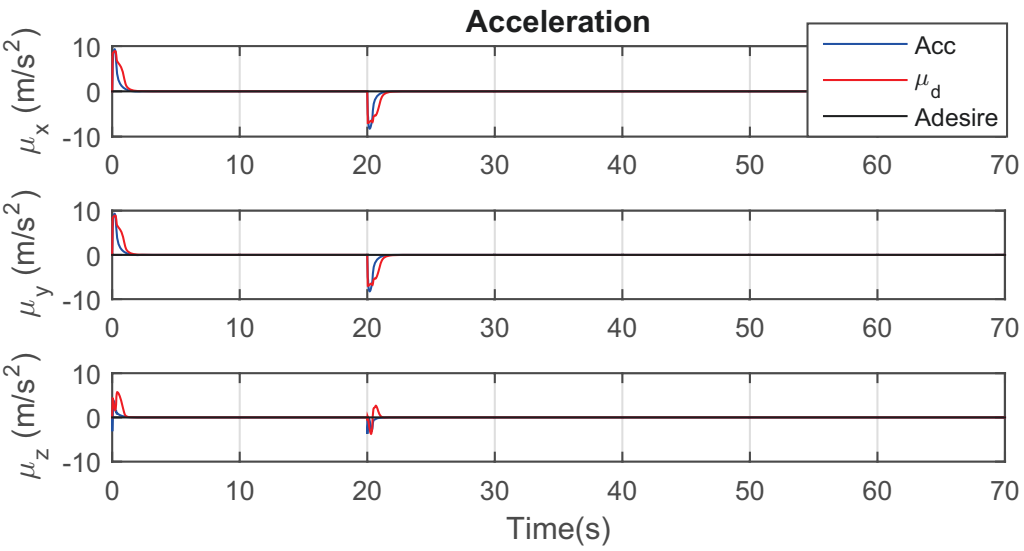

Figure 4.37: Simulation Results for Accelerations with Adaptive Method

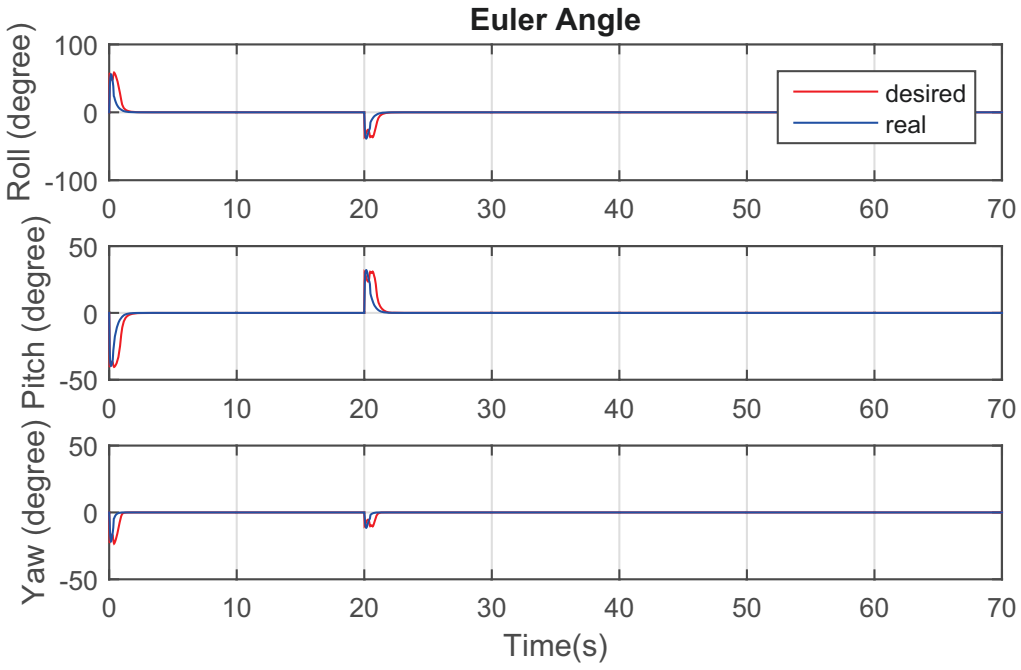

Figure 4.38: Simulation Results for Euler Angles with Adaptive Method

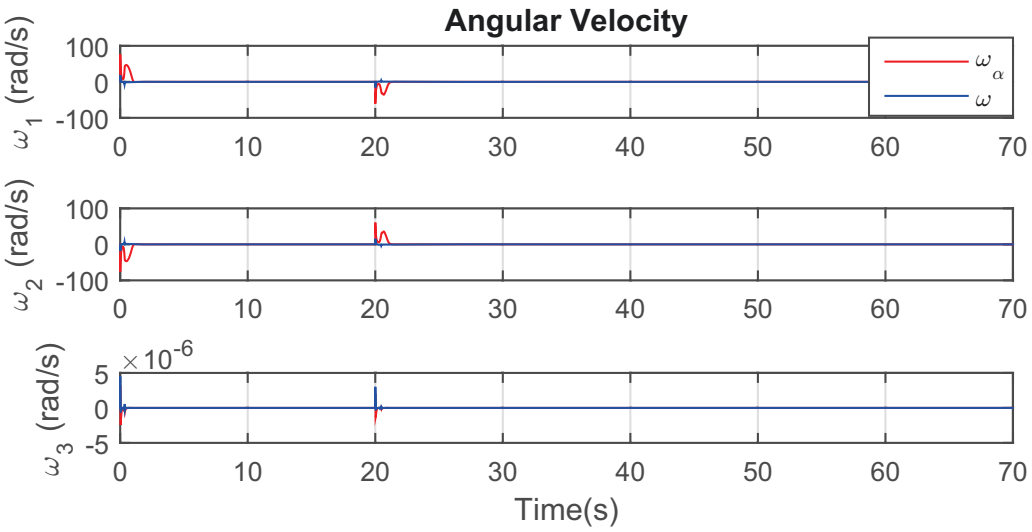

Figure 4.39: Simulation Results for Angular Velocities with Adaptive Method

Chapter 5

Conclusion

In this chapter some comparisons about the two proposed controllers are discussed. Also the achievements of the thesis is summarized. Finally, a couple of future works are discussed.

The simulation for adaptive performance conducted in previous chapter is close to the system tolerance of maximum change for the moment of inertia when adaptive method is used. According to these results, the four step controller with neural-network is able to maintain stable with a relative large change of the moment of inertia. However, without the change of the moment of inertia, the experimental results shows that the tracking performance of two step controller is better.

5.1 Achievements of the Thesis

The thesis has implemented the two potential practical algorithms for quadrotor position tracking control. The first one with four steps is based on backstepping nonlinear controller design method. The second one with two steps is simplified and improved from the first one. Both controllers are based on Lyapunov stability theory.

A complimentary filter has been applied to estimate the attitude of the quadrotor. It integrates the information from both IMU and magnetometer and generates the real time estimated attitude.

An adaptive neural-network method has been applied to estimate the nonlinear terms of the four step controller. In addition, an adaptive method has been implemented to estimate the unknown parameters of the two step controller.

An adaptive method has been applied to estimate the moment of inertia. Because the moment of inertia is difficult to be measured precisely, it is assumed to be unknown in this thesis.

The adaptive methods mentioned above is able to work with the backstepping technique.

And the system is able maintain stable when the moment of inertia is changed.

The existing code has been migrated to a new better hardware platform. It is more than 10 times faster than the old platform, which ensures the high loop rate for the system even though a complex algorithm is used.

5.2 Future Work

The current work may be extended in the future on the following aspects.

- **Altitude control**
  Currently, the altitude is manually controlled to ensure the flight safety. With a good altitude controller, a quadrotor can perform a fully automated enroute flying.
- **Auto takeoff and landing**
  The procedures of takeoff and landing for quadrotor are very dangerous processes for a flight. It is also true with other aircraft. If it can be auto-operated, it will significantly increase the flight safety. Also, it depends on a good altitude and position controller. With the introduction of automatic takeoff and landing features, a quadrotor can perform a fully automated flight.
- **Indoor position control**
  Currently, the position control can only be performed outdoor due to the dependency on GPS signals. It is much more meaningful to develop an indoor position tracking controller for a quadrotor. Currently, there are mainly two approaches for the indoor positioning system. One is based on a satellite or beacon based system like an indoor GPS. It is obviously unusable outside laboratory. The other one is based on optical flow technology. It does not rely on ground equipment. However, it can not supply an absolute position information like a GPS system.

Appendix A

Derivation of $\tilde{\mu} = W^T \mathbf{q}_e$

Define

$$\tilde{\mu} = -\mu + \mu_d \tag{A.1}$$

where $\tilde{\mu}$, μ, and μ_d denote the acceleration error, actual acceleration and desired acceleration.

According to (4.2)

$$\mu = g\mathbf{e}_3 - \frac{T}{m} R(Q)^T \mathbf{e}_3 \tag{A.2}$$

it follows that

$$\mu_d = g\mathbf{e}_3 - \frac{T}{m} R(Q_d)^T \mathbf{e}_3 \tag{A.3}$$

Substituting (A.2) and (A.3) into (A.1) results in

$$\begin{aligned} \tilde{\mu} &= \frac{T}{m} R(Q)^T \mathbf{e}_3 - \frac{T}{m} R(Q_d)^T \mathbf{e}_3 \\ &= \frac{T}{m} \left(R(Q)^T - R(Q_d)^T \right) \mathbf{e}_3 \end{aligned} \tag{A.4}$$

According to (2.30), the followings can be obtained.

$$R(Q) = \begin{bmatrix} -2q_2^2 - 2q_3^2 + 1 & 2q_0q_3 + 2q_1q_2 & 2q_1q_3 - 2q_0q_2 \\ 2q_1q_2 - 2q_0q_3 & -2q_1^2 - 2q_3^2 + 1 & 2q_0q_1 + 2q_2q_3 \\ 2q_0q_2 + 2q_1q_3 & 2q_2q_3 - 2q_0q_1 & -2q_1^2 - 2q_2^2 + 1 \end{bmatrix} \tag{A.5}$$

$$R\left(Q_d\right)=\left[\begin{array}{ccc} -2q_{d2}^2-2q_{d3}^2+1 & 2q_{d0}q_{d3}+2q_{d1}q_{d2} & 2q_{d1}q_{d3}-2q_{d0}q_{d2} \\ 2q_{d1}q_{d2}-2q_{d0}q_{d3} & -2q_{d1}^2-2q_{d3}^2+1 & 2q_{d0}q_{d1}+2q_{d2}q_{d3} \\ 2q_{d0}q_{d2}+2q_{d1}q_{d3} & 2q_{d2}q_{d3}-2q_{d0}q_{d1} & -2q_{d1}^2-2q_{d2}^2+1 \end{array}\right] \tag{A.6}$$

Then, $R\left(Q\right)^T-R\left(Q_d\right)^T$ can be expressed as below.

$$\begin{aligned} \bar{R}&=\left[\begin{array}{ccc} \bar{R}_{11} & \bar{R}_{12} & \bar{R}_{13} \\ \bar{R}_{21} & \bar{R}_{22} & \bar{R}_{23} \\ \bar{R}_{31} & \bar{R}_{32} & \bar{R}_{33} \end{array}\right]=R\left(Q\right)^T-R\left(Q_d\right)^T \\ &=\left[\begin{array}{ccc} -2q_2^2-2q_3^2+1 & 2q_0q_3+2q_1q_2 & 2q_1q_3-2q_0q_2 \\ 2q_1q_2-2q_0q_3 & -2q_1^2-2q_3^2+1 & 2q_0q_1+2q_2q_3 \\ 2q_0q_2+2q_1q_3 & 2q_2q_3-2q_0q_1 & -2q_1^2-2q_2^2+1 \end{array}\right]^T \\ &-\left[\begin{array}{ccc} -2q_{d2}^2-2q_{d3}^2+1 & 2q_{d0}q_{d3}+2q_{d1}q_{d2} & 2q_{d1}q_{d3}-2q_{d0}q_{d2} \\ 2q_{d1}q_{d2}-2q_{d0}q_{d3} & -2q_{d1}^2-2q_{d3}^2+1 & 2q_{d0}q_{d1}+2q_{d2}q_{d3} \\ 2q_{d0}q_{d2}+2q_{d1}q_{d3} & 2q_{d2}q_{d3}-2q_{d0}q_{d1} & -2q_{d1}^2-2q_{d2}^2+1 \end{array}\right]^T \end{aligned} \tag{A.7}$$

where

$$\bar{R}_{11}=2\left(-q_2^2-q_3^2+q_{d2}^2+q_{d3}^2\right)$$

$$\bar{R}_{12}=2\left(q_{d3}q_{d0}-q_{d2}q_{d1}-q_0q_3+q_1q_2\right)$$

$$\bar{R}_{13}=2\left(q_0q_2+q_1q_3-q_{d1}q_{d3}-q_{d2}q_{d0}\right)$$

$$\bar{R}_{21}=2\left(q_0q_3-q_{d2}q_{d1}-q_{d3}q_{d0}+q_1q_2\right)$$

$$\bar{R}_{22}=2\left(-q_1^2-q_3^2+q_{d3}^2+q_{d1}^2\right)$$

$$\bar{R}_{23}=2\left(q_2q_3-q_0q_1-q_{d2}q_{d3}+q_{d0}q_{d1}\right)$$

$$\bar{R}_{31}=2\left(q_{d2}q_{d0}-q_{d3}q_{d1}-q_0q_2+q_1q_3\right)$$

$$\bar{R}_{32}=2\left(q_0q_1+q_2q_3-q_{d2}q_{d3}-q_{d0}q_{d1}\right)$$

$$\bar{R}_{33}=2\left(-q_1^2-q_2^2+q_{d2}^2+q_{d1}^2\right)$$

By substituting (A.7) into (A.4), it follows that

$$\begin{aligned}\tilde{\mu} &= \frac{T}{m}\bar{R}\mathbf{e}_3 \\ &= \frac{T}{m}\begin{bmatrix} 2q_0q_2 + 2q_1q_3 - 2q_{d1}q_{d3} - 2q_{d2}q_{d0} \\ 2q_2q_3 - 2q_0q_1 - 2q_{d2}q_{d3} + 2q_{d0}q_{d1} \\ -2q_1^2 - 2q_2^2 + 2q_{d2}^2 + 2q_{d1}^2 \end{bmatrix} \\ &= 2\frac{T}{m}\begin{bmatrix} q_0q_2 + q_1q_3 - q_{d1}q_{d3} - q_{d2}q_{d0} \\ q_2q_3 - q_0q_1 - q_{d2}q_{d3} + q_{d0}q_{d1} \\ -q_1^2 - q_2^2 + q_{d2}^2 + q_{d1}^2 \end{bmatrix} \end{aligned} \tag{A.8}$$

Define a vector $\bar{\mathbf{r}} = \frac{1}{2}\bar{R}\mathbf{e}_3 = \begin{bmatrix} r_1 & r_2 & r_3 \end{bmatrix}^T$.

Then,

$$\tilde{\mu} = 2\frac{T}{m}\bar{\mathbf{r}} \tag{A.9}$$

where

$$\bar{\mathbf{r}} = \begin{bmatrix} q_0q_2 + q_1q_3 - q_{d1}q_{d3} - q_{d2}q_{d0} \\ q_2q_3 - q_0q_1 - q_{d2}q_{d3} + q_{d0}q_{d1} \\ -q_1^2 - q_2^2 + q_{d2}^2 + q_{d1}^2 \end{bmatrix} \tag{A.10}$$

It follows from (2.2.4) that

$$Q_e = Q_d^{-1} \odot Q \tag{A.11}$$

which is equivalent to

$$Q_d \odot Q_e = Q \tag{A.12}$$

The expression for Q_d can be obtained from (A.12)

$$\begin{aligned} Q_d &= Q \odot Q_e^{-1} \\ &= \begin{bmatrix} q_{e0}q_0 + q_1q_{e1} + q_2q_{e2} + q_3q_{e3} \\ q_{e0}q_1 - q_0q_{e1} + q_3q_{e2} - q_2q_{e3} \\ q_{e0}q_2 - q_0q_{e2} + q_1q_{e3} - q_3q_{e1} \\ q_{e0}q_3 - q_0q_{e3} + q_2q_{e1} - q_1q_{e2} \end{bmatrix} \end{aligned}$$

The vector part of Q_d is expressed as

$$\mathbf{q}_d = \begin{bmatrix} q_{d1} \\ q_{d2} \\ q_{d3} \end{bmatrix} = \begin{bmatrix} q_{e0}q_1 - q_0q_{e1} + q_3q_{e2} - q_2q_{e3} \\ q_{e0}q_2 - q_0q_{e2} + q_1q_{e3} - q_3q_{e1} \\ q_{e0}q_3 - q_0q_{e3} + q_2q_{e1} - q_1q_{e2} \end{bmatrix} \tag{A.13}$$

The following is given by substituting (A.13) into (A.10).

$$\begin{aligned} r_1 &= q_0q_2 + q_1q_3 - (q_{e0}q_1 - q_0q_{e1} + q_3q_{e2} - q_2q_{e3})(q_{e0}q_3 - q_0q_{e3} + q_2q_{e1} - q_1q_{e2}) \\ &\quad - (q_{e0}q_2 - q_0q_{e2} + q_1q_{e3} - q_3q_{e1})(q_{e0}q_0 + q_1q_{e1} + q_2q_{e2} + q_3q_{e3}) \\ r_2 &= q_2q_3 - q_0q_1 - (q_{e0}q_2 - q_0q_{e2} + q_1q_{e3} - q_3q_{e1})(q_{e0}q_3 - q_0q_{e3} + q_2q_{e1} - q_1q_{e2}) \\ &\quad + (q_{e0}q_0 + q_1q_{e1} + q_2q_{e2} + q_3q_{e3})(q_{e0}q_1 - q_0q_{e1} + q_3q_{e2} - q_2q_{e3}) \\ r_3 &= -q_1^2 - q_2^2 + (q_{e0}q_2 - q_0q_{e2} + q_1q_{e3} - q_3q_{e1})^2 + (q_{e0}q_1 - q_0q_{e1} + q_3q_{e2} - q_2q_{e3})^2 \end{aligned} \tag{A.14}$$

The expansion of (A.14) is

$$\begin{aligned} r_1 &= -q_0^2q_eq_{3e} + q_0^2q_{2e}q_{e0} + q_0q_2q_e^2 + q_0q_2q_{2e}^2 - q_0q_2q_{3e}^2 - q_0q_2q_{e0}^2 + q_0q_2 + 2q_0q_3q_eq_{e0} \\ &\quad + 2q_0q_3q_{2e}q_{3e} - q_1^2q_eq_{3e} + q_1^2q_{2e}q_{e0} - 2q_1q_2q_eq_{e0} - 2q_1q_2q_{2e}q_{3e} + q_1q_3q_e^2 + q_1q_3q_{2e}^2 \\ &\quad - q_1q_3q_{3e}^2 - q_1q_3q_{e0}^2 + q_1q_3 + q_2^2q_eq_{3e} - q_2^2q_{2e}q_{e0} + q_3^2q_eq_{3e} - q_3^2q_{2e}q_{e0} \end{aligned} \tag{A.15}$$

$$\begin{aligned} r_2 &= -q_0^2q_eq_{e0} - q_0^2q_{2e}q_{3e} - q_0q_1q_e^2 - q_0q_1q_{2e}^2 + q_0q_1q_{3e}^2 + q_0q_1q_{e0}^2 - q_0q_1 - 2q_0q_3q_eq_{3e} \\ &\quad + 2q_0q_3q_{2e}q_{e0} + q_1^2q_eq_{e0} + q_1^2q_{2e}q_{3e} - 2q_1q_2q_eq_{3e} + 2q_1q_2q_{2e}q_{e0} - q_2^2q_eq_{e0} - q_2^2q_{2e}q_{3e} \\ &\quad + q_2q_3q_e^2 + q_2q_3q_{2e}^2 - q_2q_3q_{3e}^2 - q_2q_3q_{e0}^2 + q_2q_3 + q_3^2q_eq_{e0} + q_3^2q_{2e}q_{3e} \end{aligned} \tag{A.16}$$

$$\begin{aligned} r_3 &= q_0^2q_e^2 + q_0^2q_{2e}^2 - 2q_0q_1q_eq_{e0} - 2q_0q_1q_{2e}q_{3e} + 2q_0q_2q_eq_{3e} - 2q_0q_2q_{2e}q_{e0} \\ &\quad + q_1^2q_{3e}^2 + q_1^2q_{e0}^2 - q_1^2 - 2q_1q_3q_eq_{3e} + 2q_1q_3q_{2e}q_{e0} + q_2^2q_{3e}^2 + q_2^2q_{e0}^2 - q_2^2 \\ &\quad - 2q_2q_3q_eq_{e0} - 2q_2q_3q_{2e}q_{3e} + q_3^2q_e^2 + q_3^2q_{2e}^2 \end{aligned} \tag{A.17}$$

By merging the similar terms in (A.15), (A.16) and (A.17), the following can be obtained.

$$\bar{\mathbf{r}} = \bar{k} \begin{bmatrix} q_{e1} \\ q_{e2} \\ q_{e3} \end{bmatrix} \tag{A.18}$$

where

$$\bar{k} = \begin{bmatrix} k_{11} & k_{12} & k_{13} \\ k_{21} & k_{22} & k_{23} \\ k_{31} & k_{32} & k_{33} \end{bmatrix} \tag{A.19}$$

with

$$k_{11} = 2\left(\left(q_0q_2 + q_1q_3\right)q_{e1} + \left(q_0q_3 - q_1q_2\right)q_{e0}\right)$$

$$k_{12} = 2\left(q_0q_2 + q_1q_3\right)q_{e2} + \left(1 - 2q_2^2 - 2q_3^2\right)q_{e0}$$

$$k_{13} = \left(1 - 2q_0^2 - 2q_1^2\right)q_{e1} + 2\left(q_0q_3 - q_1q_2\right)q_{e2}$$

$$k_{21} = \left(1 - 2q_0^2 - 2q_2^2\right)q_{e0} + 2\left(q_2q_3 - q_0q_1\right)q_{e1}$$

$$k_{22} = 2\left(\left(-q_0q_1 + q_2q_3\right)q_{e2} + \left(q_0q_3 + q_1q_2\right)q_{e0}\right)$$

$$k_{23} = \left(1 - 2q_0^2 - 2q_2^2\right)q_{e2} + 2\left(-q_0q_3 - q_1q_2\right)q_{e1}$$

$$k_{31} = \left(1 - 2q_1^2 - 2q_2^2\right)q_{e1} + 2\left(-q_0q_1 - q_2q_3\right)q_{e0}$$

$$k_{32} = \left(1 - 2q_1^2 - 2q_2^2\right)q_{e2} + 2\left(q_1q_3 - q_0q_2\right)q_{e0}$$

$$k_{33} = 2\left(\left(-q_1q_3 + q_0q_2\right)q_{e1} + \left(-q_2q_3 - q_0q_1\right)q_{e2}\right)$$

Then, the matrix representation of (A.18) can be expressed as

$$\bar{\mathbf{r}} = \bar{k}\mathbf{q}_e \tag{A.20}$$

By substituting (A.20) into (A.9), the following can be obtained.

$$\tilde{\mu} = 2\frac{T}{m}\bar{k}\mathbf{q}_e \tag{A.21}$$

Define

$$W = \left(2\frac{T}{m}\bar{k}\right)^T \tag{A.22}$$

Finally, (A.21) can be expressed as

$$\tilde{\mu} = W^T\mathbf{q}_e \tag{A.23}$$

Appendix B

Vector Multiply its Skew Matrix

Define a vector a

$$a = \begin{bmatrix} a_1 \\ a_2 \\ a_3 \end{bmatrix} \tag{B.1}$$

Then,

$$a^T S(a) = \begin{bmatrix} a_1 & a_2 & a_3 \end{bmatrix} \begin{bmatrix} 0 & -a_3 & a_2 \\ a_3 & 0 & -a_1 \\ -a_2 & a_1 & 0 \end{bmatrix} \tag{B.2}$$

$$= \begin{bmatrix} 0 & 0 & 0 \end{bmatrix} \tag{B.3}$$

Since $\omega + \omega_d$ is a column vector, no matter what value of $\omega + \omega_d$,

$$\mathbf{q}_e^T S(\mathbf{q}_e)(\omega + \omega_d) = 0 \tag{B.4}$$

Appendix C

Derivation from Desired Acceleration to Desired Quaternion

The following equation is the same as (4.31)

$$\begin{bmatrix} \mu_{d1} \\ \mu_{d2} \\ \mu_{d3} \end{bmatrix} = \begin{bmatrix} -\frac{T}{m}\left(2q_{d2}q_{d0} + 2q_{d3}q_{d1}\right) \\ -\frac{T}{m}\left(2q_{d2}q_{d3} - 2q_{d0}q_{d1}\right) \\ g + \frac{T}{m}\left(2q_{d2}^2 + 2q_{d1}^2 - 1\right) \end{bmatrix} \tag{C.1}$$

By using the unit quaternion property (2.23), μ_{d3} can be formed as

$$\begin{aligned} \mu_{d3} &= g + \frac{T}{m}\left(2q_{d2}^2 + 2q_{d1}^2 - 1\right) \\ &= g + \frac{T}{m}\left(2\left(q_{d2}^2 + q_{d1}^2\right) - 1\right) \\ &= g + \frac{T}{m}\left(2\left(1 - q_{d0}^2 - q_{d3}^2\right) - 1\right) \end{aligned}$$

By setting $q_{d3} = 0$, (C.1) can be written as

$$\mu_{d1} = -\frac{2T}{m} q_{d2}q_{d0} \tag{C.2}$$

$$\mu_{d2} = \frac{2T}{m} q_{d0}q_{d1} \tag{C.3}$$

$$\mu_{d3} = g + \frac{T}{m}\left(1 - 2q_{d0}^2\right) \tag{C.4}$$

According to (C.4), the expression for q_{d0} is given by

$$q_{d0} = \sqrt{\frac{1}{2}\left(1 - (\mu_{d3} - g)\,\frac{m}{T}\right)}$$

The expressions for q_{d1} and q_{d2} can be derived from (C.2) and (C.3)

$$q_{d1} = \frac{\mu_{d2}}{q_{d0}}\frac{m}{2T}$$
$$q_{d2} = -\frac{\mu_{d1}}{q_{d0}}\frac{m}{2T}$$

Finally, the expression of Q_d is shown below.

$$Q_d = \begin{bmatrix} \sqrt{\frac{1}{2}\left(1 - (\mu_{d3} - g)\,\frac{m}{T}\right)} \\ \frac{\mu_{d2}}{q_{d0}}\frac{m}{2T} \\ -\frac{\mu_{d1}}{q_{d0}}\frac{m}{2T} \\ 0 \end{bmatrix} \tag{C.5}$$

Appendix D

Derivation of ω_d

It follows from (4.3) that

$$\begin{aligned} \dot{Q}_d &= \frac{1}{2} Q_d \odot Q_{\omega d} \\ Q_{\omega d} &= 2 Q_d^{-1} \odot \dot{Q}_d \end{aligned} \tag{D.1}$$

By using the unit quaternion property (2.23) with respect to (C.5), the followings can be obtained.

$$\frac{1}{2}\left(1 - (\mu_{d3} - g)\frac{m}{T}\right) + \left(\frac{\mu_{d2}}{q_{d0}}\frac{m}{2T}\right)^2 + \left(-\frac{\mu_{d1}}{q_{d0}}\frac{m}{2T}\right)^2 = 1$$

$$\begin{aligned} T^2 &= (\mu_{d3} - g)^2 m^2 + \mu_{d2}^2 m^2 + \mu_{d1}^2 m^2 \\ \frac{T^2}{m^2} &= (\mu_{d3} - g)^2 + \mu_{d2}^2 + \mu_{d1}^2 = (\mu_d - g\mathbf{e}_3)^T (\mu_d - g\mathbf{e}_3) \\ \frac{T}{m} &= \|\mu_d - g\mathbf{e}_3\| \end{aligned} \tag{D.2}$$

Note that T and m are positive.

Define

$$u_t = \frac{T}{m} = \|\mu_d - g\mathbf{e}_3\| \tag{D.3}$$

Then, the time derivative of u_t is

$$\begin{aligned}\dot{u}_t &= \frac{d\sqrt{\left(\mu_d - g\mathbf{e}_3\right)^T\left(\mu_d - g\mathbf{e}_3\right)}}{dt} = \frac{1}{2}u_t^{-1}2\left(\mu_d - g\mathbf{e}_3\right)^T\dot{\mu}_d \\ &= u_t^{-1}\left(\mu_d - g\mathbf{e}_3\right)^T\dot{\mu}_d \end{aligned} \tag{D.4}$$

By substituting (D.2) into (C.5), the followings can be obtained.

$$Q_d = \begin{bmatrix} \sqrt{\frac{1}{2}\left(1 - \frac{(\mu_{d3}-g)}{u_t}\right)} \\ \frac{\mu_{d2}}{q_{d0}}\frac{1}{2u_t} \\ -\frac{\mu_{d1}}{q_{d0}}\frac{1}{2u_t} \\ 0 \end{bmatrix} \tag{D.5}$$

$$Q_d^{-1} = \begin{bmatrix} \left(\frac{1}{2}\left(1 - \frac{(\mu_{d3}-g)}{u_t}\right)\right)^{\frac{1}{2}} \\ -\frac{\mu_{d2}}{q_{d0}}\frac{1}{2u_t} \\ \frac{\mu_{d1}}{q_{d0}}\frac{1}{2u_t} \\ 0 \end{bmatrix} \tag{D.6}$$

By differentiating (D.5), the expression of $\dot{Q}_d$ is given by

$$\dot{Q}_d = \begin{bmatrix} \frac{1}{2}\left(\frac{1}{2}\left(1 - \frac{(\mu_{d3}-g)}{u_t}\right)\right)^{-\frac{1}{2}}\left(-\frac{1}{2}\frac{\dot{\mu}_{d3}u_t - (\mu_{d3}-g)\dot{u}_t}{u_t^2}\right) \\ \frac{\dot{\mu}_{d2}2u_tq_{d0} - \mu_{d2}2(\dot{u}_tq_{d0} + u_t\dot{q}_{d0})}{4u_t^2q_{d0}^2} \\ -\frac{\dot{\mu}_{d1}2u_tq_{d0} - \mu_{d1}2(\dot{u}_tq_{d0} + u_t\dot{q}_{d0})}{4u_t^2q_{d0}^2} \\ 0 \end{bmatrix} \tag{D.7}$$

Then, by substituting (D.6) and (D.7) into (D.1), $Q_{\omega d}$ can be expressed as

$$Q_{\omega d} = \begin{bmatrix} q_{\omega d0} \\ \mathbf{q}_{\omega d} \end{bmatrix} = 2Q_d^{-1} \odot \dot{Q}_d$$

that is,

$$
\begin{aligned}
q_{\omega d0} &= -\frac{1}{2}\frac{\dot{\mu}_{d3}u_t - (\mu_{d3}-g)\,\dot{u}_t}{u_t^2} + \frac{\mu_{d2}}{q_{d0}}\frac{1}{u_t}\frac{\dot{\mu}_{d2}2u_tq_{d0} - \mu_{d2}2\,(\dot{u}_tq_{d0}+u_t\dot{q}_{d0})}{4u_t^2q_{d0}^2} \\
&\quad + \frac{\mu_{d1}}{q_{d0}}\frac{1}{u_t}\frac{\dot{\mu}_{d1}2u_tq_{d0} - \mu_{d1}2\,(\dot{u}_tq_{d0}+u_t\dot{q}_{d0})}{4u_t^2q_{d0}^2} \\
\mathbf{q}_{\omega d} &= \left(\frac{1}{2}\left(1-\frac{(\mu_{d3}-g)}{u_t}\right)\right)^{-\frac{1}{2}}\left(-\frac{1}{2}\frac{\dot{\mu}_{d3}u_t-(\mu_{d3}-g)\,\dot{u}_t}{u_t^2}\right)\begin{bmatrix} -\frac{\mu_{d2}}{q_{d0}}\frac{1}{2u_t} \\ \frac{\mu_{d1}}{q_{d0}}\frac{1}{2u_t} \\ 0 \end{bmatrix} \\
&\quad + 2\left(\frac{1}{2}\left(1-\frac{(\mu_{d3}-g)}{u_t}\right)\right)^{\frac{1}{2}}\begin{bmatrix} \frac{\dot{\mu}_{d2}2u_tq_{d0}-\mu_{d2}2(\dot{u}_tq_{d0}+u_t\dot{q}_{d0})}{4u_t^2q_{d0}^2} \\ -\frac{\dot{\mu}_{d1}2u_tq_{d0}-\mu_{d1}2(\dot{u}_tq_{d0}+u_t\dot{q}_{d0})}{4u_t^2q_{d0}^2} \\ 0 \end{bmatrix} \\
&\quad + 2\begin{bmatrix} -\frac{\mu_{d2}}{q_{d0}}\frac{1}{2u_t} \\ \frac{\mu_{d1}}{q_{d0}}\frac{1}{2u_t} \\ 0 \end{bmatrix} \times \begin{bmatrix} \frac{\dot{\mu}_{d2}2u_tq_{d0}-\mu_{d2}2(\dot{u}_tq_{d0}+u_t\dot{q}_{d0})}{4u_t^2q_{d0}^2} \\ -\frac{\dot{\mu}_{d1}2u_tq_{d0}-\mu_{d1}2(\dot{u}_tq_{d0}+u_t\dot{q}_{d0})}{4u_t^2q_{d0}^2} \\ 0 \end{bmatrix}
\end{aligned} \tag{D.8}
$$

By expanding (D.8), the components of $Q_{\omega d}$ can be shown as

$$
\begin{aligned}
q_{\omega d0} = & -\frac{1}{2}\frac{\dot{\mu}_{d3}u_t - (\mu_{d3}-g)\,\dot{u}_t}{u_t^2} + \frac{(\mu_{d2}\dot{\mu}_{d2}+\mu_{d1}\dot{\mu}_{d1})\,u_t\left(\frac{1}{2}\left(1-\frac{(\mu_{d3}-g)}{u_t}\right)\right)^{\frac{1}{2}}}{q_{d0}u_t 4u_t^2 q_{d0}^2} \\
& - \frac{2\left(\mu_{d2}^2+\mu_{d1}^2\right)\left(\dot{u}_t\left(\frac{1}{2}\left(1-\frac{(\mu_{d3}-g)}{u_t}\right)\right)^{\frac{1}{2}} - \frac{1}{4}u_t\left(\frac{1}{2}\left(1-\frac{(\mu_{d3}-g)}{u_t}\right)\right)^{-\frac{1}{2}}\left(\frac{\dot{\mu}_{d3}u_t-(\mu_{d3}-g)\dot{u}_t}{u_t^2}\right)\right)}{4u_t^3 q_{d0}^3} \\
q_{\omega d1} = & \left(\frac{1}{2}-\frac{1}{2}\frac{(\mu_{d3}-g)}{u_t}\right)^{-\frac{1}{2}}\frac{\dot{\mu}_{d3}u_t-(\mu_{d3}-g)\,\dot{u}_t}{2u_t^2}\frac{\mu_{d2}}{\left(\frac{1}{2}\left(1-\frac{(\mu_{d3}-g)}{u_t}\right)\right)^{\frac{1}{2}}}\frac{1}{2u_t} \\
& + \frac{\left(\frac{1}{2}\left(1-\frac{(\mu_{d3}-g)}{u_t}\right)\right)^{\frac{1}{2}}\dot{\mu}_{d2}u_t}{u_t^2\left(\frac{1}{2}\left(1-\frac{(\mu_{d3}-g)}{u_t}\right)\right)}\left(\frac{1}{2}\left(1-\frac{(\mu_{d3}-g)}{u_t}\right)\right)^{\frac{1}{2}} \\
& - \frac{\left(\frac{1}{2}\left(1-\frac{(\mu_{d3}-g)}{u_t}\right)\right)^{\frac{1}{2}}\mu_{d2}}{u_t^2\left(\frac{1}{2}\left(1-\frac{(\mu_{d3}-g)}{u_t}\right)\right)}\left(\dot{u}_t\left(\frac{1}{2}\left(1-\frac{(\mu_{d3}-g)}{u_t}\right)\right)^{\frac{1}{2}}\right) \\
& - \frac{\left(\frac{1}{2}\left(1-\frac{(\mu_{d3}-g)}{u_t}\right)\right)^{\frac{1}{2}}\mu_{d2}u_t}{2u_t^2\left(\frac{1}{2}\left(1-\frac{(\mu_{d3}-g)}{u_t}\right)\right)}\left(\frac{1}{2}\left(1-\frac{(\mu_{d3}-g)}{u_t}\right)\right)^{-\frac{1}{2}}\left(-\frac{1}{2}\frac{\dot{\mu}_{d3}u_t-(\mu_{d3}-g)\,\dot{u}_t}{u_t^2}\right) \\
q_{\omega d2} = & -\left(\frac{1}{2}\left(1-\frac{(\mu_{d3}-g)}{u_t}\right)\right)^{-\frac{1}{2}}\frac{\dot{\mu}_{d3}u_t-(\mu_{d3}-g)\,\dot{u}_t}{2u_t^2}\frac{\mu_{d1}}{\left(\frac{1}{2}\left(1-\frac{(\mu_{d3}-g)}{u_t}\right)\right)^{\frac{1}{2}}}\frac{1}{2u_t} \\
& - \frac{\left(\frac{1}{2}\left(1-\frac{(\mu_{d3}-g)}{u_t}\right)\right)^{\frac{1}{2}}\dot{\mu}_{d1}u_t}{u_t^2\left(\frac{1}{2}\left(1-\frac{(\mu_{d3}-g)}{u_t}\right)\right)}\left(\frac{1}{2}\left(1-\frac{(\mu_{d3}-g)}{u_t}\right)\right)^{\frac{1}{2}} \\
& + \frac{\left(\frac{1}{2}\left(1-\frac{(\mu_{d3}-g)}{u_t}\right)\right)^{\frac{1}{2}}\mu_{d1}\dot{u}_t}{u_t^2\left(\frac{1}{2}\left(1-\frac{(\mu_{d3}-g)}{u_t}\right)\right)}\left(\frac{1}{2}\left(1-\frac{(\mu_{d3}-g)}{u_t}\right)\right)^{\frac{1}{2}} \\
& + \frac{\left(\frac{1}{2}\left(1-\frac{(\mu_{d3}-g)}{u_t}\right)\right)^{\frac{1}{2}}\mu_{d1}u_t}{2u_t^2\left(\frac{1}{2}\left(1-\frac{(\mu_{d3}-g)}{u_t}\right)\right)}\left(\frac{1}{2}\left(1-\frac{(\mu_{d3}-g)}{u_t}\right)\right)^{-\frac{1}{2}}\left(-\frac{1}{2}\frac{\dot{\mu}_{d3}u_t-(\mu_{d3}-g)\,\dot{u}_t}{u_t^2}\right) \\
q_{\omega d3} = & \frac{(\dot{\mu}_{d1}\mu_{d2}-\mu_{d1}\dot{\mu}_{d2})}{2u_t^2\left(\frac{1}{2}\left(1-\frac{(\mu_{d3}-g)}{u_t}\right)\right)}
\end{aligned}
\tag{D.9}
$$

Define

$$
c_1 = u_t + g - \mu_{d3} \tag{D.10}
$$

then, $1-\frac{(\mu_{d3}-g)}{u_t} = \frac{c_1}{u_t}$, $u_t - c_1 = \mu_{d3} - g$. By replacing $1-\frac{(\mu_{d3}-g)}{u_t}$ with $\frac{c_1}{u_t}$ and replacing $\mu_{d3}-g$ with $u_t - c_1$ in (D.9), $Q_{\omega d}$ can be expressed as

$$Q_{\omega d} = \begin{bmatrix} \frac{(\mu_{d2}\dot{\mu}_{d2}+\mu_{d1}\dot{\mu}_{d1})u_t\left(\frac{c_1}{2u_t}\right)^{\frac{1}{2}} - \left(\mu_{d2}^2+\mu_{d1}^2\right)\left(\dot{u}_t\left(\frac{c_1}{2u_t}\right)^{\frac{1}{2}} - \left(\frac{c_1}{2u_t}\right)^{-\frac{1}{2}}\frac{\dot{\mu}_{d3}u_t-(u_t-c_1)\dot{u}_t}{4u_t}\right)}{2u_t^3 q_{d0}^3} - \frac{\dot{\mu}_{d3}u_t-(u_t-c_1)\dot{u}_t}{2u_t^2} \\ \frac{1}{2}\frac{\dot{\mu}_{d3}u_t-(u_t-c_1)\dot{u}_t}{u_t^2}\frac{\mu_{d2}}{c_1} + \frac{\dot{\mu}_{d2}c_1-\frac{1}{2}\mu_{d2}\left(\frac{c_1\dot{u}_t}{u_t}-\dot{\mu}_{d3}+\dot{u}_t\right)}{u_t c_1} \\ -\frac{1}{2}\frac{\dot{\mu}_{d3}u_t-(u_t-c_1)\dot{u}_t}{u_t^2}\frac{\mu_{d1}}{c_1} - \frac{\dot{\mu}_{d1}c_1-\frac{1}{2}\mu_{d1}\left(\frac{c_1\dot{u}_t}{u_t}-\dot{\mu}_{d3}+\dot{u}_t\right)}{u_t c_1} \\ \frac{(\dot{\mu}_{d1}\mu_{d2}-\mu_{d1}\dot{\mu}_{d2})}{u_t c_1} \end{bmatrix}$$

The first component of $Q_{\omega d}$ is zero due to the definition of Q_ω in (4.3). As shown in (D.11), ω_d is the vector part of $Q_{\omega d}$.

$$\begin{aligned} \omega_d &= \begin{bmatrix} \frac{1}{2}\frac{(\dot{\mu}_{d3}u_t-(u_t-c_1)\dot{u}_t)\mu_{d2}}{u_t^2 c_1} + \frac{1}{2}\frac{2\dot{\mu}_{d2}c_1u_t-\mu_{d2}(c_1\dot{u}_t-u_t\dot{\mu}_{d3}+u_t\dot{u}_t)}{u_t^2c_1} \\ -\frac{1}{2}\frac{(\dot{\mu}_{d3}u_t-(u_t-c_1)\dot{u}_t)\mu_{d1}}{u_t^2 c_1} - \frac{1}{2}\frac{2\dot{\mu}_{d1}c_1u_t-\mu_{d1}(c_1\dot{u}_t-u_t\dot{\mu}_{d3}+u_t\dot{u}_t)}{u_t^2c_1} \\ \frac{(\dot{\mu}_{d1}\mu_{d2}-\mu_{d1}\dot{\mu}_{d2})}{u_t c_1} \end{bmatrix} \\ &= \begin{bmatrix} \frac{(\dot{\mu}_{d3}u_t-(u_t-c_1)\dot{u}_t)\mu_{d2}-\mu_{d2}(c_1\dot{u}_t-u_t\dot{\mu}_{d3}+u_t\dot{u}_t)+2\dot{\mu}_{d2}c_1u_t}{2u_t^2c_1} \\ -\frac{(\dot{\mu}_{d3}u_t-(u_t-c_1)\dot{u}_t)\mu_{d1}-\mu_{d1}(c_1\dot{u}_t-u_t\dot{\mu}_{d3}+u_t\dot{u}_t)+2\dot{\mu}_{d1}c_1u_t}{2u_t^2c_1} \\ \frac{(\dot{\mu}_{d1}\mu_{d2}-\mu_{d1}\dot{\mu}_{d2})}{u_t c_1} \end{bmatrix} \\ &= \begin{bmatrix} \frac{u_t\dot{\mu}_{d3}\mu_{d2}-u_t\dot{u}_t\mu_{d2}+\dot{\mu}_{d2}c_1u_t}{u_t^2c_1} \\ -\frac{u_t\dot{\mu}_{d3}\mu_{d1}-u_t\dot{u}_t\mu_{d1}+\dot{\mu}_{d1}c_1u_t}{u_t^2c_1} \\ \frac{(\dot{\mu}_{d1}\mu_{d2}-\mu_{d1}\dot{\mu}_{d2})}{u_t c_1} \end{bmatrix} \\ &= \frac{1}{u_t c_1}\begin{bmatrix} \dot{\mu}_{d3}\mu_{d2} - \dot{u}_t\mu_{d2} + \dot{\mu}_{d2}c_1 \\ -\left(\dot{\mu}_{d3}\mu_{d1} - \dot{u}_t\mu_{d1} + \dot{\mu}_{d1}c_1\right) \\ \left(\dot{\mu}_{d1}\mu_{d2} - \mu_{d1}\dot{\mu}_{d2}\right) \end{bmatrix} \end{aligned} \tag{D.11}$$

By substituting (D.4) into (D.11), ω_d can be shown as

$$\begin{aligned} \omega_d &= \frac{1}{u_t c_1}\begin{bmatrix} \dot{\mu}_{d3}\mu_{d2} - u_t^{-1}\left(\mu_d - g\mathbf{e}_3\right)^T\dot{\mu}_d\mu_{d2} + \dot{\mu}_{d2}c_1 \\ -\left(\dot{\mu}_{d3}\mu_{d1} - u_t^{-1}\left(\mu_d - g\mathbf{e}_3\right)^T\dot{\mu}_d\mu_{d1} + \dot{\mu}_{d1}c_1\right) \\ \left(\dot{\mu}_{d1}\mu_{d2} - \mu_{d1}\dot{\mu}_{d2}\right) \end{bmatrix} \\ &= \frac{1}{u_t^2 c_1}\begin{bmatrix} u_t\dot{\mu}_{d3}\mu_{d2} - \left(\mu_d - g\mathbf{e}_3\right)^T\dot{\mu}_d\mu_{d2} + u_t\dot{\mu}_{d2}c_1 \\ -u_t\dot{\mu}_{d3}\mu_{d1} + \left(\mu_d - g\mathbf{e}_3\right)^T\dot{\mu}_d\mu_{d1} - u_t\dot{\mu}_{d1}c_1 \\ u_t\left(\dot{\mu}_{d1}\mu_{d2} - \mu_{d1}\dot{\mu}_{d2}\right) \end{bmatrix} \end{aligned} \tag{D.12}$$

$\left(\mu_d - g\mathbf{e}_3\right)^T\dot{\mu}_d$ can be expanded as follows:

$$\left(\mu_d - g\mathbf{e}_3\right)^T\dot{\mu}_d = \mu_{d1}\dot{\mu}_{d1} + \mu_{d2}\dot{\mu}_{d2} + \left(\mu_{d3} - g\right)\dot{\mu}_{d3} \tag{D.13}$$

By substituting (D.13) into (D.12), it follows that

$$\begin{aligned}
\omega_d &= \frac{1}{u_t^2 c_1}\begin{bmatrix} u_t\mu_{d2}\dot{\mu}_{d3} - \left(\mu_{d1}\dot{\mu}_{d1} + \mu_{d2}\dot{\mu}_{d2} + \left(\mu_{d3} - g\right)\dot{\mu}_{d3}\right)\mu_{d2} + u_t\dot{\mu}_{d2}c_1 \\ -u_t\mu_{d1}\dot{\mu}_{d3} + \left(\mu_{d1}\dot{\mu}_{d1} + \mu_{d2}\dot{\mu}_{d2} + \left(\mu_{d3} - g\right)\dot{\mu}_{d3}\right)\mu_{d1} - u_t\dot{\mu}_{d1}c_1 \\ u_t\left(\dot{\mu}_{d1}\mu_{d2} - \mu_{d1}\dot{\mu}_{d2}\right) \end{bmatrix} \\
&= \frac{1}{u_t^2 c_1}\begin{bmatrix} -\mu_{d1}\mu_{d2}\dot{\mu}_{d1} + \left(u_t c_1 - \mu_{d2}^2\right)\dot{\mu}_{d2} + c_1\mu_{d2}\dot{\mu}_{d3} \\ \left(\mu_{d1}^2 - u_t c_1\right)\dot{\mu}_{d1} + \mu_{d1}\mu_{d2}\dot{\mu}_{d2} - c_1\mu_{d1}\dot{\mu}_{d3} \\ u_t\mu_{d2}\dot{\mu}_{d1} - u_t\mu_{d1}\dot{\mu}_{d2} \end{bmatrix} \\
&= \frac{1}{u_t^2 c_1}\begin{bmatrix} -\mu_{d1}\mu_{d2} & -\mu_{d2}^2 + u_t c_1 & \mu_{d2}c_1 \\ \mu_{d1}^2 - u_t c_1 & \mu_{d1}\mu_{d2} & -\mu_{d1}c_1 \\ \mu_{d2}u_t & -\mu_{d1}u_t & 0 \end{bmatrix}\begin{bmatrix} \dot{\mu}_{d1} \\ \dot{\mu}_{d2} \\ \dot{\mu}_{d3} \end{bmatrix}
\end{aligned}$$

Define M as

$$M\left(\mu_d\right) = \frac{1}{u_t^2 c_1}\begin{bmatrix} -\mu_{d1}\mu_{d2} & -\mu_{d2}^2 + u_t c_1 & \mu_{d2}c_1 \\ \mu_{d1}^2 - u_t c_1 & \mu_{d1}\mu_{d2} & -\mu_{d1}c_1 \\ \mu_{d2}u_t & -\mu_{d1}u_t & 0 \end{bmatrix} \tag{D.14}$$

Finally, ω_d can be expressed as

$$\omega_d = M\left(\mu_d\right)\dot{\mu}_d$$

Appendix E

Boundedness of $\frac{\partial M(\mu_d)}{\partial \mu_{dk}}$ with $k = 1, 2, 3$

According to (D.3), u_t can be rewritten as

$$\begin{aligned} u_t &= \|\mu_d - g\mathbf{e}_3\| = \sqrt{(\mu_d - g\mathbf{e}_3)^T (\mu_d - g\mathbf{e}_3)} \\ &= \sqrt{\mu_{d1}^2 + \mu_{d2}^2 + (g - \mu_{d3})^2} \end{aligned}$$

The components and their upper bounds of $\frac{\partial u_t}{\partial \mu_d}$ can be computed as follows.

$$\frac{\partial u_t}{\partial \mu_{dk}} = \frac{1}{2} \frac{2\mu_{dk}}{\sqrt{\mu_{d1}^2 + \mu_{d2}^2 + (g - \mu_{d3})^2}} = \frac{\mu_{dk}}{\sqrt{\mu_{d1}^2 + \mu_{d2}^2 + (g - \mu_{d3})^2}}, k = 1, 2$$

$$\left| \frac{\partial u_t}{\partial \mu_{dk}} \right| = \frac{|\mu_{dk}|}{\sqrt{\mu_{d1}^2 + \mu_{d2}^2 + (g - \mu_{d3})^2}} \leq \frac{\sqrt{\mu_{d1}^2 + \mu_{d2}^2 + (g - \mu_{d3})^2}}{\sqrt{\mu_{d1}^2 + \mu_{d2}^2 + (g - \mu_{d3})^2}} \leq 1, k = 1, 2$$

$$\frac{\partial u_t}{\partial \mu_{dk}} = \frac{1}{2} \frac{-2(g - \mu_{d3})}{\sqrt{\mu_{d1}^2 + \mu_{d2}^2 + (g - \mu_{d3})^2}} = \frac{-(g - \mu_{d3})}{\sqrt{\mu_{d1}^2 + \mu_{d2}^2 + (g - \mu_{d3})^2}}, k = 3$$

$$\left| \frac{\partial u_t}{\partial \mu_{dk}} \right| \leq \frac{|g - \mu_{d3}|}{\sqrt{\mu_{d1}^2 + \mu_{d2}^2 + (g - \mu_{d3})^2}} \leq \frac{\sqrt{\mu_{d1}^2 + \mu_{d2}^2 + (g - \mu_{d3})^2}}{\sqrt{\mu_{d1}^2 + \mu_{d2}^2 + (g - \mu_{d3})^2}} \leq 1, k = 3$$

So, $\frac{\partial u_t}{\partial \mu_{dk}}$ is bounded by 1 for $k = 1, 2, 3$. Then, with (D.10), it can be verified that the following is true.

$$\frac{\partial c_1}{\partial \mu_{dk}} = \frac{\partial c_1}{\partial u_t} \frac{\partial u_t}{\partial \mu_{dk}} = \frac{\partial u_t}{\partial \mu_{dk}}, k = 1, 2$$

As a result, the boundedness of $\frac{\partial c_1}{\partial \mu_{dk}}$ inherits from the boundedness of $\frac{\partial u_t}{\partial \mu_{dk}}$ for $k = 1, 2$. For $k = 3$, the boundedness of $\frac{\partial c_1}{\partial \mu_{dk}}$ can be verified by

$$\begin{aligned}
\frac{\partial c_1}{\partial \mu_{dk}} &= \frac{\partial c_1}{\partial u_t}\frac{\partial u_t}{\partial \mu_{dk}} - 1 = \frac{\partial u_t}{\partial \mu_{dk}} - 1 = \frac{-(g-\mu_{d3})}{\sqrt{\mu_{d1}^2 + \mu_{d2}^2 + (g-\mu_{d3})^2}} - 1 \\
&= \frac{-(g-\mu_{d3}) - \sqrt{\mu_{d1}^2 + \mu_{d2}^2 + (g-\mu_{d3})^2}}{\sqrt{\mu_{d1}^2 + \mu_{d2}^2 + (g-\mu_{d3})^2}}, k = 3 \\
\left|\frac{\partial c_1}{\partial \mu_{dk}}\right| &= \left|\frac{-(g-\mu_{d3}) - \sqrt{\mu_{d1}^2 + \mu_{d2}^2 + (g-\mu_{d3})^2}}{\sqrt{\mu_{d1}^2 + \mu_{d2}^2 + (g-\mu_{d3})^2}}\right| \\
&\leq \frac{|g-\mu_{d3}| + \sqrt{\mu_{d1}^2 + \mu_{d2}^2 + (g-\mu_{d3})^2}}{\sqrt{\mu_{d1}^2 + \mu_{d2}^2 + (g-\mu_{d3})^2}} \\
&\leq \frac{\sqrt{\mu_{d1}^2 + \mu_{d2}^2 + (g-\mu_{d3})^2} + \sqrt{\mu_{d1}^2 + \mu_{d2}^2 + (g-\mu_{d3})^2}}{\sqrt{\mu_{d1}^2 + \mu_{d2}^2 + (g-\mu_{d3})^2}} \leq 2
\end{aligned}$$

So, $\frac{\partial c_1}{\partial \mu_{dk}}$ is bounded by 2 for $k = 1, 2, 3$.

According to Assumption 1, (D.3), and (D.10), the following inequalities can be obtained.

$$\begin{aligned}
&\mu_{d3} \leq g - s \Rightarrow g - \mu_{d3} \geq s > 0 \\
&u_t = \|\mu_d - g\mathbf{e}_3\| \geq \sqrt{\mu_{d1}^2 + \mu_{d2}^2 + s^2} \geq s > 0 \\
&c_1 = u_t + g - \mu_{d3} \geq \sqrt{\mu_{d1}^2 + \mu_{d2}^2 + s^2} + s \geq 2s > 0
\end{aligned}$$

In addition, if $\|\mu_d\| \leq \mu_{d\max}$, then it can be verified that

$$\begin{aligned}
&u_t = \|\mu_d - g\mathbf{e}_3\| \leq \|\mu_d\| + \|g\mathbf{e}_3\| \leq \mu_{d\max} + g \\
&c_1 = u_t + g - \mu_{d3} \leq |u_t| + |g - \mu_{d3}| \leq 2\,|u_t| \leq 2\,(\mu_{d\max} + g)
\end{aligned}$$

It can be verified that the following is true.

$$\left|\frac{1}{u_t^2 c_1}\right| = \frac{1}{\left(\mu_{d1}^2 + \mu_{d2}^2 + (g-\mu_{d3})^2\right)\left(\sqrt{\mu_{d1}^2 + \mu_{d2}^2 + (g-\mu_{d3})^2} + g - \mu_{d3}\right)} \leq \frac{1}{2s^3}$$

The upper bound of $\frac{\partial}{\partial \mu_{dk}}\left(\frac{1}{u_t^2 c_1}\right)$ can be calculated as follows.

$$\frac{\partial}{\partial \mu_{dk}}\left(\frac{1}{u_t^2 c_1}\right) = \frac{-2u_t c_1 \frac{\partial u_t}{\partial \mu_{dk}} - u_t^2 \frac{\partial c_1}{\partial \mu_{dk}}}{u_t^4 c_1^2} = \frac{-2c_1 \frac{\partial u_t}{\partial \mu_{dk}} - u_t \frac{\partial c_1}{\partial \mu_{dk}}}{u_t^3 c_1^2}$$

$$\left|\frac{\partial}{\partial \mu_{dk}}\left(\frac{1}{u_t^2 c_1}\right)\right| = \left|\frac{2c_1 \frac{\partial u_t}{\partial \mu_{dk}} + u_t \frac{\partial c_1}{\partial \mu_{dk}}}{u_t^3 c_1^2}\right| \leq \frac{2c_1 \left|\frac{\partial u_t}{\partial \mu_{dk}}\right| + u_t \left|\frac{\partial c_1}{\partial \mu_{dk}}\right|}{u_t^3 c_1^2}$$

$$\leq \frac{2\left|\frac{\partial u_t}{\partial \mu_{dk}}\right|}{u_t^3 c_1} + \frac{\left|\frac{\partial c_1}{\partial \mu_{dk}}\right|}{u_t^2 c_1^2} \leq \frac{2}{2s^3 s} + \frac{2}{4s^2 s^2} = \frac{3}{2s^4}$$

So, $\frac{\partial}{\partial \mu_{dk}}\left(\frac{1}{u_t^2 c_1}\right)$ is bounded by $\frac{3}{2s^4}$ for $k = 1, 2, 3$.

By differentiating $M(\mu_d)$ in (D.14), $\frac{\partial M(\mu_d)}{\partial \mu_{d1}}$ can be expressed as

$$\frac{\partial M(\mu_d)}{\partial \mu_{d1}} = \left(\frac{\partial\left(\frac{1}{u_t^2 c_1}\right)}{\partial \mu_{d1}}\right)\begin{bmatrix} -\mu_{d1}\mu_{d2} & -\mu_{d2}^2 + u_t c_1 & \mu_{d2} c_1 \\ \mu_{d1}^2 - u_t c_1 & \mu_{d1}\mu_{d2} & -\mu_{d1} c_1 \\ \mu_{d2} u_t & -\mu_{d1} u_t & 0 \end{bmatrix}$$
$$+ \frac{1}{u_t^2 c_1}\begin{bmatrix} -\mu_{d2} & \frac{\partial u_t c_1}{\partial \mu_{d1}} & \mu_{d2}\frac{\partial c_1}{\partial \mu_{d1}} \\ 2\mu_{d1} - \frac{\partial u_t c_1}{\partial \mu_{d1}} & \mu_{d2} & -c_1 - \mu_{d1}\frac{\partial c_1}{\partial \mu_{d1}} \\ \mu_{d2}\frac{\partial u_t}{\partial \mu_{d1}} & -u_t - \mu_{d1}\frac{\partial u_t}{\partial \mu_{d1}} & 0 \end{bmatrix}$$
$$= \left(\frac{\partial\left(\frac{1}{u_t^2 c_1}\right)}{\partial \mu_{d1}}\right)\begin{bmatrix} -\mu_{d1}\mu_{d2} & -\mu_{d2}^2 + u_t c_1 & \mu_{d2} c_1 \\ \mu_{d1}^2 - u_t c_1 & \mu_{d1}\mu_{d2} & -\mu_{d1} c_1 \\ \mu_{d2} u_t & -\mu_{d1} u_t & 0 \end{bmatrix}$$
$$+ \frac{1}{u_t^2 c_1}\begin{bmatrix} -\mu_{d2} & c_1\frac{\partial u_t}{\partial \mu_{d1}} + u_t\frac{\partial c_1}{\partial \mu_{d1}} & \mu_{d2}\frac{\partial c_1}{\partial \mu_{d1}} \\ 2\mu_{d1} - \left(c_1\frac{\partial u_t}{\partial \mu_{d1}} + u_t\frac{\partial c_1}{\partial \mu_{d1}}\right) & \mu_{d2} & -c_1 - \mu_{d1}\frac{\partial c_1}{\partial \mu_{d1}} \\ \mu_{d2}\frac{\partial u_t}{\partial \mu_{d1}} & -u_t - \mu_{d1}\frac{\partial u_t}{\partial \mu_{d1}} & 0 \end{bmatrix}$$

Due to the boundedness of $\frac{\partial\left(\frac{1}{u_t^2 c_1}\right)}{\partial \mu_{d1}}$, $\frac{1}{u_t^2 c_1}$, u_t, c_1, μ_{d1}, $\frac{\partial u_t}{\partial \mu_{d1}}$, and $\frac{\partial c_1}{\partial \mu_{d1}}$, all the components of $\frac{\partial M(\mu_d)}{\partial \mu_{d1}}$ are bounded, which implies that $\frac{\partial M(\mu_d)}{\partial \mu_{d1}}$ is bounded.

By differentiating $M(\mu_d)$ in (D.14), $\frac{\partial M(\mu_d)}{\partial \mu_{d2}}$ can be expressed as

$$\frac{\partial M\left(\mu_d\right)}{\partial \mu_{d2}} = \left(\frac{\partial \frac{1}{u_t^2 c_1}}{\partial \mu_{d2}}\right) \begin{bmatrix} -\mu_{d1}\mu_{d2} & -\mu_{d2}^2 + u_t c_1 & \mu_{d2} c_1 \\ \mu_{d1}^2 - u_t c_1 & \mu_{d1}\mu_{d2} & -\mu_{d1} c_1 \\ \mu_{d2} u_t & -\mu_{d1} u_t & 0 \end{bmatrix}$$
$$+ \frac{1}{u_t^2 c_1} \begin{bmatrix} -\mu_{d1} & -2\mu_{d2} + \frac{\partial u_t c_1}{\partial \mu_{d2}} & c_1 + \mu_{d2}\frac{\partial c_1}{\partial \mu_{d2}} \\ -\frac{\partial u_t c_1}{\partial \mu_{d2}} & \mu_{d1} & -\mu_{d1}\frac{\partial c_1}{\partial \mu_{d2}} \\ u_t + \mu_{d2}\frac{\partial u_t}{\partial \mu_{d2}} & -\mu_{d1}\frac{\partial u_t}{\partial \mu_{d2}} & 0 \end{bmatrix}$$
$$= \left(\frac{\partial \frac{1}{u_t^2 c_1}}{\partial \mu_{d2}}\right) \begin{bmatrix} -\mu_{d1}\mu_{d2} & -\mu_{d2}^2 + u_t c_1 & \mu_{d2} c_1 \\ \mu_{d1}^2 - u_t c_1 & \mu_{d1}\mu_{d2} & -\mu_{d1} c_1 \\ \mu_{d2} u_t & -\mu_{d1} u_t & 0 \end{bmatrix}$$
$$+ \frac{1}{u_t^2 c_1} \begin{bmatrix} -\mu_{d1} & -2\mu_{d2} + c_1\frac{\partial u_t}{\partial \mu_{d2}} + u_t\frac{\partial c_1}{\partial \mu_{d2}} & c_1 + \mu_{d2}\frac{\partial c_1}{\partial \mu_{d2}} \\ -\left(c_1\frac{\partial u_t}{\partial \mu_{d2}} + u_t\frac{\partial c_1}{\partial \mu_{d2}}\right) & \mu_{d1} & -\mu_{d1}\frac{\partial c_1}{\partial \mu_{d2}} \\ u_t + \mu_{d2}\frac{\partial u_t}{\partial \mu_{d2}} & -\mu_{d1}\frac{\partial u_t}{\partial \mu_{d2}} & 0 \end{bmatrix}$$

Due to the boundedness of $\frac{\partial\left(\frac{1}{u_t^2 c_1}\right)}{\partial \mu_{d2}}$, $\frac{1}{u_t^2 c_1}$, u_t, c_1, μ_d, $\frac{\partial u_t}{\partial \mu_{d2}}$, and $\frac{\partial c_1}{\partial \mu_{d2}}$, all the components of $\frac{\partial M(\mu_d)}{\partial \mu_{d2}}$ are bounded, which implies that $\frac{\partial M(\mu_d)}{\partial \mu_{d2}}$ is bounded.

By differentiating $M\left(\mu_d\right)$ in (D.14), $\frac{\partial M(\mu_d)}{\partial \mu_{d3}}$ can be expressed as

$$\frac{\partial M\left(\mu_d\right)}{\partial \mu_{d3}} = \left(\frac{\partial \frac{1}{u_t^2 c_1}}{\partial \mu_{d3}}\right) \begin{bmatrix} -\mu_{d1}\mu_{d2} & -\mu_{d2}^2 + u_t c_1 & \mu_{d2} c_1 \\ \mu_{d1}^2 - u_t c_1 & \mu_{d1}\mu_{d2} & -\mu_{d1} c_1 \\ \mu_{d2} u_t & -\mu_{d1} u_t & 0 \end{bmatrix}$$
$$+ \frac{1}{u_t^2 c_1} \begin{bmatrix} 0 & \frac{\partial u_t c_1}{\partial \mu_{d3}} & \mu_{d2}\frac{\partial c_1}{\partial \mu_{d3}} \\ -\frac{\partial u_t c_1}{\partial \mu_{d3}} & 0 & -\mu_{d1}\frac{\partial c_1}{\partial \mu_{d3}} \\ \mu_{d2}\frac{\partial u_t}{\partial \mu_{d3}} & -\mu_{d1}\frac{\partial u_t}{\partial \mu_{d3}} & 0 \end{bmatrix}$$
$$= \left(\frac{\partial \frac{1}{u_t^2 c_1}}{\partial \mu_{d3}}\right) \begin{bmatrix} -\mu_{d1}\mu_{d2} & -\mu_{d2}^2 + u_t c_1 & \mu_{d2} c_1 \\ \mu_{d1}^2 - u_t c_1 & \mu_{d1}\mu_{d2} & -\mu_{d1} c_1 \\ \mu_{d2} u_t & -\mu_{d1} u_t & 0 \end{bmatrix}$$
$$+ \frac{1}{u_t^2 c_1} \begin{bmatrix} 0 & c_1\frac{\partial u_t}{\partial \mu_{d3}} + u_t\frac{\partial c_1}{\partial \mu_{d3}} & \mu_{d2}\frac{\partial c_1}{\partial \mu_{d3}} \\ -\left(c_1\frac{\partial u_t}{\partial \mu_{d3}} + u_t\frac{\partial c_1}{\partial \mu_{d3}}\right) & 0 & -\mu_{d1}\frac{\partial c_1}{\partial \mu_{d3}} \\ \mu_{d2}\frac{\partial u_t}{\partial \mu_{d3}} & -\mu_{d1}\frac{\partial u_t}{\partial \mu_{d3}} & 0 \end{bmatrix}$$

Due to the boundedness of $\frac{\partial\left(\frac{1}{u_t^2 c_1}\right)}{\partial \mu_{d3}}$, $\frac{1}{u_t^2 c_1}$, u_t, c_1, μ_d, $\frac{\partial u_t}{\partial \mu_{d3}}$, and $\frac{\partial c_1}{\partial \mu_{d3}}$, all the components of $\frac{\partial M(\mu_d)}{\partial \mu_{d3}}$ are bounded, which implies that $\frac{\partial M(\mu_d)}{\partial \mu_{d3}}$ is bounded.

Appendix F

The Boundedness of $\frac{\partial h(\mathbf{x},\varepsilon_1,\varepsilon_2)}{\partial \mathbf{x}}$ and $\frac{\partial^2 h(\mathbf{x},\varepsilon_1,\varepsilon_2)}{\partial \mathbf{x}^2}$

Define $\mathbf{x} = \begin{bmatrix} x_1 & x_2 & x_3 \end{bmatrix}^T$. Then, $h_i = \frac{x_i}{\left(\varepsilon_1+\varepsilon_2\left(x_1^2+x_2^2+x_3^2\right)\right)^{\frac{1}{2}}}$. Therefore, the components of $\frac{\partial h(\mathbf{x},\varepsilon_1,\varepsilon_2)}{\partial \mathbf{x}}$ can be calculated by

$$\begin{aligned}\frac{\partial h_i}{\partial x_j} &= \frac{\partial}{\partial x_j}\left(\frac{x_i}{\left(\varepsilon_1+\varepsilon_2\left(x_1^2+x_2^2+x_3^2\right)\right)^{\frac{1}{2}}}\right)\\ &= \frac{-\varepsilon_2 x_i x_j}{\left(\varepsilon_1+\varepsilon_2\left(x_1^2+x_2^2+x_3^2\right)\right)^{3/2}}\end{aligned}$$

for $i \neq j$ and

$$\begin{aligned}\frac{\partial h_i}{\partial x_j} &= \frac{\partial}{\partial x_i}\left(\frac{x_i}{\left(\varepsilon_1+\varepsilon_2\left(x_1^2+x_2^2+x_3^2\right)\right)^{\frac{1}{2}}}\right)\\ &= \frac{1}{\left(\varepsilon_1+\varepsilon_2\left(x_1^2+x_2^2+x_3^2\right)\right)^{1/2}} + \frac{-\varepsilon_2 x_i x_i}{\left(\varepsilon_1+\varepsilon_2\left(x_1^2+x_2^2+x_3^2\right)\right)^{3/2}}\\ &= \frac{\left(\varepsilon_1+\varepsilon_2\left(x_1^2+x_2^2+x_3^2\right)\right)-\varepsilon_2 x_i^2}{\left(\varepsilon_1+\varepsilon_2\left(x_1^2+x_2^2+x_3^2\right)\right)^{3/2}}\\ &= \frac{\varepsilon_1+\varepsilon_2\sum_{s\neq i} x_s^2}{\left(\varepsilon_1+\varepsilon_2\left(x_1^2+x_2^2+x_3^2\right)\right)^{3/2}}\end{aligned}$$

for $i = j$. It can be verified that the followings are true.

$$|\sqrt{\varepsilon_2}x_i| = \sqrt{\varepsilon_2 x_i^2} \leq \sqrt{\varepsilon_1 + \varepsilon_2\left(x_1^2 + x_2^2 + x_3^2\right)} \tag{F.1}$$

$$\varepsilon_2 \sum_{s\neq i} x_s^2 \leq \varepsilon_1 + \varepsilon_2\left(x_1^2 + x_2^2 + x_3^2\right) \tag{F.2}$$

for $i = 1, 2, 3$. With this inequalities, it follows that for $i \neq j$

$$\begin{aligned}
\left|\frac{\partial h_i}{\partial x_j}\right| &= \left|\frac{-\varepsilon_2 x_i x_j}{\left(\varepsilon_1 + \varepsilon_2\left(x_1^2 + x_2^2 + x_3^2\right)\right)^{3/2}}\right| \\
&= \frac{\left|\sqrt{\varepsilon_2}x_i\right|\left|\sqrt{\varepsilon_2}x_j\right|}{\left(\varepsilon_1 + \varepsilon_2\left(x_1^2 + x_2^2 + x_3^2\right)\right)^{3/2}} \\
&\leq \frac{\sqrt{\varepsilon_1 + \varepsilon_2\left(x_1^2 + x_2^2 + x_3^2\right)}\sqrt{\varepsilon_1 + \varepsilon_2\left(x_1^2 + x_2^2 + x_3^2\right)}}{\left(\varepsilon_1 + \varepsilon_2\left(x_1^2 + x_2^2 + x_3^2\right)\right)^{3/2}} \\
&\leq \frac{1}{\left(\varepsilon_1 + \varepsilon_2\left(x_1^2 + x_2^2 + x_3^2\right)\right)^{\frac{1}{2}}} \leq \frac{1}{\sqrt{\varepsilon_1}}
\end{aligned}$$

and for $i \neq j$

$$\begin{aligned}
\left|\frac{\partial h_i}{\partial x_j}\right| &= \left|\frac{\varepsilon_1 + \varepsilon_2 \sum_{s\neq i} x_s^2}{\left(\varepsilon_1 + \varepsilon_2\left(x_1^2 + x_2^2 + x_3^2\right)\right)^{3/2}}\right| \\
&= \frac{\varepsilon_1 + \varepsilon_2 \sum_{s\neq i} x_s^2}{\left(\varepsilon_1 + \varepsilon_2\left(x_1^2 + x_2^2 + x_3^2\right)\right)^{3/2}} \\
&\leq \frac{1}{\left(\varepsilon_1 + \varepsilon_2\left(x_1^2 + x_2^2 + x_3^2\right)\right)^{\frac{1}{2}}} \leq \frac{1}{\sqrt{\varepsilon_1}}
\end{aligned}$$

Therefore, all the components of $\frac{\partial h(\mathbf{x},\varepsilon_1,\varepsilon_2)}{\partial \mathbf{x}}$ are bounded by $\frac{1}{\sqrt{\varepsilon_1}}$. Furthermore, the components of $\frac{\partial^2 h(\mathbf{x},\varepsilon_1,\varepsilon_2)}{\partial \mathbf{x}^2}$ and their upper bounds can be computed as

$$\begin{aligned}
\frac{\partial^2 h_i}{\partial x_k \partial x_j} &= \frac{\partial}{\partial x_k}\left(\frac{\partial h_i}{\partial x_j}\right) = \frac{\partial}{\partial x_k}\left(\frac{-\varepsilon_2 x_i x_j}{\left(\varepsilon_1+\varepsilon_2\left(x_1^2+x_2^2+x_3^2\right)\right)^{3/2}}\right) \\
&= \frac{3\varepsilon_2^2 x_i x_j x_k}{\left(\varepsilon_1+\varepsilon_2\left(x_1^2+x_2^2+x_3^2\right)\right)^{5/2}} \\
\left|\frac{\partial^2 h_i}{\partial x_k \partial x_j}\right| &= \frac{3\sqrt{\varepsilon_2}\left|\sqrt{\varepsilon_2}x_i\right|\left|\sqrt{\varepsilon_2}x_j\right|\left|\sqrt{\varepsilon_2}x_k\right|}{\left(\varepsilon_1+\varepsilon_2\left(x_1^2+x_2^2+x_3^2\right)\right)^{5/2}} \\
&\leq \frac{3\sqrt{\varepsilon_2}\left(\varepsilon_1+\varepsilon_2\left(x_1^2+x_2^2+x_3^2\right)\right)^{3/2}}{\left(\varepsilon_1+\varepsilon_2\left(x_1^2+x_2^2+x_3^2\right)\right)^{5/2}} \\
&\leq \frac{3\sqrt{\varepsilon_2}}{\left(\varepsilon_1+\varepsilon_2\left(x_1^2+x_2^2+x_3^2\right)\right)} \leq \frac{3\sqrt{\varepsilon_2}}{\varepsilon_1}
\end{aligned}$$

for $k \neq i \neq j$,

$$\begin{aligned}
\frac{\partial^2 h_i}{\partial x_k \partial x_j} &= \frac{\partial}{\partial x_k}\left(\frac{\partial h_i}{\partial x_j}\right) = \frac{\partial}{\partial x_k}\left(\frac{-\varepsilon_2 x_i x_j}{\left(\varepsilon_1+\varepsilon_2\left(x_1^2+x_2^2+x_3^2\right)\right)^{3/2}}\right) \\
&= \frac{-\varepsilon_2 x_j}{\left(\varepsilon_1+\varepsilon_2\left(x_1^2+x_2^2+x_3^2\right)\right)^{3/2}} + \frac{3\varepsilon_2^2 x_j x_k^2}{\left(\varepsilon_1+\varepsilon_2\left(x_1^2+x_2^2+x_3^2\right)\right)^{5/2}} \\
&= \frac{-\varepsilon_2 x_j\left(\varepsilon_2 x_2^2+\varepsilon_2 x_3^2+\varepsilon_2 x_4^2+\varepsilon_1\right)+3\varepsilon_2^2 x_j x_k^2}{\left(\varepsilon_1+\varepsilon_2\left(x_1^2+x_2^2+x_3^2\right)\right)^{5/2}} \\
&= \frac{\varepsilon_2 x_j\left[-\left(\varepsilon_1+\varepsilon_2\left(x_1^2+x_2^2+x_3^2\right)\right)+3\varepsilon_2 x_k^2\right]}{\left(\varepsilon_1+\varepsilon_2\left(x_1^2+x_2^2+x_3^2\right)\right)^{5/2}} \\
\left|\frac{\partial^2 h_i}{\partial x_k \partial x_j}\right| &= \frac{\sqrt{\varepsilon_2}\sqrt{\varepsilon_2}\left|x_j\right|\left|-\left(\varepsilon_1+\varepsilon_2\left(x_1^2+x_2^2+x_3^2\right)\right)+3\varepsilon_2 x_k^2\right|}{\left(\varepsilon_1+\varepsilon_2\left(x_1^2+x_2^2+x_3^2\right)\right)^{5/2}} \\
&\leq \frac{\sqrt{\varepsilon_2}\left[\left|-\left(\varepsilon_1+\varepsilon_2\left(x_1^2+x_2^2+x_3^2\right)\right)\right|+\left|3\varepsilon_2 x_k^2\right|\right]}{\left(\varepsilon_1+\varepsilon_2\left(x_1^2+x_2^2+x_3^2\right)\right)^2} \\
&\leq \frac{4\sqrt{\varepsilon_2}\left(\varepsilon_1+\varepsilon_2\left(x_1^2+x_2^2+x_3^2\right)\right)}{\left(\varepsilon_1+\varepsilon_2\left(x_1^2+x_2^2+x_3^2\right)\right)^2} \\
&\leq \frac{4\sqrt{\varepsilon_2}}{\left(\varepsilon_1+\varepsilon_2\left(x_1^2+x_2^2+x_3^2\right)\right)} \leq \frac{4\sqrt{\varepsilon_2}}{\varepsilon_1}
\end{aligned}$$

for $k = i$ and $i \neq j$,

$$\begin{aligned}
\frac{\partial^2 h_i}{\partial x_k \partial x_j} &= \frac{\partial}{\partial x_k}\left(\frac{\partial h_i}{\partial x_j}\right) = \frac{\partial}{\partial x_k}\left(\frac{-\varepsilon_2 x_i x_j}{\left(\varepsilon_1+\varepsilon_2\left(x_1^2+x_2^2+x_3^2\right)\right)^{3/2}}\right) \\
&= \frac{-\varepsilon_2 x_i}{\left(\varepsilon_1+\varepsilon_2\left(x_1^2+x_2^2+x_3^2\right)\right)^{3/2}} + \frac{3\varepsilon_2^2 x_i x_k^2}{\left(\varepsilon_1+\varepsilon_2\left(x_1^2+x_2^2+x_3^2\right)\right)^{5/2}} \\
&= \frac{-\varepsilon_2 x_i\left(\varepsilon_1+\varepsilon_2\left(x_1^2+x_2^2+x_3^2\right)\right)+3\varepsilon_2^2 x_i x_k^2}{\left(\varepsilon_1+\varepsilon_2\left(x_1^2+x_2^2+x_3^2\right)\right)^{5/2}} \\
&= \frac{\varepsilon_2 x_i\left[-\left(\varepsilon_1+\varepsilon_2\left(x_1^2+x_2^2+x_3^2\right)\right)+3\varepsilon_2 x_k^2\right]}{\left(\varepsilon_1+\varepsilon_2\left(x_1^2+x_2^2+x_3^2\right)\right)^{5/2}} \\
\left|\frac{\partial^2 h_i}{\partial x_k \partial x_j}\right| &= \frac{\sqrt{\varepsilon_2}\sqrt{\varepsilon_2}\left|x_i\right|\left|-\left(\varepsilon_1+\varepsilon_2\left(x_1^2+x_2^2+x_3^2\right)\right)+3\varepsilon_2 x_k^2\right|}{\left(\varepsilon_1+\varepsilon_2\left(x_1^2+x_2^2+x_3^2\right)\right)^{5/2}} \\
&\leq \frac{\sqrt{\varepsilon_2}\left[\left|-\left(\varepsilon_1+\varepsilon_2\left(x_1^2+x_2^2+x_3^2\right)\right)\right|+\left|3\varepsilon_2 x_k^2\right|\right]}{\left(\varepsilon_1+\varepsilon_2\left(x_1^2+x_2^2+x_3^2\right)\right)^{2}} \\
&\leq \frac{4\sqrt{\varepsilon_2}\left(\varepsilon_1+\varepsilon_2\left(x_1^2+x_2^2+x_3^2\right)\right)}{\left(\varepsilon_1+\varepsilon_2\left(x_1^2+x_2^2+x_3^2\right)\right)^{2}} \\
&\leq \frac{4\sqrt{\varepsilon_2}}{\left(\varepsilon_1+\varepsilon_2\left(x_1^2+x_2^2+x_3^2\right)\right)} \leq \frac{4\sqrt{\varepsilon_2}}{\varepsilon_1}
\end{aligned}$$

for $k = j$ and $i \neq j$,

$$\begin{aligned}
\frac{\partial}{\partial x_k}\left(\frac{\partial h_i}{\partial x_j}\right) &= \frac{\partial}{\partial x_k}\left(\frac{\varepsilon_1+\varepsilon_2\sum_{s\neq i} x_s^2}{\left(\varepsilon_1+\varepsilon_2\left(x_1^2+x_2^2+x_3^2\right)\right)^{3/2}}\right) \\
&= \frac{-3\varepsilon_2 x_k\left(\varepsilon_1+\varepsilon_2\sum_{s\neq i} x_s^2\right)}{\left(\varepsilon_1+\varepsilon_2\left(x_1^2+x_2^2+x_3^2\right)\right)^{5/2}} \\
\left|\frac{\partial}{\partial x_k}\left(\frac{\partial h_i}{\partial x_j}\right)\right| &= \frac{3\sqrt{\varepsilon_2}\sqrt{\varepsilon_2}\left|x_k\right|\left(\varepsilon_1+\varepsilon_2\sum_{s\neq i} x_s^2\right)}{\left(\varepsilon_1+\varepsilon_2\left(x_1^2+x_2^2+x_3^2\right)\right)^{5/2}} \\
&\leq \frac{3\sqrt{\varepsilon_2}\left(\varepsilon_1+\varepsilon_2\left(x_1^2+x_2^2+x_3^2\right)\right)}{\left(\varepsilon_1+\varepsilon_2\left(x_1^2+x_2^2+x_3^2\right)\right)^{2}} \\
&\leq \frac{3\sqrt{\varepsilon_2}}{\left(\varepsilon_1+\varepsilon_2\left(x_1^2+x_2^2+x_3^2\right)\right)} \leq \frac{3\sqrt{\varepsilon_2}}{\varepsilon_1}
\end{aligned}$$

for $k = i = j$, and

$$
\begin{aligned}
\frac{\partial}{\partial x_k}\left(\frac{\partial h_i}{\partial x_i}\right) &= \frac{\partial}{\partial x_k}\left(\frac{\varepsilon_1+\varepsilon_2\sum_{s\neq i}x_s^2}{\left(\varepsilon_1+\varepsilon_2\left(x_1^2+x_2^2+x_3^2\right)\right)^{3/2}}\right)\\
&= \frac{2\varepsilon_2 x_k}{\left(\varepsilon_1+\varepsilon_2\left(x_1^2+x_2^2+x_3^2\right)\right)^{3/2}}+\frac{-3\varepsilon_2 x_k\left(\varepsilon_1+\varepsilon_2\sum_{s\neq i}x_s^2\right)}{\left(\varepsilon_1+\varepsilon_2\left(x_1^2+x_2^2+x_3^2\right)\right)^{5/2}}\\
&= \frac{2\varepsilon_2 x_k\left(\varepsilon_1+\varepsilon_2\left(x_1^2+x_2^2+x_3^2\right)\right)-3\varepsilon_2 x_k\left(\varepsilon_1+\varepsilon_2\sum_{s\neq i}x_s^2\right)}{\left(\varepsilon_1+\varepsilon_2\left(x_1^2+x_2^2+x_3^2\right)\right)^{5/2}}\\
&= \frac{\varepsilon_2 x_k\left[2\left(\varepsilon_1+\varepsilon_2\left(x_1^2+x_2^2+x_3^2\right)\right)-3\left(\varepsilon_1+\varepsilon_2\sum_{s\neq i}x_s^2\right)\right]}{\left(\varepsilon_1+\varepsilon_2\left(x_1^2+x_2^2+x_3^2\right)\right)^{5/2}}\\
\left|\frac{\partial}{\partial x_k}\left(\frac{\partial h_i}{\partial x_i}\right)\right| &= \frac{\sqrt{\varepsilon_2}\sqrt{\varepsilon_2}\,|x_k|\left|\left[2\left(\varepsilon_1+\varepsilon_2\left(x_1^2+x_2^2+x_3^2\right)\right)-3\left(\varepsilon_1+\varepsilon_2\sum_{s\neq i}x_s^2\right)\right]\right|}{\left(\varepsilon_1+\varepsilon_2\left(x_1^2+x_2^2+x_3^2\right)\right)^{5/2}}\\
&\leq \frac{\sqrt{\varepsilon_2}\left[\left|2\left(\varepsilon_1+\varepsilon_2\left(x_1^2+x_2^2+x_3^2\right)\right)\right|+\left|-3\left(\varepsilon_1+\varepsilon_2\sum_{s\neq i}x_s^2\right)\right|\right]}{\left(\varepsilon_1+\varepsilon_2\left(x_1^2+x_2^2+x_3^2\right)\right)^{2}}\\
&\leq \frac{\sqrt{\varepsilon_2}\left[2\left(\varepsilon_1+\varepsilon_2\left(x_1^2+x_2^2+x_3^2\right)\right)+3\left(\varepsilon_1+\varepsilon_2\left(x_1^2+x_2^2+x_3^2\right)\right)\right]}{\left(\varepsilon_1+\varepsilon_2\left(x_1^2+x_2^2+x_3^2\right)\right)^{2}}\\
&\leq \frac{5\sqrt{\varepsilon_2}}{\left(\varepsilon_1+\varepsilon_2\left(x_1^2+x_2^2+x_3^2\right)\right)}\leq\frac{5\sqrt{\varepsilon_2}}{\varepsilon_1}
\end{aligned}
$$

for $k\neq i=j$. Therefore, all the components of $\frac{\partial^2 h(\mathbf{x},\varepsilon_1,\varepsilon_2)}{\partial \mathbf{x}^2}$ are bounded by $\frac{5\sqrt{\varepsilon_2}}{\varepsilon_1}$.

Appendix G

Motor Characteristics

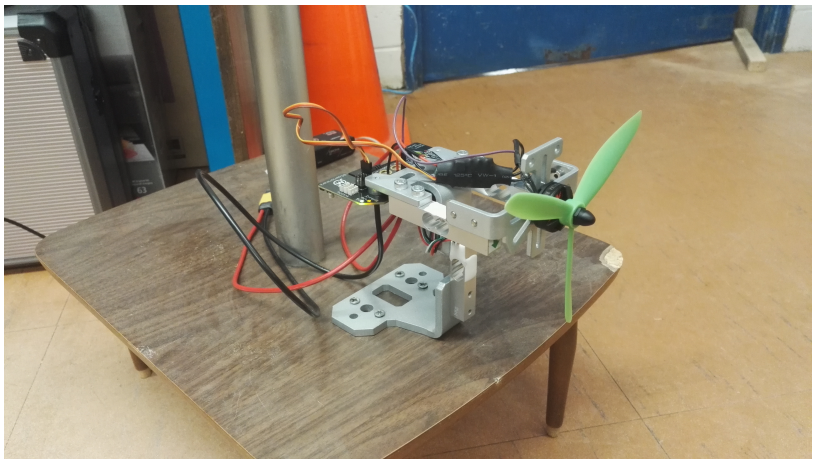

Figure G.1: Motor Test Stand

Motors used in the thesis are BLDC motors. Although called DC motor, the BLDC motor is actually powered by a 3 phase AC. So a ESC is required. The ESC converts DC power to AC power in order to drive the motor. Also, it reads the PWM signal from the receiver of the RC system and converts it to the actual thrust force by the motor and propeller. So it is inaccurate to call it a speed controller. The control object of an regular ESC is not the motor's angular velocity. Only in helicopter mode, the ESC is used as an actual speed controller because the main task for a helicopter ESC is to maintain a constant angular velocity by a constant PWM signal. To verify the relationship between the PWM signal and angular velocity of the motor or the thrust of the propeller, several experimental tests were conducted. The result is shown as in Fig. G.2 and Fig. G.3. It can be concluded from the test result that the relationship between the PWM signal and the thrust of the propeller is nearly linear and the relationship between the PWM signal and angular velocity of the motor is nonlinear. Besides, the torque generated by the motor is also closed to linear with the input PWM signal as shown in Fig. G.4.

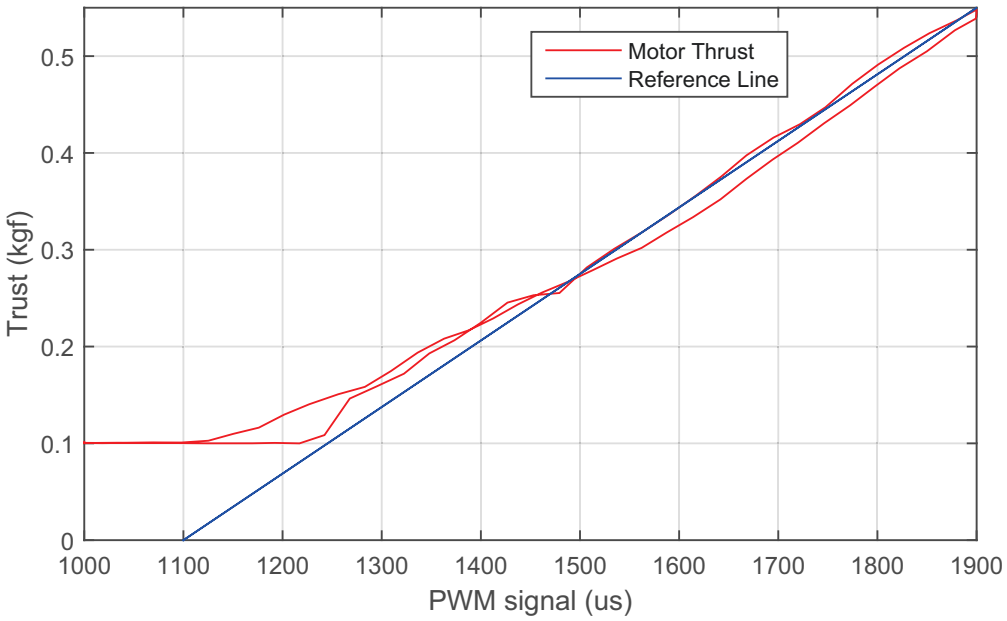

Figure G.2: Relationship between PWM and Thrust

G.1 Output Relationships

From the proposed controller, only the torque on the body fixed frame can be obtained. It is not an issue for the simulation because the input of the model is just only the torque. However, in the practical experiment, it is not able to control the torque on body fixed frame directly. The torque on the body fixed frame is generated by rotors. Therefore, the relationship between the PWM signals for motors and the torque introduced on the quadrotor body need to be determined.

According to the physical definition, torque is the product of the force and the force arm. So the following equations can be obtained.

$$l_1(F_{fl} + F_{bl}) - l_1(F_{fr} + F_{br}) = \tau_r \tag{G.1}$$
$$l_2(F_{fl} + F_{fr}) - l_2(F_{bl} + F_{br}) = \tau_p \tag{G.2}$$
$$(\tau_{fr} + \tau_{bl}) - (\tau_{fl} + \tau_{br}) = \tau_y \tag{G.3}$$
$$F_{fl} + F_{fr} + F_{bl} + F_{br} = F_{set} \tag{G.4}$$

where l_1 is half of the distance from the FL motor axis to the FR motor axis and l_2 is half of the distance from the FL motor axis to the BL motor axis. τ_r, τ_p, and τ_y are the torque on body fixed frame with roll, pitch and yaw axis. τ_{fr}, τ_{bl}, τ_{fl}, and τ_{br} are the torque generated by FR, BL, FL, and BR motors. F_{fl}, F_{fr}, F_{bl}, and F_{br} are the thrust force generated by FL, FR, BL, and BR motors. The definition of FL, FR, BL, and BR motors can be refereed to Fig. 2.8. F_{set} is the general thrust set by input. It should be close to the gravity force when the quadrotor is hovering.

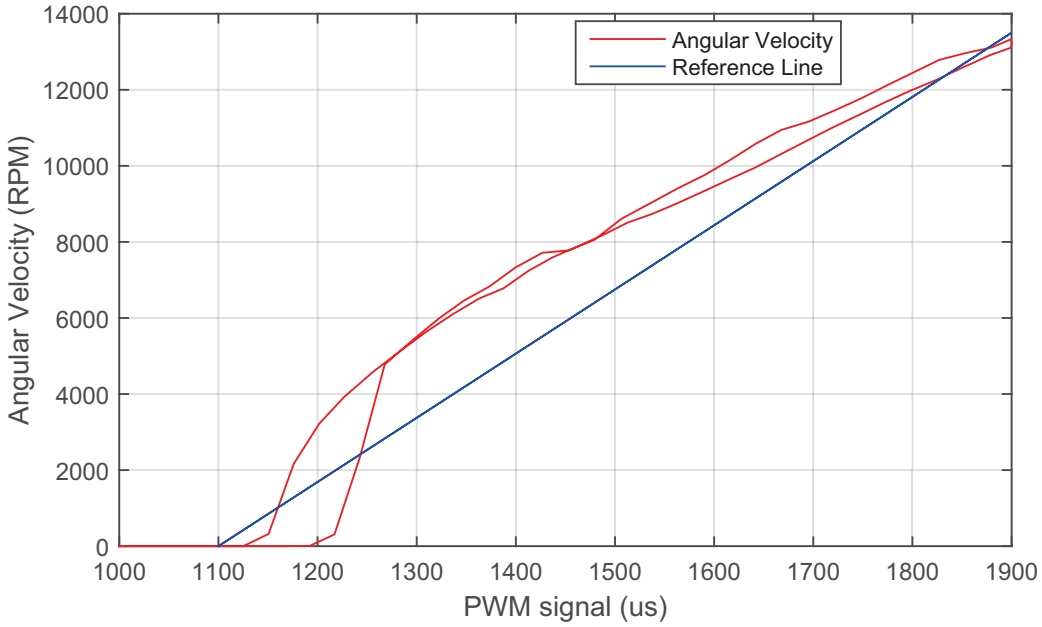

Figure G.3: Relationship between PWM and Angular Velocity

From Fig. G.2, the following relationship can be determined.

$$F_m = (P - 1100)c_F \tag{G.5}$$

where F_m is the thrust generated by the rotor. P is the high logic time of the PWM signal in microsecond. c_F is a constant and in this case $c_F = g/1454.5$. g is the gravity constant.

From Fig. G.4, the following relationship can be determined.

$$\tau_m = (P - 1100)c_\tau \tag{G.6}$$

where τ_m is the torque generated by the rotor. P is the high logic time of the PWM signal in microseconds. c_τ is a constant and in this case $c_\tau = 0.00008375$

By substituting (G.5) and (G.6) to (G.1), (G.2), (G.3), and (G.4), the following relationships can be obtained.

$$P_{fl} = \frac{1}{4}\left(P_{set} + \frac{\tau_r}{c_F l_1} + \frac{\tau_p}{c_F l_2} - \frac{\tau_y}{c_\tau} + 3300\right) \tag{G.7}$$

$$P_{bl} = \frac{1}{4}\left(P_{set} + \frac{\tau_r}{c_F l_1} - \frac{\tau_p}{c_F l_2} + \frac{\tau_y}{c_\tau} + 3300\right) \tag{G.8}$$

$$P_{fr} = \frac{1}{4}\left(P_{set} - \frac{\tau_r}{c_F l_1} + \frac{\tau_p}{c_F l_2} + \frac{\tau_y}{c_\tau} + 3300\right) \tag{G.9}$$

$$P_{br} = \frac{1}{4}\left(P_{set} - \frac{\tau_r}{c_F l_1} - \frac{\tau_p}{c_F l_2} - \frac{\tau_y}{c_\tau} + 3300\right) \tag{G.10}$$

where P_{fl}, P_{bl}, P_{fr}, and P_{br} are the high logic time in microseconds for the PWM signal of FL, BL, FR, and BR motors. P_{set} is the thrust input of the system in PWM siganl.

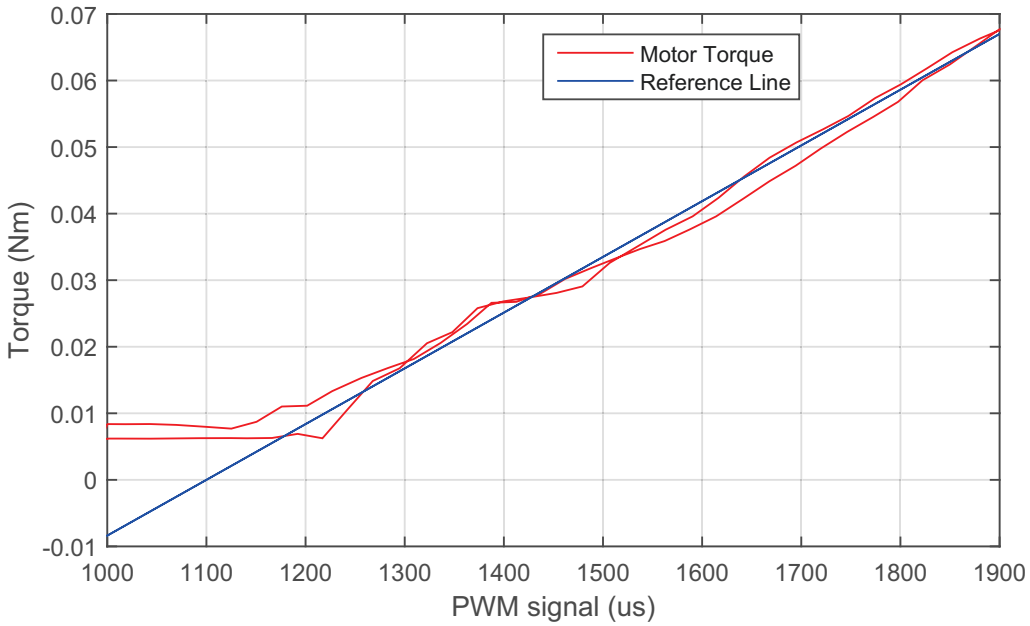

Figure G.4: Relationship between PWM and Motor Torque

Bibliography

[1] *Unmanned Aircraft Systems (UAS)*. ICAO, 2011. ISBN: 978-92-9231-751-5 https://www.icao.int/Meetings/UAS/Documents/Circular%20328_en.pdf.

[2] http://www.northropgrumman.com/Capabilities/GlobalHawk/Pages/default.aspx.

[3] http://www.af.mil/About-Us/Fact-Sheets/Display/Article/104470/mq-9-reaper/.

[4] http://www.northropgrumman.com/Capabilities/FireScout/Documents/pageDocuments/MQ-8B_Fire_Scout_Data_Sheet.pdf.

[5] https://www.arm.gov/news/features/post/37859.

[6] https://www.festo.com/group/en/cms/10238.htm.

[7] J. D. DeLaurier, "An ornithopter wing design," *Canadian Aeronautics and Space Journal*, vol. 40, no. 1, pp. 10–18, 1994.

[8] L. R. G. Carrillo, A. E. D. López, R. Lozano, and C. Pégard, *Quad Rotorcraft Control: Vision-based Hovering and Navigation*. Springer Science & Business Media, 2012.

[9] A. Tayebi and S. McGilvray, "Attitude stabilization of a VTOL quadrotor aircraft," *IEEE Transactions on Control Systems Technology*, vol. 14, no. 3, pp. 562–571, May 2006.

[10] E. Altug, J. P. Ostrowski, and R. Mahony, "Control of a quadrotor helicopter using visual feedback," in *Proceedings of IEEE International Conference on Robotics and Automation*, vol. 1, pp. 72–77, 2002.

[11] https://www.dji.com/phantom-4-adv/info#specs.

[12] https://www.dji.com/inspire-2/info#specs.

[13] R. E. Kalman, "A new approach to linear filtering and prediction problems," *Journal of Basic Engineering*, vol. 82, no. 1, pp. 35–45, 1960.

[14] S. F. Schmidt, "The Kalman filter - its recognition and development for aerospace applications," *Journal of Guidance, Control and Dynamics*, vol. 4, no. 1, pp. 4–7, 1981.

[15] M. S. Grewal and A. P. Andrews, *Kalman Filtering: Theory and Practice Using MATLAB*. 2001.

[16] M. S. Grewal, "Kalman filtering," in *International Encyclopedia of Statistical Science*, pp. 705–708, Springer, 2011.

[17] D. Simon, "Kalman filtering, embedded systems programming," *Embedded. com Article*, 2001.

[18] M. S. Grewal and A. P. Andrews, "Applications of Kalman filtering in aerospace 1960 to the present [historical perspectives]," *IEEE Control Systems*, vol. 30, no. 3, pp. 69–78, 2010.

[19] E. J. Lefferts, F. L. Markley, and M. D. Shuster, "Kalman filtering for spacecraft attitude estimation," *Journal of Guidance, Control and Dynamics*, vol. 5, no. 5, pp. 417–429, 1982.

[20] A. M. Sabatini, "Quaternion-based extended Kalman filter for determining orientation by inertial and magnetic sensing," *IEEE Transactions on Biomedical Engineering*, vol. 53, no. 7, pp. 1346–1356, 2006.

[21] J. L. Marins, X. Yun, E. R. Bachmann, R. B. McGhee, and M. J. Zyda, "An extended Kalman filter for quaternion-based orientation estimation using marg sensors," in *Proceedings of IEEE/RSJ International Conference on Intelligent Robots and Systems*, vol. 4, pp. 2003–2011, 2001.

[22] S. J. Julier and J. K. Uhlmann, "A new extension of the Kalman filter to nonlinear systems," in *Proceedings of AeroSense: The 11th International Symposium on Aerospace/Defense Sensing, Simulation and Controls*, vol. 3, pp. 182–193, Orlando, FL, 1997.

[23] J. J. LaViola, "A comparison of unscented and extended Kalman filtering for estimating quaternion motion," in *Proceedings of American Control Conference*, vol. 3, pp. 2435–2440, 2003.

[24] K. D. Sebesta and N. Boizot, "A real-time adaptive high-gain EKF, applied to a quadcopter inertial navigation system," *IEEE Transactions on Industrial Electronics*, vol. 61, no. 1, pp. 495–503, 2014.

[25] T. Hamel and R. Mahony, "Attitude estimation on SO(3) based on direct inertial measurements," in *Proceedings of IEEE International Conference on Robotics and Automation*, pp. 2170–2175, 2006.

[26] R. Mahony, T. Hamel, and J. M. Pflimlin, "Nonlinear complementary filters on the special orthogonal group," *IEEE Transactions on Automatic Control*, vol. 53, no. 5, pp. 1203–1218, 2008.

[27] M. D. Hua, G. Ducard, T. Hamel, R. Mahony, and K. Rudin, "Implementation of a nonlinear attitude estimator for aerial robotic vehicles," *IEEE Transactions on Control Systems Technology*, vol. 22, no. 1, 2014.

[28] S. O. H. Madgwick, A. J. Harrison, and R. Vaidyanathan, "Estimation of IMU and MARG orientation using a gradient descent algorithm," in *Proceedings of IEEE International Conference on Rehabilitation Robotics*, pp. 1–7, 2011.

[29] S. O. H. Madgwick, "An efficient orientation filter for inertial and inertial/magnetic sensor arrays," *Report x-io and University of Bristol (UK)*, vol. 25, 2010.

[30] A. L. Salih, M. Moghavvemi, H. A. Mohamed, and K. S. Gaeid, "Modelling and PID controller design for a quadrotor unmanned air vehicle," in *Proceedings of IEEE International Conference on Automation Quality and Testing Robotics*, vol. 1, pp. 1–5, 2010.

[31] S. Bouabdallah, A. Noth, and R. Siegwart, "PID vs LQR control techniques applied to an indoor micro quadrotor," in *Proceedings of IEEE/RSJ International Conference on Intelligent Robots and Systems*, vol. 3, pp. 2451–2456, 2004.

[32] L. M. Argentim, W. C. Rezende, P. E. Santos, and R. A. Aguiar, "PID, LQR and LQR-PID on a quadcopter platform," in *Proceedings of International Conference on Informatics, Electronics and Vision*, pp. 1–6, May 2013.

[33] S. Bouabdallah and R. Siegwart, "Backstepping and sliding-mode techniques applied to an indoor micro quadrotor," in *Proceedings of the IEEE International Conference on Robotics and Automation*, pp. 2247–2252, 2005.

[34] T. Madani and A. Benallegue, "Backstepping control for a quadrotor helicopter," in *Proceedings of IEEE/RSJ International Conference on Intelligent Robots and Systems*, pp. 3255–3260, 2006.

[35] A. Soumelidis, P. Gáspár, G. Regula, and B. Lantos, "Control of an experimental mini quad-rotor UAV," in *Proceedings of 16th Mediterranean Conference on Control and Automation*, pp. 1252–1257, 2008.

[36] X. Cui, "Intelligent backstepping quadrotor position control using neural network," *Master Thesis, Lakehead University, Ontario, Canada*, 2016.

[37] K. Zhao, "Attitude control for a quadrotor UAV using adaptive fuzzy backstepping," *Master Thesis, Lakehead University, Ontario, Canada*, 2017.

[38] M. Huang, B. Xian, C. Diao, K. Yang, and Y. Feng, "Adaptive tracking control of underactuated quadrotor unmanned aerial vehicles via backstepping," in *Proceedings of American Control Conference*, pp. 2076–2081, 2010.

[39] A. A. Mian and D. Wang, "Modeling and backstepping-based nonlinear control strategy for a 6 DOF quadrotor helicopter," *Chinese Journal of Aeronautics*, vol. 21, no. 3, pp. 261–268, 2008.

[40] G. V. Raffo, M. G. Ortega, and F. R. Rubio, "Backstepping/nonlinear H_∞ control for path tracking of a quadrotor unmanned aerial vehicle," in *Proceedings of American Control Conference*, pp. 3356–3361, 2008.

[41] H. Bouadi, S. S. Cunha, A. Drouin, and F. Mora-Camino, "Adaptive sliding mode control for quadrotor attitude stabilization and altitude tracking," in *Proceedings of IEEE 12th International Symposium on Computational Intelligence and Informatics (CINTI)*, pp. 449–455, 2011.

[42] D. Cabecinhas, R. Cunha, and C. Silvestre, "A nonlinear quadrotor trajectory tracking controller with disturbance rejection," *Control Engineering Practice*, vol. 26, pp. 1–10, 2014.

[43] D. Lee, H. J. Kim, and S. Sastry, "Feedback linearization vs. adaptive sliding mode control for a quadrotor helicopter," *International Journal of Control, Automation and Systems*, vol. 7, no. 3, pp. 419–428, 2009.

[44] Z. T. Dydek, A. M. Annaswamy, and E. Lavretsky, "Adaptive control of quadrotor UAVs: a design trade study with flight evaluations," *IEEE Transactions on Control Systems Technology*, vol. 21, no. 4, pp. 1400–1406, 2013.

[45] C. Nicol, C. Macnab, and A. Ramirez-Serrano, "Robust adaptive control of a quadrotor helicopter," *Mechatronics*, vol. 21, no. 6, pp. 927–938, 2011.

[46] C. Coza and C. J. B. Macnab, "A new robust adaptive-fuzzy control method applied to quadrotor helicopter stabilization," in *Proceedings of Annual Meeting of the North American Fuzzy Information Processing Society*, pp. 454–458, 2006.

[47] G. V. Raffo, M. G. Ortega, and F. R. Rubio, "An integral predictive/nonlinear H_∞ control structure for a quadrotor helicopter," *Automatica*, vol. 46, no. 1, pp. 29–39, 2010.

[48] K. Hornik, M. Stinchcombe, and H. White, "Multilayer feedforward networks are universal approximators," *Neural Networks*, vol. 2, no. 5, pp. 359–366, 1989.

[49] J. Park and I. W. Sandberg, "Universal approximation using radial-basis-function networks," *Neural Computation*, vol. 3, no. 2, pp. 246–257, 1991.

[50] V. Kŭrková, "Kolmogorov's theorem and multilayer neural networks," *Neural Networks*, vol. 5, no. 3, pp. 501–506, 1992.

[51] A. R. Barron, "Universal approximation bounds for superpositions of a sigmoidal function," *IEEE Transactions on Information Theory*, vol. 39, no. 3, pp. 930–945, 1993.

[52] M. Ö. Efe, "Neural network assisted computationally simple $\mathrm{PI}^\lambda\mathrm{D}^\mu$ control of a quadrotor UAV," *IEEE Transactions on Industrial Informatics*, vol. 7, no. 2, pp. 354–361, 2011.

[53] T. Dierks and S. Jagannathan, "Output feedback control of a quadrotor UAV using neural networks," *IEEE Transactions on Neural Networks*, vol. 21, no. 1, pp. 50–66, 2010.

[54] Y. C. Choi and H. S. Ahn, "Nonlinear control of quadrotor for point tracking: actual implementation and experimental tests," *IEEE/ASME Transactions on Mechatronics*, vol. 20, no. 3, pp. 1179–1192, 2015.

[55] A. Roberts and A. Tayebi, "Adaptive position tracking of VTOL UAVs," *IEEE Transactions on Robotics*, vol. 27, no. 1, pp. 129–142, February 2011.

[56] M. Wang, "Attitude control of a quadrotor UAV," *Master Thesis, Lakehead University, Ontario, Canada*, 2015.

[57] M. R. Jardin and E. R. Mueller, "Optimized measurements of UAV mass moment of inertia with a bifilar pendulum," in *Proceedings of AIAA Guidance, Navigation and Control Conference and Exhibit, Hilton Head, SC, USA*, 2007.

[58] M. D. Shuster, "A survey of attitude representations," *The Journal of the Astronautical Science*, vol. 41, no. 4, pp. 439–517, 1993.

[59] A. Chovancová, T. Fico, P. Hubinskỳ, and F. Duchoň, "Comparison of various quaternion-based control methods applied to quadrotor with disturbance observer and position estimator," *Robotics and Autonomous Systems*, vol. 79, pp. 87–98, 2016.

[60] J. D. Barton, "Fundamentals of small unmanned aircraft flight," *Johns Hopkins APL Technical Digest*, vol. 31, no. 2, 2012.

[61] J. T.-Y. Wen and K. Kreutz-Delgado, "The attitude control problem," *IEEE Transactions on Automatic Control*, vol. 36, no. 10, 1991.

[62] J. B. Kuipers, *Quaternions and Rotation Sequences*. Princeton University Press, 1999.

[63] D. Finkelstein, J. M. Jauch, S. Schiminovich, and D. Speiser, "Foundations of quaternion quantum mechanics," *Journal of Mathematical Physics*, vol. 3, no. 2, pp. 207–220, 1962.

[64] S. M. Joshi, A. G. Kelkar, and J. T.-Y. Wen, "Robust attitude stabilization of spacecraft using nonlinear quaternion feedback," *IEEE Transactions on Automatic Control*, vol. 40, no. 10, 1995.

[65] F. Lizarralde and J. T. Wen, "Attitude control without angular velocity measurement: a passivity approach," *IEEE Transactions on Automatic Control*, vol. 41, no. 3, 1996.

[66] K. Shoemake, "Animating rotation with quaternion curves," in *Proceedings of the 12th Annual Conference on Computer Graphics and Interactive Techniques*, vol. 19, pp. 245–254, 1985.

[67] http://www.tarotrc.com/Product/Detail.aspx?Lang=en&Id=3fe0db37-a0e3-47dc-a372-eb08653ef93f.

[68] https://www.fasttech.com/product/4049301-apm2-8-autopilot-module-flight-controller-board.

[69] Datasheet, STM32F427XX/STM32F429XX, http://www.st.com/content/ccc/resource/technical/document/datasheet/03/b4/b2/36/4c/72/49/29/DM00071990.pdf/files/DM00071990.pdf/jcr:content/translations/en.DM00071990.pdf.

[70] https://pixhawk.org/modules/pixhawk.

[71] A. Tayebi, A. Roberts, and A. Benallegue, "Inertial measurements based dynamic attitude estimation and velocity-free attitude stabilization," in *Proceedings of 2011 American Control Conference*, pp. 1027–1032, 2011.

[72] A. Tayebi, "Unit quaternion-based output feedback for the attitude tracking problem," *IEEE Transactions on Automatic Control*, vol. 53, no. 6, pp. 1516–1520, July 2008.

[73] T. Hamel, R. Mahony, R. Lozano, and J. Ostrowski, "Dynamic modelling and configuration stabilization for an x4-flyer," *IFAC Proceedings Volumes*, vol. 35, no. 1, pp. 217–222, 2002.

[74] L. R. G. Carrillo, A. E. D. López, R. Lozano, and C. Pégard, *Quad Rotorcraft Control*. Springer, 2013.

[75] http://renaissance.ucsd.edu/courses/mae207/wie_chap5.pdf, pp. 332–323.

[76] K. Gopalsamy, *Stability and Oscillations in Delay Differential Equations of Population Dynamics*. Springer, 1992.

[77] A. Abdessameud and A. Tayebi, *Motion Coordination for VTOL Unmanned Aerial Vehicles: Attitude Synchronisation and Formation Control*. Springer Science & Business Media, 2013.

[78] S. J. McGilvray, "Attitude stabilization of a quadrotor aircraft," *Master Thesis, Lakehead University, Ontario, Canada*, 2004.

[79] H. K. Khalil, *Noninear Systems*. Prentice-Hall, New Jersey, 1996.

[80] A. Roberts and A. Tayebi, "On the attitude estimation of accelerating rigid-bodies using GPS and IMU measurements," in *Proceedings of 50th IEEE Conference on Decision and Control and European Control Conference*, pp. 8088–8093, 2011.

[81] A. Tayebi, S. McGilvray, A. Roberts, and M. Moallem, "Attitude estimation and stabilization of a rigid body using low-cost sensors," in *Decision and Control, 2007 46th IEEE Conference on*, pp. 6424–6429, 2007.

[82] A. Tayebi, A. Roberts, and A. Benallegue, "Inertial vector measurements based velocity-free attitude stabilization," *IEEE Transactions on Automatic Control*, vol. 58, no. 11, pp. 2893–2898, 2013.

[83] A. Roberts and A. Tayebi, "A new position regulation strategy for VTOL UAVs using IMU and GPS measurements," *Automatica*, vol. 49, no. 2, pp. 434–440, 2013.